Universidad de Bogotá Jorge Tadeo Lozano - Universidad Central

Modelling & Simulation Master's degree

Modelling and Simulation of propagation of light in isotropic and anisotropic media with magneto-optic activity

---

Author:
Bernardo Garibello

Supervisor:
Nicolás Avilán Ph.D. Universidad Central, Departamento de Matemáticas.
César Herreño Ph.D. Universidad Distrital, Facultad de Ciencias y Educación.

November 30, 2018

"*Physics isn't the most important thing. Love is.*"

Richard Feynman

UNIVERSIDAD DE BOGOTÁ JORGE TADEO LOZANO - UNIVERSIDAD CENTRAL

Abstract

Faculty of Basic Sciences and Engineering
Modelling & Simulation Master's degree

Modelling & Simulation Master's degree

Modelling and Simulation of propagation of light in isotropic and anisotropic media with magneto-optic activity

by Bernardo GARIBELLO

Light propagation through thin film isotropic layers as well as anisotropic have been studied since the middle of the twenty century with applications in chemistry, biology, optical communications and materials engineering. Theoretical development has been made in order to find Fresnel coefficients, optical functions as reflectance, transmittance and when Joule effect is present absorptance. The transfer matrix method 2×2 for isotropic media is followed finding the Fresnel coefficients and optical functions with angular dependence. Explicit expressions for electric field module as function of transversal component of the structure for three media are derived and simulated, an iterated method is derived to find the electric field in a structured multilayer for isotropic stratified media. Three approaches are tested for light propagation in anisotropic multilayer systems, first the 4×4 transfer matrix method introduced by Yeh, but due to the method do not work on the limits of the isotropy the immersion method proposed by Cojocaru is programmed instead. This second method was programmed and an analytical solution of electric field was derived and calculated via software. The scattering matrix approach was used finally to avoid numerical overflows present in electric fields calculated by Cojocaru's method, optical functions are calculated as well as the transversal magneto-optic Kerr effect. Results were contrasted with those calculated in literature. Flux diagrams at the end of each chapter were included to give some clarity of the programming developed in Matlab.

Acknowledgements

Agradezco a mis padres que me dieron el apoyo que nunca me ha faltado, a mi mejor amiga, compañera, colega, confidente y orientadora Yadira Martín por su aportes y finalmente a mis profesores Nicolás Avilán y César Herreño por su paciencia, sus aportes siempre tan acertados y su incondicional apoyo. . . .

Contents

List of Figures

Physical Constants

Speed of Light	$c = 2.99792458 \times 10^{8}\ \mathrm{m\,s^{-1}}$ (exact)
Permitivitty of Vacuum	$\epsilon_0 = 8.85 \times 10^{-12}\ \mathrm{C^2\,N^{-1}\,m^{-2}}$
Permeability of Vacuum	$\mu_0 = 4\pi \times 10^{-7}\ \mathrm{N\,A^{-2}}$

List of Symbols

n	refraction index	dimensionless
E	Electric Field	$\mathrm{V\,m^{-1}}$
H	Magnetic Field	$\mathrm{A\,m^{-1}}$
D	Displacement Electric	$\mathrm{C\,m^{-2}}$
B	Magnetic Induction	$\mathrm{Wb\,m^{-2}}$
λ	wavelength	m
ω	angular frequency	$\mathrm{rad\,s^{-1}}$
δ	skin deep	Np m

Dedicated to. . . Juana Yadira Martín Perico

Chapter 1

Optics of two isotropic media

1.1 Introduction

The foundations of light propagation from the classical point of view is based on the Maxwell equations. This chapter describe the propagation of light for simple interfaces defining and finding expressions for Fresnel coefficients and optical functions principally reflectance and transmittance. A program was developed in order to shows graphics where Brewster's angle and total internal reflection are present, finally some characteristics dielectric-metal interface was showed, simulating optical functions contrasted with results reported in literature.

1.2 Laws of Reflection and Refraction

The Maxwell's equations are the starting point of all the theory that is implied in this thesis. For conducting linear media, in the differential form they are:

$$\nabla \cdot \mathbf{E} = \frac{\rho}{\varepsilon} \tag{1.1}$$

$$\nabla \cdot \mathbf{H} = 0 \tag{1.2}$$

$$\nabla \times \mathbf{E} = -\mu \frac{\partial \mathbf{H}}{\partial t} \tag{1.3}$$

$$\nabla \times \mathbf{H} = \mu \mathbf{J} + \mu\varepsilon \frac{\partial \mathbf{E}}{\partial t} \tag{1.4}$$

Where ρ is the charge density, ε is the electric permittivity of the medium and μ is the magnetic permeability of the medium. $\nabla \cdot \mathbf{A}$ is the divergence of the field $\mathbf{A}$ and $\nabla \times \mathbf{A}$ represents the curl of the field $\mathbf{A}$. $\mathbf{E}$ and $\mathbf{H}$ are the electric and magnetic fields respectively. Permittivity and permeability are defined for isotropic media as: $\varepsilon = \varepsilon_0 \varepsilon_r$, ε_r is the relative permittivity of the medium respect to the vacuum and $\mu = \mu_0 \mu_r$, μ_r is the relative permeability that is 1 for most materials.
The continuity for the plane of incidence components for electric and magnetic fields through several media can be derived from Maxwell's equations integral form. The relations are given by a set of equations named **boundary conditions** (equations 1.5 - 1.8):

$$\varepsilon_1 E_{1n} - \varepsilon_2 E_{2n} = \sigma \tag{1.5}$$

$$\mathbf{E}_{t1} = \mathbf{E}_{t2} \tag{1.6}$$

$$\mu_1 H_{1n} = \mu_2 H_{2n} \tag{1.7}$$

$$\mathbf{H}_{t1} - \mathbf{H}_{t2} = \mathbf{K} \times \mathbf{n} \tag{1.8}$$

Where σ is the superficial charge density, $\mathbf{K}$ is superficial current, $\mathbf{n}$ is the normal vector to the surface, σ and $\mathbf{K}$ are considered to be zero for all purposes of this work. Constants ϵ_1 and ϵ_2 are the permittivities in the media 1 and 2, likewise, μ_1 and μ_2 are the permeabilities in the media 1 and 2.

By decoupling the Maxwell's equations, it is found that the electric and magnetic fields satisfy the wave equation. They can be written as a monochromatic wave in the form: $\mathbf{E} = \mathbf{E}_0 e^{i(\mathbf{k}\cdot\mathbf{r}-\omega t)}$ and $\mathbf{H} = \mathbf{H}_0 e^{i(\mathbf{k}\cdot\mathbf{r}-\omega t)}$. $\mathbf{E}_0$ and $\mathbf{H}_0$ are the corresponding amplitudes to the electromagnetic wave complex vectors that indicates its amplitudes and directions. The vector $\mathbf{k}$ is called **wave vector** and indicates the direction of propagation of the electromagnetic wave; $k = |\mathbf{k}|$ is the wave number and is given by $k = \frac{2\pi}{\lambda}$, here λ is the wavelength and is related to the frequency by $c = \lambda f$, $\mathbf{r}$ is the position coordinate. $\omega = 2\pi f$ is the angular frequency, defined by the source and t is the time.

The electric and magnetic fields are related by the wave velocity v and the permeability of the medium μ with the vector $\mathbf{k}$ by:

$$\mathbf{H} = \frac{1}{\mu v}(\mathbf{k} \times \mathbf{E}) \tag{1.9}$$

If a monochromatic wave is travelling from an isotropic medium 1 to another isotropic medium 2, there are three waves involved. First, the incident wave $\mathbf{E}_1$; second, the reflected wave $\mathbf{E}_1'$ and third, the transmitted (or refracted) wave $\mathbf{E}_2$.

In the first and second chapters of this thesis it is assumed that the medium is linear, homogeneous and isotropic, so the constitutive relations will be: $\mathbf{D} = \varepsilon\mathbf{E}$, $\mathbf{D}$ is the displacement electric vector, and $\mathbf{B} = \mu\mathbf{H}$, $\mathbf{B}$ is called the magnetic induction. The velocity of the wave in a medium on the direction of propagation is: $v = \frac{1}{\sqrt{\varepsilon\mu}} = \frac{c}{n}$, where n is defined by $n \equiv \sqrt{\frac{\varepsilon\mu}{\varepsilon_0\mu_0}}$ and is named *the refraction index*. In presence of non-magnetic material $\mu \cong \mu_0$ (i.e. $\mu_r \cong 1$) so $n \cong \sqrt{\varepsilon_r}$.

The figure 1.1 is a schematic representation of incident, reflected and transmitted rays for a monochromatic wave that travels from the medium 1 to the medium 2. The incident, reflected and transmitted angles are measured respect the normal (z-axis) in this geometry.

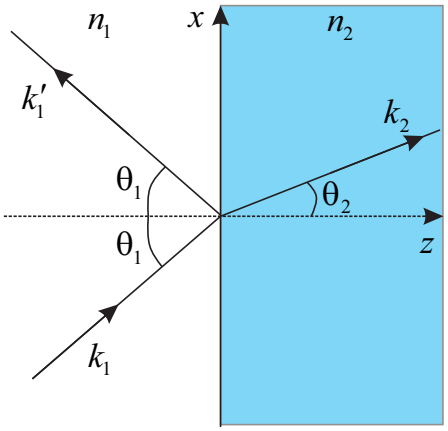

FIGURE 1.1: Wave vectors representing an incoming wave to an interface bounding two media and the corresponding transmitted and reflected vector waves.

It is possible to demonstrate that $\mathbf{k}_1, \mathbf{k}'_1$ and $\mathbf{k}_2$ -the incident, reflected and transmitted wave vectors-, (see figure 1.1) are in the same plane, named the *incident plane*. The wave numbers of the incident, reflected and transmitted waves (k_1, k'_1, k_2) are related with the angular frequency by: $\omega = 2\pi f = k_i v_i$. Using the boundary conditions for tangential electric fields, $k_{1x} = k_{2x} = k'_{1x}$, or $k_1 \sin\theta_1 = k'_1 \sin\theta'_1 = k_2 \sin\theta_2$, where θ_1 is the **angle of incidence**, θ'_1 is the **angle of reflection** and θ_2 is the angle of transmission, known as **angle of refraction** with respect to the normal. Therefore magnitudes of the wave numbers are equal $k_1 = k'_1$ so $\theta_1 = \theta'_1$ for complete zero roughness, (for a treatment of roughness interfaces in isotropic media see (Windt, 1998)) as a consequence:

$$n_1 \sin\theta_1 = n_2 \sin\theta_2 \tag{1.10}$$

Expression known as **Snell's Law**.

1.3 Fresnel coefficients, reflectance and transmittance for *p*-Polarization

The polarization of a wave is refereed to the direction of the electric field vector. The *p*-polarization makes reference to a *parallel* field to the incidence plane, so the propagation vectors (k_1, k'_1, k_2) and the electric field vectors (E_1, E'_1, E_2) are in the plane (xz). This plane is shown in the figure 1.2, the magnetic field vectors are perpendicular (out or in) to the paper.

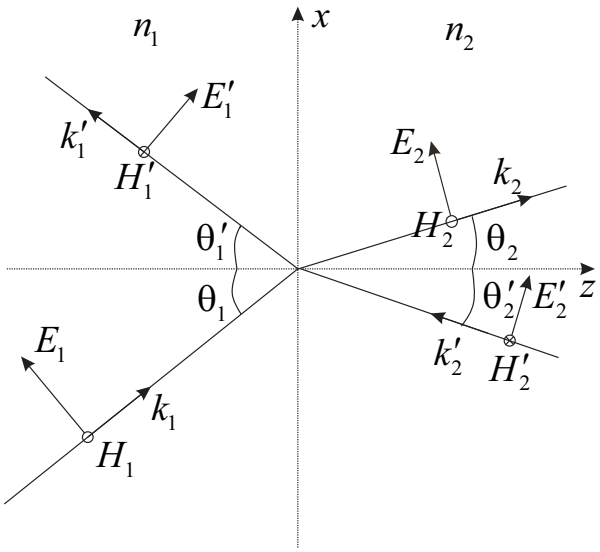

FIGURE 1.2: *p*-Polarization for a oblique inicident wave through two dielectric media

The wave defined by k'_2 coming form the right is drawn for future analysis. From equations (1.6) and (1.8) in the boundary conditions, assuming a couple of dielectric media with no charges or superficial current densities and leading to zero the value of E'_2, is possible decomposing the vectors in the form:

$$E_1 \cos\theta_1 + E'_1 \cos\theta'_1 = E_2 \cos\theta_2 \tag{1.11}$$

$$\frac{1}{\mu_1 v_1}(E_1 - E'_1) = \frac{1}{\mu_2 v_2} E_2 \tag{1.12}$$

Previously was mentioned that $\theta_1 = \theta_1'$, is possible rewrite the equation (1.11) as:

$$E_1 + E_1' = \alpha E_2 \tag{1.13}$$

Where $\alpha = \frac{\cos\theta_2}{\cos\theta_1}$ [1]. Likewise, the equation (1.12) becomes:

$$E_1 - E_1' = \beta E_2 \tag{1.15}$$

Where $\beta = \frac{\mu_1 v_1}{\mu_2 v_2} = \frac{\mu_1 n_2}{\mu_2 n_1} \cong \frac{n_2}{n_1}$ if the medium 1 and medium 2 are not magnetic ($\mu_1 \cong \mu_2 \cong 1$). Solving the equations (1.13) and (1.15) for the quotient of the reflected and transmitted amplitudes over the incident field:

$$r_{12p} = \frac{E_2}{E_1} = \frac{\alpha - \beta}{\alpha + \beta} \tag{1.16}$$

$$t_{12p} = \frac{E_2}{E_1} = \frac{2}{\alpha + \beta} \tag{1.17}$$

Equation (1.16) define what is known as *reflection Fresnel coefficient* and is a ratio between the reflected respect to the incident electric field. In a similar way the equation 1.17 is the *transmission Fresnel coefficient* of transmitted and incident electric field. Both of them are dimensionless and can be written as a function of the angle of incidence θ_1.

The first simulation created for the previous model is shown in the figure 1.3. Both Fresnel coefficients are drawn as functions of the angle of incidence θ_1, for a monochromatic source of light with wavelength $\lambda = 633nm$ that travels from air with refraction index $n_1 = 1$ to optical glass or BK7, with refraction index $n_2 = 1.51$. The negative values of the figure 1.3 indicates that the wave is out of phase 180° with the incident beam.

In terms of energy, there are a couple of functions that relate on one hand, the energy of the incident wave respect to the energy of the reflected wave (**Reflectance**), on the other hand, the energy of the incident wave respect to the energy of the transmitted wave (**Transmittance**). For two media, they are given by the expressions (1.18), and (1.19):

$$R = rr^* \tag{1.18}$$

$$T = \frac{n_2 \cos\theta_2}{n_1 \cos\theta_1} tt^* \tag{1.19}$$

Where r is the Fresnel coefficient for reflection, r^* is the conjugate complex of r, as well as t is the Fresnel coefficient for transmission, t^* is the conjugate complex of t. n_1, n_2 are the refraction indexes of media 1 and 2, respectively and θ_1, θ_2 are the angle of incidence and the angle of refraction respectively. Explicit expressions for p-polarization are given as follows:

[1] Using the Snell's law is possible show that α can be rewritten in terms of the incident angle as:

$$\alpha = \frac{\sqrt{1 - \left(\frac{n_1}{n_2}\sin\theta_1\right)^2}}{\cos\theta_1} \tag{1.14}$$

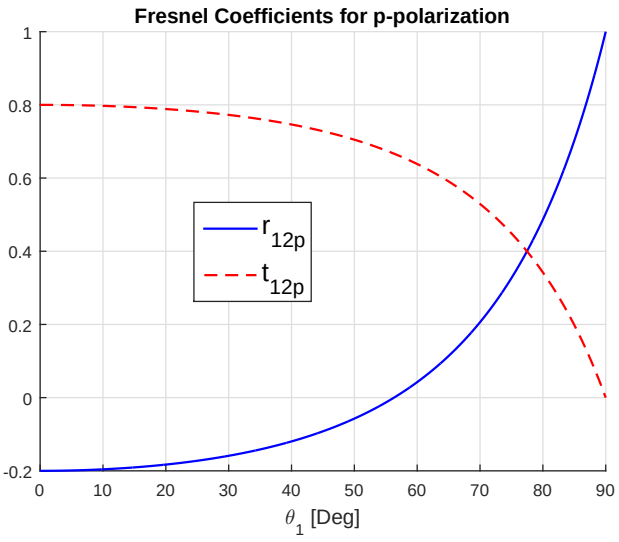

FIGURE 1.3: Fresnel coefficients for transmitted and reflected waves as functions of the angle of incidence θ_1 for p-polarization, in a simple interface Air||BK7, $\lambda = 633nm$.

$$R_p = \left(\frac{\alpha - \beta}{\alpha + \beta}\right)^2 \tag{1.20}$$

$$T_p = \alpha\beta\left(\frac{2}{\alpha + \beta}\right)^2 \tag{1.21}$$

For the same air||BK7 interface the figure 1.4 shows the functions of R_p and T_p depending of the angle of incidence θ_1. Note that $R_p + T_p = 1$ for all values of θ_1, so there is no stored energy in the interface.

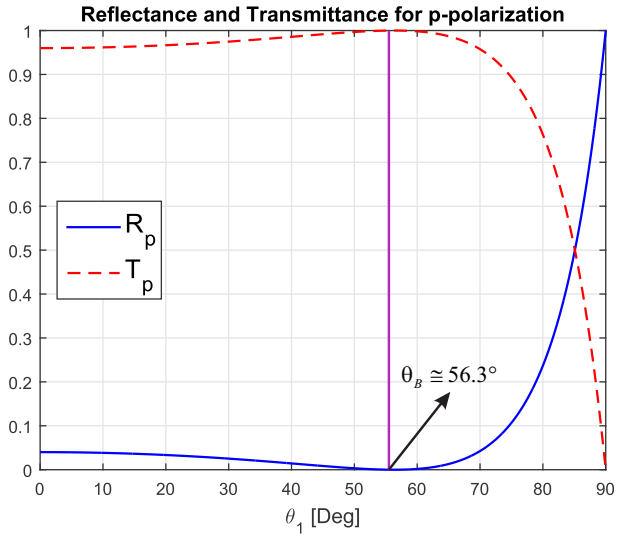

FIGURE 1.4: Reflectance and Transmittance as functions of the angle of incidence θ_1 for p-polarization, interface Air||BK7 for $\lambda = 633nm$.

From the figure 1.4 is clear that the Reflectance reaches a zero value for a specific angle, on this angle there is not reflected wave $R_p = 0$. The expression for this angle can be derived from equation (1.20) setting $R_p = 0$, using the fact that $\cos^2\theta = 1 - \sin^2\theta$, and assuming that $\mu_0 = \mu$ (i.e. $\mu_r = 1$ for both media) is possible find:

$$\tan\theta_B = \frac{n_2}{n_1} \tag{1.22}$$

This angle of total transmission (exclusive for p-waves) is called: **Brewster's angle**. For the same interface air||BK7; $\tan\theta_B = \frac{1.5}{1}$, then, $\theta \simeq 56.3°$ as can be seen in the figure 1.4.

1.4 Fresnel coefficients, reflectance and transmittance for s-Polarization

In a similar way it is possible to deduce the same equations for s-waves (s for "senkrecht" the German word for perpendicular). Now the electrical field is perpendicular to the plane of incidence xz. Using the boundary conditions (1.6) and (1.7) based on the figure 1.5 we set the equations:

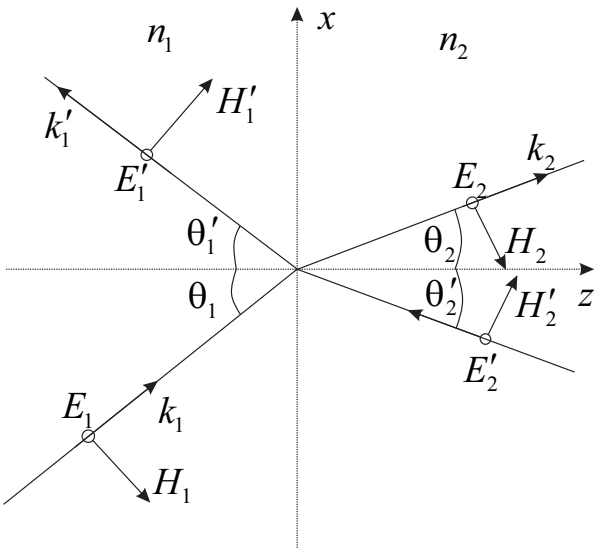

FIGURE 1.5: s-Polarization for a oblique incident wave through two isotropic dielectric media

$$-\mu_1 H_1 \cos\theta_1 + \mu_1 H_1' \cos\theta_1' = -\mu_2 H_2 \cos\theta_2 \tag{1.23}$$

$$E_1 + E_1' = E_2 \tag{1.24}$$

Rewriting the equation (1.23) and using the fact that $\mathbf{H}_1 = \frac{1}{\mu v}(\mathbf{k}_1 \times \mathbf{E}_1)$, is possible to find the expression:

$$E_1 - E_1' = \alpha\beta E_2 \tag{1.25}$$

The previous two equations combined will give:

$$r_{12s} = \frac{E_1'}{E_1} = \frac{1 - \alpha\beta}{1 + \alpha\beta} \tag{1.26}$$

$$t_{12s} = \frac{E_2}{E_1} = \frac{2}{1+\alpha\beta} \tag{1.27}$$

Where r_{12s} represents the ratio of reflected amplitude to the incident for s-wave travelling from medium 1 to medium 2 for s-polarization. Likewise, t_{12s} describes the ratio of the transmitted amplitude to the incident for a s-wave travelling from medium 1 to medium 2. This couple of coefficients are the *Fresnel coefficients* for s-polarization for a monochromatic wave with oblique incidence.

Once again, the Fresnel coefficients were calculated via software as functions of the angle of incidence θ_1, for a source of monochromatic incident light form air ($n_1 = 1$) to optical glass or BK7 ($n_2 = 1.51$) at $\lambda = 633nm$, see figure 1.6.

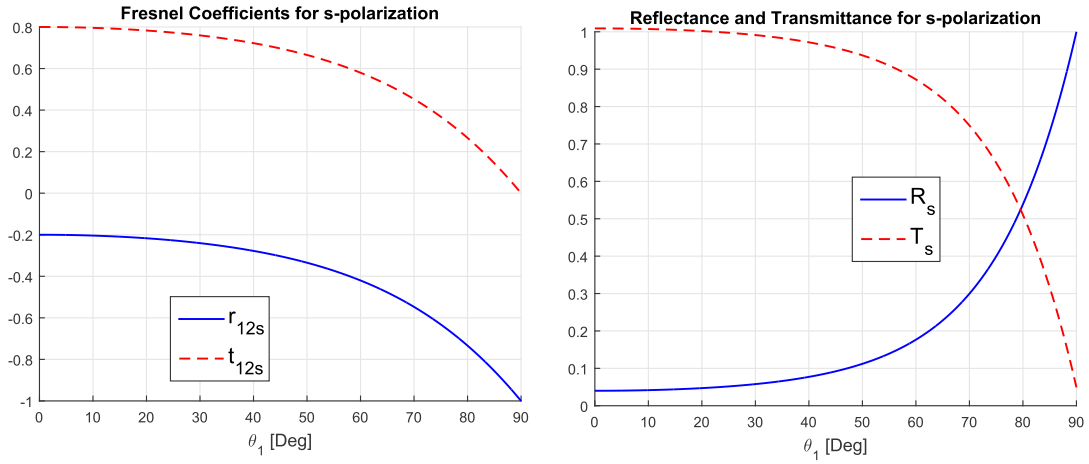

FIGURE 1.6: (Left) Fresnel coefficients for reflected and transmitted waves as functions of the angle of incidence θ_1, for s-polarization waves interface Air||BK7 at $\lambda = 633nm$. (Right) Reflectance and Transmittance as functions of the angle of incidence θ_1 for s-polarization waves same geometry.

Using the expressions for reflectance and transmittance (1.18, 1.19) explicit expressions for s-polarization are given by:

$$R_s = \left(\frac{1-\alpha\beta}{1+\alpha\beta}\right)^2 \tag{1.28}$$

$$T_s = \alpha\beta\left(\frac{2}{1+\alpha\beta}\right)^2 \tag{1.29}$$

For the same air||BK7 interface the figure 1.6 shows the reflectance R_s and transmittance T_s as functions of θ_1. Note that as the p-polarization, $R_s + T_s = 1$ for all values of θ_1, as required by conservation energy, and as a consequence there is no energy stored in the boundary of the two media.

There is no Brewster's angle in this case (a similar procedure for p-polarization will lead us to $n_1 = n_2$), this fact can be observed in the figure 1.6 where the coefficent R_s never search the zero value.

The Fresnel coefficients, the reflectance and transmittance for both p and s-polarization were exemplified via two nonconducting media where the refraction index of the incident wave (n_1) is less than the

medium 2 (n_2) i.e. $n_1 < n_2$. In the opposite case ($n_1 > n_2$), emerge a concept named *critical angle*, that is a particular angle when all the incident wave is totally reflected. From the Snell's law, the critical angle is found via:

$$\sin\theta_c = \frac{n_2}{n_1} \tag{1.30}$$

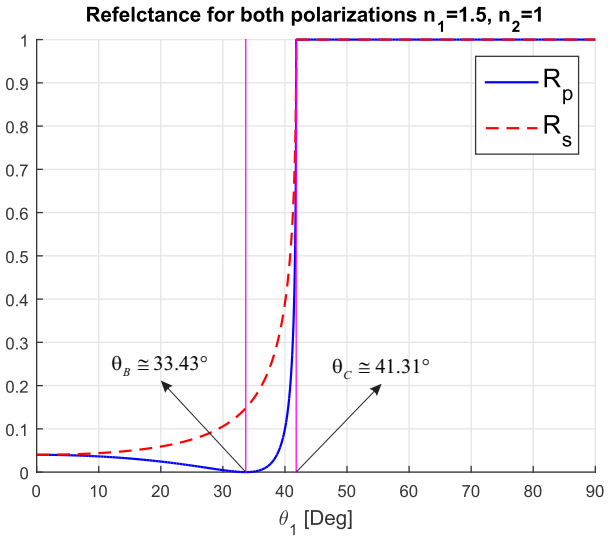

FIGURE 1.7: Reflectance for p and s-polarizations as functions of the angle of incidence θ_1 for $n_1 = 1.5 > n_2 = 1$, the Brewster angle only for p-polarization in $\theta_B = 33.43°$ and critical angle for both polarizations is in $\theta_c = 47.31°$

The figure 1.7 shows the reflectance for p and s-polarization for an incident light from a medium $n_1 = 1.51$ to a medium $n_2 = 1$. The Brewster's angle is only valid for the p-polarization (For these parameters $\theta_B = 33.43°$) and the angle for total internal reflection reach its value on $\theta_c = 41.31°$.

With Fresnel coefficients (equations 1.16, 1.17, 1.26 and 1.27) and the functions of reflectance and transmittance, we have a complete solution of the boundary value problem for a wave with arbitrary polarization at oblique incidence for two dielectric isotropic media.

1.5 Propagation of light in interface dielectric-conductor

Until now, we have seen the propagation of a wave through two media with an oblique incidence for non-conducting (or dielectric) media. In this section we are going to analyse the behaviour of the wave that travels from a medium with a real refraction index n_1 (transparent medium) to a good conductor, that represents an absorptive material, treatment here is for Ohmic metals.

Applying the curl to the equation (1.3), using the Ohm's law $\mathbf{J} = \sigma\mathbf{E}$, where $\mathbf{E}$ is the electric field vector, σ is the conductivity and $\mathbf{J}$ is the current density is possible to obtain:

$$\nabla^2\mathbf{E} = \mu\sigma\frac{\partial\mathbf{E}}{\partial t} + \mu\varepsilon\frac{\partial^2\mathbf{E}}{\partial t^2} \tag{1.31}$$

The previous equation admit plane wave solution:

$$\mathbf{E}(\mathbf{r},t) = \mathbf{E}_0 e^{i(\mathbf{k}\cdot\mathbf{r}-\omega t)} \tag{1.32}$$

But in this case the element $\mathbf{k} = \mathbf{k}_2$ in the second medium is a complex vector. To find an expression of the norm of the vector $||\mathbf{k}_2||$, first we replace the equation (1.32) in the (1.31). Finding that:

$$||\mathbf{k}_2||^2 = \mu\sigma\omega^2 + i\mu\epsilon\omega \tag{1.33}$$

Then $||\mathbf{k}_2|| = k_{re} + ik_{im}$ so, $||\mathbf{k}_2||^2 = {k_{re}}^2 - {k_{im}}^2 + 2ik_{re}k_{im}$. The real part of $||\mathbf{k}_2||^2$ will be:

$${k_{re}}^2 - {k_{im}}^2 = \mu\sigma\omega^2 \tag{1.34}$$

Also, the module of $||\mathbf{k}_2||^2$ is $|||\mathbf{k}_2||^2| = {k_{re}}^2 + {k_{im}}^2$, so:

$${k_{re}}^2 + {k_{im}}^2 = \sqrt{(\mu\sigma\omega^2)^2 + (\mu\epsilon\omega)^2} \tag{1.35}$$

Adding and subtracting the equations (1.34) and (1.35), the real and imaginary parts of k are given by:

$$k_{re} = \omega\sqrt{\frac{\epsilon\mu}{2}}\left(\sqrt{1+\left(\frac{\sigma}{\epsilon\omega}\right)^2}+1\right)^{\frac{1}{2}} \tag{1.36}$$

$$k_{im} = \omega\sqrt{\frac{\epsilon\mu}{2}}\left(\sqrt{1+\left(\frac{\sigma}{\epsilon\omega}\right)^2}-1\right)^{\frac{1}{2}} \tag{1.37}$$

If the ray has a normal incidence $\mathbf{k} = k_z\hat{\mathbf{z}}$, $||\mathbf{k}|| = k_z = k_{re} + ik_{im}$, replacing in (1.32), it is possible to find that:

$$\mathbf{E}(z,t) = \mathbf{E}_0 e^{-k_{im}z} e^{i(k_{re}z-\omega t)} \tag{1.38}$$

The real part of k_z (i.e. k_{re}) determines, according to Reitz et. al. (Reitz, Milford, and Christy, 2008): 1. The wave length: $\lambda = \frac{2\pi}{k_{re}}$, 2. Propagation velocity: $v = \frac{\omega}{k_{re}}$ and 3. The refraction index: $n = \frac{c}{\omega}k_{re}$, where c is the light velocity in vacuum.

The imaginary part in (1.38) allows us to know the wave is attenuated exponentially with the distance in z. The distance that reduce the amplitude of the wave to a 36% is called **skin deep** in Nepers per meter and is given by: $\delta_m = \frac{1}{k_{im}}$.

The electromagnetic wave not only is attenuated with the distance in z. It is possible to demonstrate, based on Griffiths (Griffiths, 2013) that the electric and magnetic components of the wave are no longer in phase. If the complex amplitudes of the fields are given by: $\mathbf{E}_0 = E_0 e^{i\delta_E}$ and $\mathbf{H}_0 = H_0 e^{i\delta_H}$, using the fact that $\mathbf{H}_{0_2} = \frac{\mathbf{k}_2}{\mu\omega}\mathbf{E}_{0_2}$, simplifying we obtain that there is a lag between the electric and magnetic fields given by $\phi = \delta_H - \delta_E$. The attenuation effect and the change of phase of the fields are shown in the figure 1.8[2].

The Fresnel coefficients are equal to those who were deduced in the previous section, but the values of α and β are now complex.

[2]Adapted from (Griffiths, 2013)

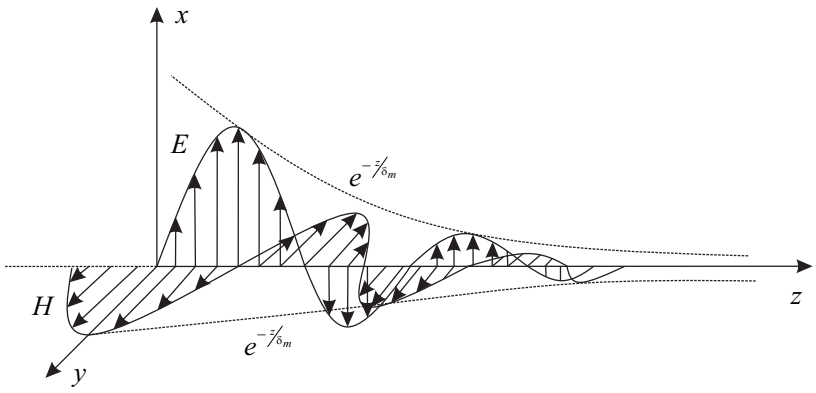

FIGURE 1.8: Attenuation and lags of electric and magnetic fields of a wave in a medium with Ohmic conductivity

Since $\mathbf{k}_2$ is a complex vector over a conducting medium ($||\mathbf{k}_2|| = k_{re} + ik_{im}$) could be drawn and decomposed in its x and z components via unit vectors $\mathbf{i} = (1, 0, 0)$ and $\mathbf{k} = (0, 0, 1)$ as the figure 1.9.

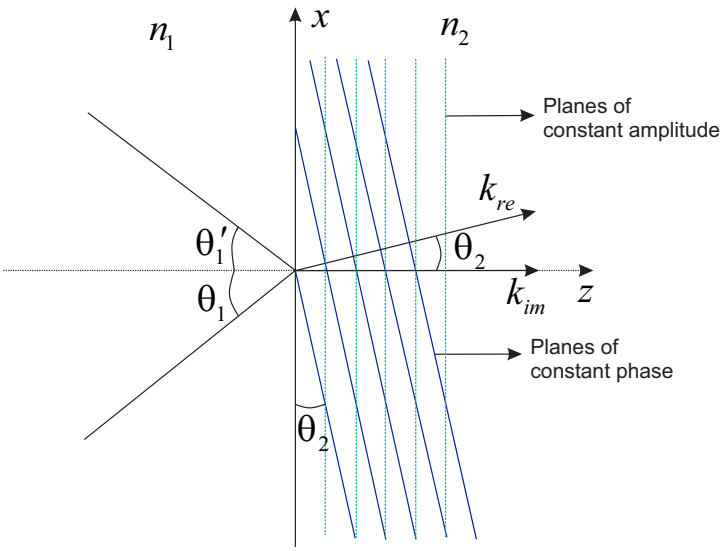

FIGURE 1.9: Planes of constant amplitude and phase for a wave in a conducting media.

k_{re} defines the planes of constant phase and k_{im} states the planes of constant amplitude:

$$\mathbf{k}_2 = k_{re} \sin\theta_2 \mathbf{i} + (k_{re} \cos\theta_2 + ik_{im})\mathbf{k}$$

Using the Snell's law $n_1 \sin\theta_1 = n_2 \sin\theta_2$.

$$\mathbf{k}_2 = k_1 \sin\theta_1 \mathbf{i} + (k_{re} \cos\theta_2 + ik_{im})\mathbf{k}$$

Also, writing $||\mathbf{k}_2|| = k_2$:

$$k_2 \cos\theta_2 = \frac{\omega}{c}(p + iq) \tag{1.39}$$

or

$$n_2 \cos\theta_2 = p + iq$$

Squaring both sides and applying: $\cos^2\theta = 1 - \sin^2\theta$:

$$\begin{aligned} n_2^2 \cos^2\theta_2 &= p^2 - q^2 + 2ipq \\ n_2^2 - n_2^2 \sin^2\theta_2 &= p^2 - q^2 + 2ipq \\ n_2^2 - n_1^2 \sin^2\theta_1 &= p^2 - q^2 + 2ipq \end{aligned}$$

Since $n_2^2 = \varepsilon_2$, where $\varepsilon_2 = \varepsilon' + i\varepsilon''$, and $n_1^2 = \varepsilon_1$, it is possible rewrite the last equation as:

$$\begin{aligned} \varepsilon_2 - \varepsilon_1 \sin^2\theta_1 &= p^2 - q^2 + 2ipq \\ \varepsilon' + i\varepsilon'' - \varepsilon_1 \sin^2\theta_1 &= p^2 - q^2 + 2ipq \end{aligned}$$

Solving for p and q

$$\begin{aligned} p &= \sqrt{\tfrac{1}{2}[(\varepsilon' - \varepsilon_1 \sin^2\theta_1) + \sqrt{(\varepsilon' - \varepsilon_1 \sin^2\theta_1)^2 + \varepsilon''^2}]} \\ q &= \sqrt{\tfrac{1}{2}[-(\varepsilon' - \varepsilon_1 \sin^2\theta_1) + \sqrt{(\varepsilon' - \varepsilon_1 \sin^2\theta_1)^2 + \varepsilon''^2}]} \end{aligned} \tag{1.40}$$

The expressions for p and q are generalized forms for the real and complex parts of n_2 depending on one hand, on the incidence angle θ_1, on the other hand on the permittivities of both media. For an interface BK7||Au was simulated the variation of the refraction index with the angle of incidence, figure 1.10. Note, that the variation is minimal for both components, while the real component remains constant, the imaginary part change lightly, so the variations of n_2 with the angle of incidence will be omitted in further analysis.

The same program that was previously used for propagation of light in interfaces dielectric-dielectric is used now in the interface dielectric-metal for an interface BK7||Au, the figure 1.11, shows the reflectance both polarizations. The interface Air || Ag for $\lambda = 500nm$ was simulated too contrasting the result with the one obtained by Yeh (Yeh, 2005).

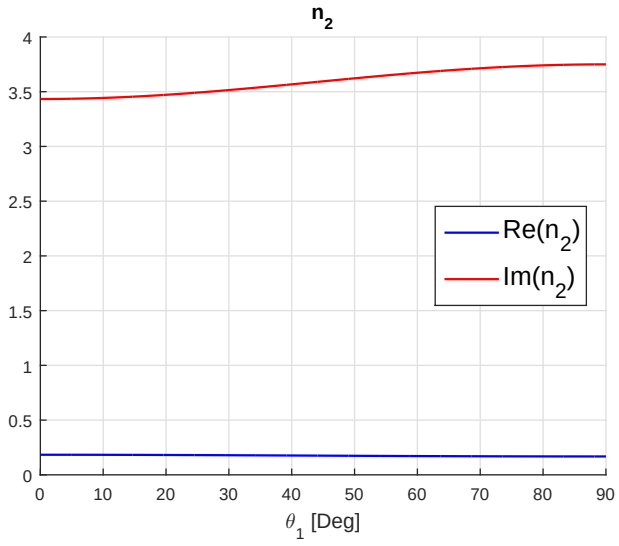

FIGURE 1.10: Variation of index of refraction as function of the angle of incidence for an interface BK7||Au.

1.6 Flux diagram two isotropic media

In the figure 1.12 is shown the flux diagram followed to find the Fresnel coefficients and optical functions with angular dependence for two isotropic media:

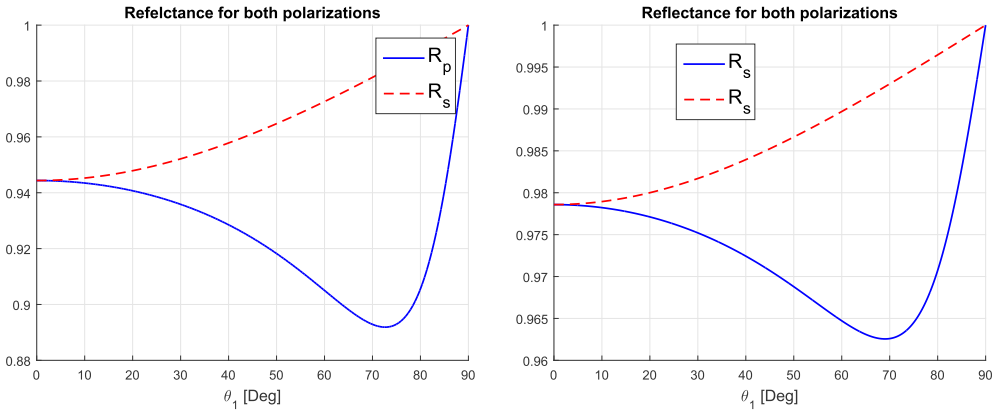

FIGURE 1.11: (Left) Reflectance for both polarizations as functions of θ_1, interface BK7||Au, $\lambda = 633nm$. (Right) Reflectance for both polarizations as functions of θ_1, interface Air||Ag, $\lambda = 500nm$.

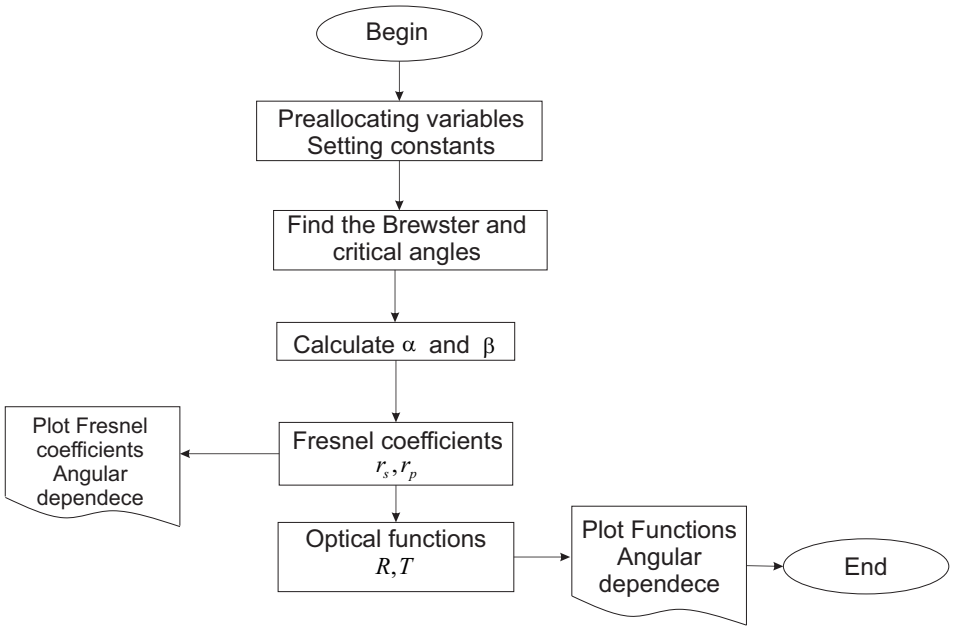

FIGURE 1.12: Flux diagram to find Brewster angle, critical angle, Fresnel coefficients and optical functions for two isotropic media.

Chapter 2

Optics of three and more isotropic media

2.1 Introduction

In this chapter the Fresnel coefficients for reflection and transmission as well as, expressions for reflectance and transmittance initially for three media and then for N-media are derived. For three media, the study was based on a deduction carried out by G.B. Airy in 1833 and it was designed a program to obtain the optical functions. Autonomous expressions are derived for electrical field for a monolayer. The Kretschmann & Raether geometry was simulated in order to test the results. Then, the matrix method is developed based on the studies of Yeh to find the optical functions for N-layers and are found autonomous expressions for electrical fields along the inner layers.

2.1.1 Airy's Formulas

The deduction here is adapted from Reitz et. al. (Reitz, Milford, and Christy, 2008). The first goal is to obtain the spatial phase shift due to the inner layer. The phase difference to be calculated is on the paths $O'X$ and OZX, according to figure 2.1.

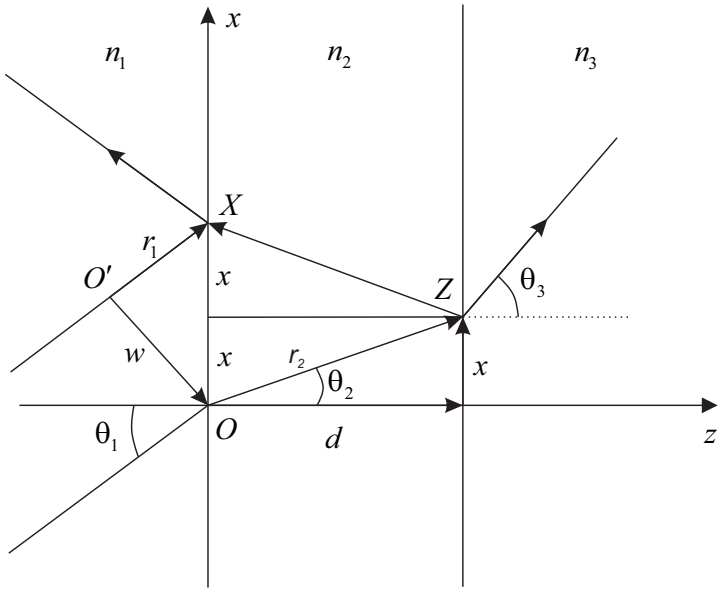

FIGURE 2.1: Incident, reflected and transmitted wave in three layers.

The spatial phase difference is found by the expression:

$$\phi = 2\mathbf{k}_2 \cdot \mathbf{r}_2 - \mathbf{k}_1 \cdot \mathbf{r}_1$$

Decomposing $\mathbf{r}_1$ and $\mathbf{r}_2$ in its components:

$$\begin{aligned} \mathbf{r}_1 &= 2x\mathbf{i} - w\mathbf{p}_1 \\ \mathbf{r}_2 &= x\mathbf{i} + d\mathbf{k}, \end{aligned}$$

where x is the amplitude of the wave vector on the x-axis, d is the thickness of the layer, $\mathbf{r}_2$ is the amplitude of the wave vector projected on the thickness, w is an auxiliary vector orthogonal to $\mathbf{r}_1$ which is on the direction of the wave vector in the incidence medium, $\mathbf{p}_1 = \mathbf{j} \times \mathbf{u}_1$ ($\mathbf{j} = (0, 1, 0)$ in $\mathbb{R}^3$), $\mathbf{p}_1$ is perpendicular to $\mathbf{k}_1 = k_1\mathbf{u}_1$, so $\mathbf{p}_1 \cdot \mathbf{u}_1 = 0$. Then, the phase ϕ can be written as:

$$\phi = 2x(\mathbf{k}_2 \cdot \mathbf{i} - \mathbf{k}_1 \cdot \mathbf{i}) + 2d\mathbf{k}_2 \cdot \mathbf{k}.$$

The component along $\mathbf{i}$ goes to 0 because of the Snell's law:

$$\mathbf{k}_2 \cdot \mathbf{i} - \mathbf{k}_1 \cdot \mathbf{i} = k_2 \sin\theta_2 - k_1 \sin\theta_1 = 0.$$

Furthermore, $\mathbf{k}_2 \cdot \mathbf{k} = k_2 \cos\theta_2$, so the phase difference between $O'X$ and OZX is given (using equation (1.39)) by:

$$\phi = 2d\frac{\omega}{c}n_2 \cos\theta_2 \tag{2.1}$$

The phase difference is proportional to the transversal distance in the inner layer, the wavelength and the refraction index, and inversely proportional to the light velocity in vacuum.

The real part of ϕ gives the real phase shift, and the imaginary part of ϕ gives the attenuation due to two traversals of the slab.

The figure 2.2 is quite helpful to derive equations for the Fresnel coefficients r and t independent of the polarization. To find the result for both polarizations it is enough setting the subscripts p and s. First of all, assume that the incident wave has amplitude 1, so, the reflected wave has an amplitude given by r_{12} and the amplitude of the transmitted wave t_{12}. When the transmitted wave travels along the layer, is affected by the spatial phase, so, when the wave arrives to the boundary of the interface of the media 2 and 3, has an amplitude $t_{12}e^{\frac{1}{2}i\phi}$. This wave is refracted to the third medium producing a wave that has an amplitude $t_{23}t_{12}e^{\frac{1}{2}i\phi}$, the wave reflected has an amplitude of $r_{23}t_{12}e^{\frac{1}{2}i\phi}$. This wave travels back from in the medium 2 and at the boundary of the media 2-1 has an amplitude of $r_{23}t_{12}e^{i\phi}$. This model will consider repeating this process until the infinite.

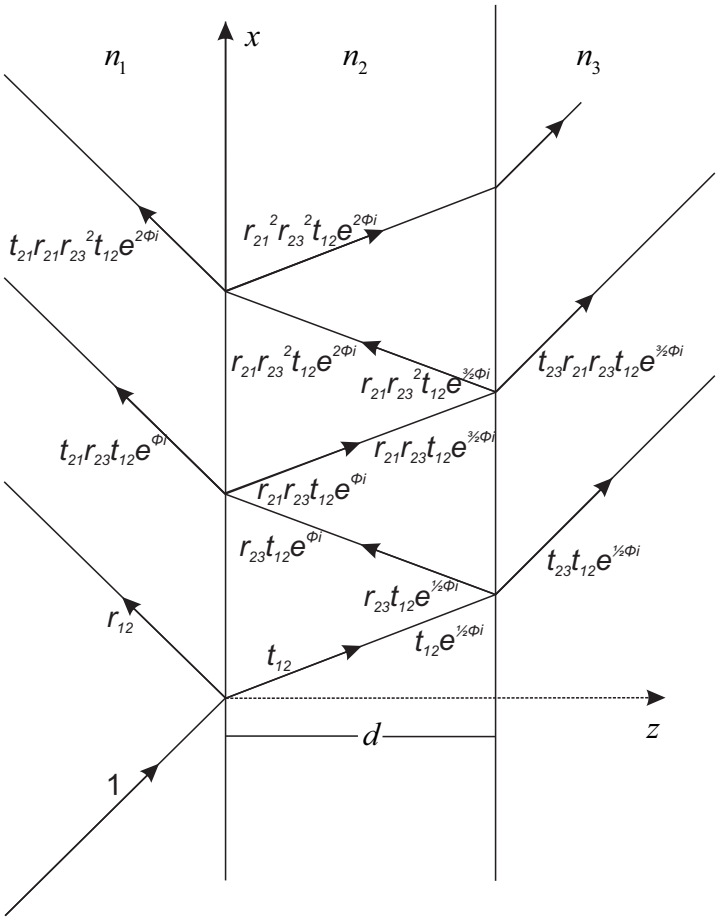

FIGURE 2.2: Incident, reflected and transmitted wave in a monolayer system.

For the reflection coefficient, adding up all the reflected coefficients of the waves (at the left side of the figure 2.2):

$$\begin{aligned} r &= r_{12} + t_{21}r_{23}t_{12}e^{i\phi} + t_{21}r_{21}r_{23}^2t_{12}e^{2i\phi} + ... \\ r &= r_{12} + t_{12}r_{23}t_{21}e^{i\phi}\left[1 + r_{21}r_{23}e^{i\phi} + (r_{21}r_{23}e^{i\phi})^2 + ...\right] \end{aligned}$$

Using the geometric series, the Fresnel coefficient for reflection can be written in the form:

$$\begin{aligned} r &= r_{12} + \frac{t_{12}r_{23}t_{21}e^{i\phi}}{1 - r_{21}r_{23}e^{i\phi}} \\ r &= \frac{r_{12} + r_{23}\left(t_{12}t_{21} - r_{12}r_{21}\right)e^{i\phi}}{1 - r_{21}r_{23}e^{i\phi}} \end{aligned}$$

Using the Stokes' relations ($r_{12} = -r_{21}$ and $r_{12}^2 + t_{12}t_{21} = 1$), the reflection coefficient becomes:

$$r = \frac{r_{12} + r_{23}e^{i\phi}}{1 + r_{12}r_{23}e^{i\phi}} \tag{2.2}$$

A similar deduction can be used to obtain the transmission coefficient:

$$t = \frac{t_{12}t_{23}e^{i\frac{1}{2}\phi}}{1 + r_{12}r_{23}e^{i\phi}} \tag{2.3}$$

If the media 1 and 3 are both dielectric, the reflectance and transmittance are respectively:

$$R = rr^* = |r|^2 \tag{2.4}$$

$$T = \frac{n_3 \cos\theta_3}{n_1 \cos\theta_1}|t|^2 \tag{2.5}$$

Explicit expressions for Fresnel coefficients, reflectance and transmittance; are different for p and s polarization, but the general form is given by the equations (2.2), (2.3), (2.4) and (2.5) they are omitted here and programmed via Matlab.

If the layer between the semi-infinite media n_1 and n_3 is dielectric then $R + T = 1$, instead of this, if the slab is a conducting medium, $R + T + A = 1$, where A is the **absorptance** in the inner layer and is a measure of the energy absorbed by the conductor (via Joule effect).

Based on the Airy's formulas for Fresnel coefficients, using the equations (2.4), (2.5) and the fact that $R + T + A = 1$, a program was designed to find the optical functions (R, T and A) as functions of the angle of incidence θ_1. The figure 2.3 shows the reflectance, transmittance and absorptance for a monochromatic wave of $\lambda = 633nm$ that travels from BK7 ($n_1 = 1.51$) to gold ($n_2 = 0.1834 + i3.4332$), and goes out by air ($n_3 = 1$) [1] for p-polarization, the gold has a thickness of $d = 47nm$. This is a classic monolayer geometry called *Kretschmann-Raether* and is useful to show unusual absorptions in the inner layer (gold), these unusual absorptions are produced by the presence of surface plasmons at a specific angle called *plasmon angle* θ_p, for this geometry $\theta_P = 43.84°$. An introduction to optical excitation of surface plasmons can be found in Sambles and colaborators(Sambles, Bradbery, and Yang, 1991).

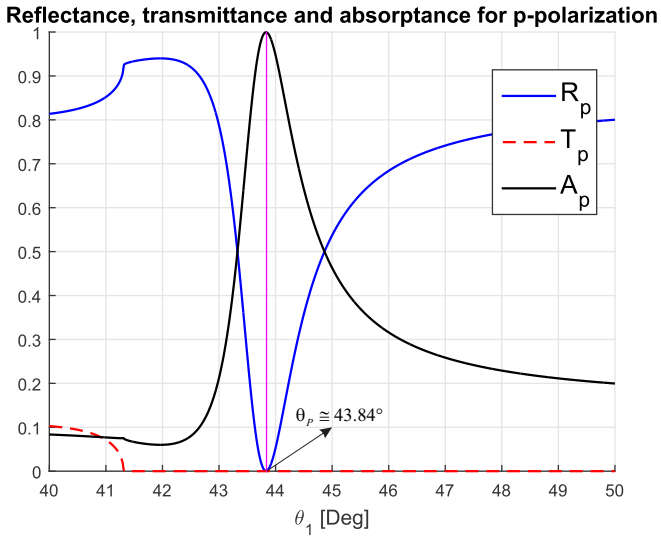

FIGURE 2.3: Reflectance, transmittance and absoprtance with p-polarization for the monolayer BK7||Au||Air and $d_{Au} = 47nm$ for $\lambda = 633nm$, the plasmon angle is on $\theta_p = 43.84°$

[1] All data of refraction indexes were taken from: **https://refractiveindex.info/**

2.1.2 Electric Field in the slab for three media

The unusual absorption in the Kretschmann-Raether geometry on the figure 2.3 is due to the matching of free electrons in the metal (Au) with the incident wave, they will oscillate at the same frequency creating a surface plasmon polariton (SPP). Since, the gold thickness is only $47nm$, to create a laboratory design in order to find an experimental measure of the electric field or magnetic field along the structure is impossible. Then, a simulation along the thickness of gold of the electric field $E(z)$ is relevant (a similar function for magnetic field can be found via Ampere's law). Expressions for both polarizations will be shown. Though, p-polarization is the mode in which the surface plasmons are excited and could be appreciate an enhancement of the electric field.

An easy way to deduce the electric field is defining it for s-polarization, based on the figure 1.5, the electric field along y-component (outside the page) moving towards z direction is given by the equation (2.6):

$$E_y(z) = \begin{cases} A_s e^{ik_{1z}z} + B_s e^{-ik_{1z}z} & if \quad z \leq 0 \\ C_s e^{ik_{2z}z} + D_s e^{-ik_{2z}z} & if \quad 0 < z \leq d \\ F_s e^{ik_{3z}(z-d)} & if \quad z > d \end{cases} \tag{2.6}$$

Where $k_{iz} = (\frac{\omega}{c})n_i \cos\theta_i$, $i = 1, 2, 3$. The complex constants A_s, B_s, C_s, D_s, F_s are the amplitudes of the electric field reflected and transmitted in the materials: n_1, n_2, n_3. If $A_s = 1$ or a known amplitude defined by the source, then: $B_s = r_s$ and $F_s = t_s$ (i. e. the Fresnel coefficients for reflection and transmission). Knowing the materials (its refraction indexes), the thickness of the inner layer and the wavelength of the source the goal is to find the constants C_s and D_s, these will give the behaviour of the field along the slab ($0 < z \leq d$).

The boundary condition in equation (1.6) states that the parallel component of the electric field must be continuous at the interfaces on $z = 0$ and $z = d$, then from equation (2.6):

$$\begin{aligned} 1 + r_s &= C_s + D_s \\ C_s e^{ik_{2z}d} + D_s e^{-ik_{2z}d} &= t_s \end{aligned}$$

Solving for C_s and D_s:

$$\begin{aligned} C_s &= \frac{t_s e^{ik_{2z}d} - (1 + r_s)}{e^{2ik_{2z}d} - 1} \\ D_s &= 1 + r_s - \frac{t_s e^{ik_{2z}d} - (1 + r_s)}{e^{2ik_{2z}d} - 1} \end{aligned}$$

The behaviour of the module of electric field for s-polarization in the Kretschmann-Raether geometry in the slab is shown on the figure 2.4 for two different incident angles $\theta_1 = 40°$ and plasmon angle $\theta_1 = 43.84°$. The z-axis is the thickness of gold.

The electric field has a different behaviour for both polarizations. For p-polarization, the figure 1.2 can be used. Decomposing the electric field vector in a tangent (x-axis) and normal (z-axis) vectors as

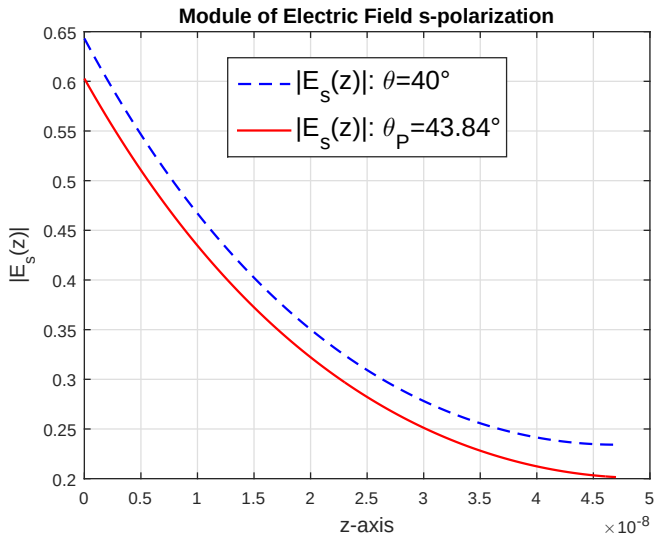

FIGURE 2.4: Module of the electric field for s-polarization in the gold layer ($d = 47nm$) for Kretschmann-Raether geometry.

can be seen in the appendix A.1 due to the continuity of the tangential electric field when is parallel to the discontinuity, the electric field on x-axis will be:

$$\mathbf{E}_x(z) = \begin{cases} (A_p e^{ik_{1z}z} + B_p e^{-ik_{1z}z})\cos\theta_1 & if \quad z \leq 0 \\ (C_p e^{ik_{2z}z} + D_p e^{-ik_{2z}z})\cos\theta_2 & if \quad 0 < z \leq d \\ (F_p e^{ik_{3z}(z-d)})\cos\theta_3 & if \quad z > d \end{cases} \tag{2.7}$$

We consider again that $A_p = 1$ or a known amplitude defined by the source, $r_p = \frac{B_p}{A_p}, t_p = \frac{F_p}{A_p}$ the Fresnel coefficients for p-polarization. Using the boundary condition (1.6) of the tangential electric field for $z = 0$ and $z = d$ and using the equation (2.7), are found the equations:

$$\begin{aligned} (1 + r_p)\cos\theta_1 &= (C_p + D_p)\cos\theta_2 \\ (C_p e^{ik_{2z}d} + D_p e^{-ik_{2z}d})\cos\theta_2 &= t_p \cos\theta_3 \end{aligned}$$

Solving for C_p and D_p:

$$\begin{aligned} C_p &= \frac{\alpha_{12}\alpha_{23}t_p e^{ik_{2z}d} - (1 + r_p)}{\alpha_{12}(e^{2ik_{2z}d} - 1)} \\ D_p &= \frac{1 + r_p}{\alpha_{12}} - \frac{\alpha_{12}\alpha_{23}t_p e^{ik_{2z}d} - (1 + r_p)}{\alpha_{12}(e^{2ik_{2z}d} - 1)} \end{aligned}$$

Where $\alpha_{12} = \frac{\cos\theta_2}{\cos\theta_1}$ and $\alpha_{23} = \frac{\cos\theta_3}{\cos\theta_2}$, using the Snell's law the equations can be written in terms only of the incident angle θ_1. The behaviour of the electric field for p-polarization is shown in the figure 2.5 for

the same two angles, $\theta_1 = 40°$ and plasmon angle, $\theta_1 = 43.84°$, for the Kretschmann-Raether monolayer structure.

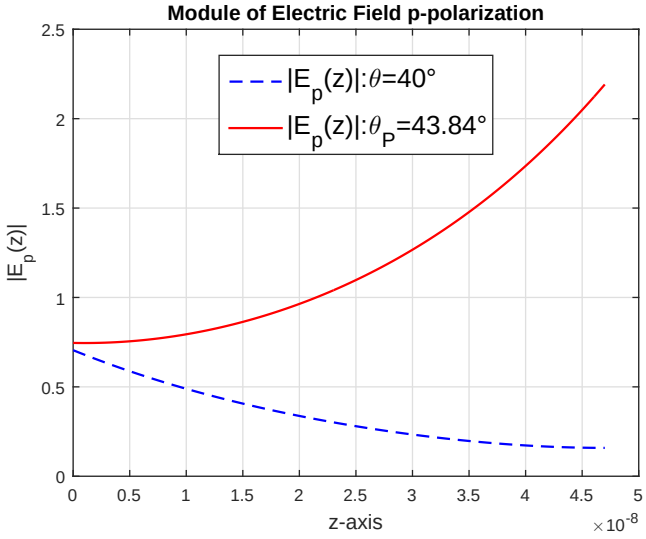

FIGURE 2.5: Module of the electric field for p-polarization in a gold layer ($d = 47nm$) for Kretschmann-Raether geometry at $\lambda = 633nm$.

In the plasmon angle for p-polarization (red continuous curve), there is an enhance of the amplitude of the electric field three times the initial amplitude, due to the unusual absorption that produce oscillating plasma at the interface Au || Air.

In the deduction of the module of electric field for p-polarization was considered the tangential component of the electric field. However, using the boundary condition for normal electric field, equation (1.5), assuming no superficial charges, it is possible to find equivalent expressions for C_p and D_p. The computational simulations give exactly the same values for these constants and the same behaviour for the module of electric field (see Appendix A).

2.2 Incident Light for N isotropic media. 2×2 transfer matrix method

In this section the 2×2 transfer matrix method introduced by Yeh (Yeh, 2005) is shown, in order to determinate the Fresnel coefficients, the reflectance and transmittance for isotropic multilayer thin films.

2.2.1 Matrix method for two isotropic media

Recalling the figure for p-polarization (1.2), and including the fields E_2' and B_2', the equations (1.11) and (1.12), can be written as:

$$\begin{aligned}(E_{1p}+E_{1p}')\cos\theta_1 &= (E_{2p}+E_{2p}')\cos\theta_2\\ \sqrt{\frac{\varepsilon_1}{\mu_1}}(E_{1p}'-E_{1p}) &= \sqrt{\frac{\varepsilon_2}{\mu_2}}(E_2-E_{2p}')\end{aligned}$$

In a matrix form the previous equations can be written as:

$$\begin{bmatrix}\cos\theta_1 & \cos\theta_1\\ \sqrt{\frac{\varepsilon_1}{\mu_1}} & -\sqrt{\frac{\varepsilon_1}{\mu_1}}\end{bmatrix}\begin{bmatrix}E_{1p}\\ E_{1p}'\end{bmatrix}=\begin{bmatrix}\cos\theta_2 & \cos\theta_2\\ \sqrt{\frac{\varepsilon_2}{\mu_2}} & -\sqrt{\frac{\varepsilon_2}{\mu_2}}\end{bmatrix}\begin{bmatrix}E_{2p}\\ E_{2p}'\end{bmatrix}$$

Or:

$$D_p(1)\begin{bmatrix}E_{1p}\\ E_{1p}'\end{bmatrix}=D_p(2)\begin{bmatrix}E_{2p}\\ E_{2p}'\end{bmatrix}$$

Where, ε_1,μ_1 are the permittivity and permeability of the medium 1 and ε_2,μ_2 are the permittivity and permeability of the medium 2. Also, the matrices $D_p(1)$ and $D_p(2)$ can be written, for any layer as:

$$D_p(i)=\begin{bmatrix}\cos\theta_i & \cos\theta_i\\ \sqrt{\frac{\varepsilon_i}{\mu_i}} & -\sqrt{\frac{\varepsilon_i}{\mu_i}}\end{bmatrix} \tag{2.8}$$

The matrix (2.8) is called *dynamical matrix* for p-polarization in the i-th medium. For non-magnetic media equation (2.8) can be presented in terms of the refraction indexes as:

$$D_p(i)=\begin{bmatrix}\cos\theta_i & \cos\theta_i\\ n_i & -n_i\end{bmatrix} \tag{2.9}$$

In a similar way, based on the figure 1.5 for s-polarization, the equations (1.23) and (1.24), can be written as:

$$\begin{aligned}(-B_{1s}+B_{1s}')\cos\theta_1 &= (-B_{2s}+B_{2s}')\cos\theta_2\\ E_{1s}+E_{1s}' &= E_{2s}+E_{2s}'\end{aligned}$$

In terms of the electric field:

$$\begin{aligned}\sqrt{\frac{\varepsilon_1}{\mu_1}}(E_{1s}-E'_{1s})\cos\theta_1 &= \sqrt{\frac{\varepsilon_2}{\mu_2}}(E_{2s}-E'_{2s})\cos\theta_2\\ E_{1s}+E'_{1s} &= E_{2s}+E'_{2s}\end{aligned}$$

Written as a matrix equation:

$$D_s(1)\begin{bmatrix}E_{1s}\\E'_{1s}\end{bmatrix} = D_s(2)\begin{bmatrix}E_{2s}\\E'_{2s}\end{bmatrix},$$

where the matrices $D_s(1)$ and $D_s(2)$ are given by the general expression:

$$D_s(i) = \begin{bmatrix}1 & 1\\ \sqrt{\frac{\varepsilon_i}{\mu_i}}\cos\theta_i & -\sqrt{\frac{\varepsilon_i}{\mu_i}}\cos\theta_i\end{bmatrix}, \tag{2.10}$$

Assuming non magnetic media:

$$D_s(i) = \begin{bmatrix}1 & 1\\ n_i\cos\theta_i & -n_i\cos\theta_i\end{bmatrix} \tag{2.11}$$

The matrix (2.11) is called *dynamical matrix* for s-polarization in the i-th medium.

Independent of the polarization, for two media, the amplitudes of the medium 1, can be expressed in terms of the dynamical matrices and by the amplitudes of the medium 2, reversing the matrix $D_s(1)$ or $D_p(1)$, and multiplying at left:

$$\begin{bmatrix}E_1\\E'_1\end{bmatrix} = D_1^{-1}D_2\begin{bmatrix}E_2\\E'_2\end{bmatrix}. \tag{2.12}$$

Futhermore, considering the electric field as an incident and reflected wave in each medium it could be written as: $E(z) = Ae^{ik_{iz}z} + Be^{-ik_{iz}z}$ or, in a reduced way $E(z) = A(z) + B(z)$. Being $A(z)$ the incident wave and $B(z)$ the reflected wave. The equation (2.12) can be written as:

$$\begin{bmatrix}A_1\\B_1\end{bmatrix} = D_1^{-1}D_2\begin{bmatrix}A'_2\\B'_2\end{bmatrix}. \tag{2.13}$$

2.2.2 Matrix method for three isotropic media

The figure 2.6 shows a simplified form of a monochromatic incident wave for three media. The reflected and transmitted waves has been written in terms of the electric field as previously mentioned.

The relation between A'_2, A_2, and B'_2, B_2, based on the figure 2.2, are given by: $A_2 = A'_2e^{i\frac{\phi}{2}}$, $B'_2 = B_2e^{i\frac{\phi}{2}}$, where ϕ is given by the equation (2.1), solving for A'_2 and B'_2:

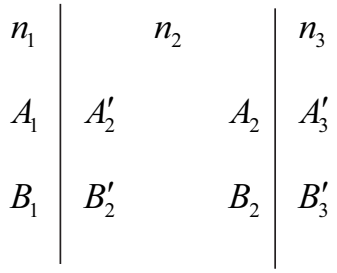

FIGURE 2.6: Amplitudes of electric field on three layer media

$$A_2' = e^{-i\frac{\phi}{2}} A_2 \tag{2.14}$$
$$B_2' = e^{i\frac{\phi}{2}} B_2 \tag{2.15}$$

In matrix form:

$$\begin{bmatrix} A_2' \\ B_2' \end{bmatrix} = \begin{bmatrix} e^{-i\frac{\phi}{2}} & 0 \\ 0 & e^{i\frac{\phi}{2}} \end{bmatrix} \begin{bmatrix} A_2 \\ B_2 \end{bmatrix} = P_2 \begin{bmatrix} A_2 \\ B_2 \end{bmatrix},$$

where:

$$P_2 = \begin{bmatrix} e^{-i\frac{\phi}{2}} & 0 \\ 0 & e^{i\frac{\phi}{2}} \end{bmatrix} \tag{2.16}$$

The matrix P_2 is called *propagation matrix* for the medium 2. Using equations (2.13) and (2.16), then:

$$\begin{bmatrix} A_1 \\ B_1 \end{bmatrix} = D_1^{-1} D_2 P_2 \begin{bmatrix} A_2 \\ B_2 \end{bmatrix}$$

As well as the equation (2.13), gives an expression for the fields in both sides of the two first layers, in a same way for the second and third layer:

$$\begin{bmatrix} A_2 \\ B_2 \end{bmatrix} = D_2^{-1} D_3 \begin{bmatrix} A_3' \\ B_3' \end{bmatrix}$$

Thus, the amplitude of the incident and reflected field on the media 1 and 3 are related through the dynamical and propagation matrices by the expression:

$$\begin{bmatrix} A_1 \\ B_1 \end{bmatrix} = D_1^{-1} \left(D_2 P_2 D_2^{-1} \right) D_3 \begin{bmatrix} A_3' \\ B_3' \end{bmatrix} \tag{2.17}$$

2.2.3 Matrix method for N-isotropic media

In order to find an expression that allows us to determinate the Fresnel coefficients, based on the amplitudes of the electric field for the monochromatic waves, the matrix method can be generalized doing the analysis previously made for N layers as is represented by the figure 2.7. The matrix product becomes repeatedly with the factors $D_i P_i D_i^{-1}$. So, a general expression that relate the amplitudes of the incident medium A_0, B_0 with the amplitudes A'_{N+1}, B'_{N+1} of the medium $N+1$ called substrate, has the shape:

$$\begin{bmatrix} A_0 \\ B_0 \end{bmatrix} = D_0^{-1} \left(\prod_{i=1}^{N} D_i P_i D_i^{-1} \right) D_{N+1} \begin{bmatrix} A'_{N+1} \\ B'_{N+1} \end{bmatrix} \tag{2.18}$$

Since, dynamic and propagation matrices has dimension 2×2. The resulting matrix product $D_0^{-1} \left(\prod_{i=1}^{N} D_i P_i D_i^{-1} \right) D_{N+1}$ will give a 2×2 matrix, so in a compactness way:

$$\begin{bmatrix} A_0 \\ B_0 \end{bmatrix} = \begin{bmatrix} M_{11} & M_{12} \\ M_{21} & M_{22} \end{bmatrix} \begin{bmatrix} A'_{N+1} \\ B'_{N+1} \end{bmatrix} \tag{2.19}$$

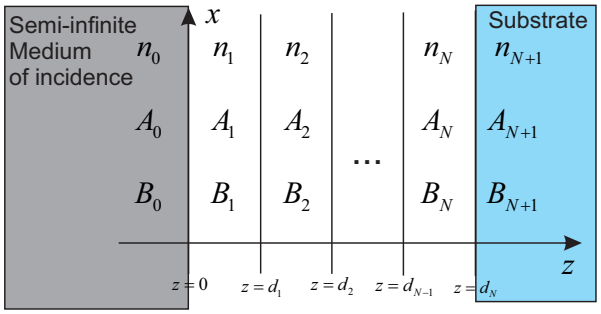

FIGURE 2.7: Amplitudes of electric field on N layered media. The incidence medium is at the left while the substrate is at the right.

2.2.4 Reflectance and transmittance for N layered media

If a monochromatic wave travels from the semi-infinite medium (n_0), and pass through the N layers, the 2×2 matrix method gives the Fresnel coefficients via:

$$r = \left(\frac{B_0}{A_0} \right)_{B'_{N+1}=0} \tag{2.20}$$

$$t = \left(\frac{A'_{N+1}}{A_0} \right)_{B'_{N+1}=0} \tag{2.21}$$

The subscript $B'_{N+1} = 0$ is refereed to the fact that there is no incident wave from the medium $N + 1$ (substrate). In terms of the components of the matrix:

$$r = \frac{M_{21}}{M_{11}} \tag{2.22}$$

$$t = \frac{1}{M_{11}} \tag{2.23}$$

If the semi-infinite media with refraction indexes n_0 and n_{N+1} are dielectric, the reflectance and transmittance are:

$$R = \left|\frac{M_{21}}{M_{11}}\right|^2 \tag{2.24}$$

$$T = \frac{n_{N+1}\cos\theta_{N+1}}{n_0\cos\theta_0}\left|\frac{1}{M_{11}}\right|^2 \tag{2.25}$$

If one of the inner materials have complex refractive index the wave is attenuated via Joule heating and the dissipated energy is described in terms of the absorptance as: $A = 1 - R - T$.

2.2.5 Electric Field in N layered media

For a multilayer thin film structure, the behaviour of the electric field between the layers determine unusual absorptions in presence of an incident electromagnetic waves. Experimentally is impossible to carry out a measure of the electric field module in each layer of a material, therefore a simulation is relevant in order to find in which layer(s) there are optical excitations of the Surface Polariton Plasmons (SPP) and consequently an enhancement of electric field. For s-polarization wave travelling in a multilayer media, the electric field has the general form:

$$\mathbf{E}_y(z) = \begin{cases} A_0 e^{ik_{0z}z} + B_0 e^{-ik_{0z}z} & if \quad z < 0 \\ A_1 e^{ik_{1z}z} + B_1 e^{-ik_{1z}z} & if \quad 0 < z < d_1 \\ A_2 e^{ik_{2z}(z-d_1)} + B_2 e^{-ik_{2z}(z-d_1)} & if \quad d_1 < z < d_2 \\ \vdots & \\ A_N e^{ik_{Nz}(z-d_{N-1})} + B_N e^{-ik_{Nz}(z-d_{N-1})} & if \quad d_{N-1} < z < d_N \\ A_{N+1} e^{ik_{(N+1)z}(z-d_N)} + B_{N+1} e^{-ik_{(N+1)z}(z-d_N)} & if \quad d_N < z \end{cases}$$

Where A_0 is the amplitude of the incident wave, B_0 is the amplitude of the reflected wave. Also, $k_{iz} = \frac{\omega}{c} n_i \cos\theta_i$, ω is the angular frequency ($\omega = 2\pi f$), c is the velocity of light in the vacuum, n_i is the refraction index at the i-th layer and θ_i is the incident angle at the i-th layer.

If only two materials are present the amplitudes of the field can be obtained via dynamical matrices:

$$\begin{bmatrix} A_0 \\ B_0 \end{bmatrix} = D_0^{-1} D_1 \begin{bmatrix} A_1' \\ B_1' \end{bmatrix} \tag{2.26}$$

The value of A_0 is the amplitude of the incident field and $B_1' = 0$, which generates a couple of equations with two variables B_0 and A_1', that will be the Fresnel coefficients for reflection and transmission (knowing the amplitudes $B_0 = r$ and $A_1' = t$).

The interest of the electric field becomes important when three materials are involved. Thus the module of the electric field on the middle layer can be calculated if the values of A_1' and B_1' are known.

The calculus of B_0 and A'_2 are useful for the Fresnel coefficients, the reflectance, transmittance and absorptance. Using the matrix approach it is known that:

$$\begin{bmatrix} A'_1 \\ B'_1 \end{bmatrix} = P_1 D_1^{-1} D_2 \begin{bmatrix} A'_2 \\ B'_2 \end{bmatrix} \tag{2.27}$$

For matrices in the equations (2.26) and (2.27) there are four unknown quantities (B_0, A'_1, B'_1 and A'_2) in a system of four equation. As well as, for two materials the quantity A_0 is known and $B'_2 = 0$. The values of the matrices depend on the structure of the materials, the optical constants and the angle of incidence. Analytical expressions for B_0, A'_1, B'_1 and A'_2 are neglected, instead of this, a program was created in Matlab.

In presence of four materials two layers are involved, and there are six equations with six unknown quantities, in general for $N+2$ materials with N layers will be $2(N+1)$ equations with $2(N+1)$ unknown quantities, given by the set of matrices (2.28) - (2.31):

$$\begin{bmatrix} A_0 \\ B_0 \end{bmatrix} = D_0^{-1} D_1 \begin{bmatrix} A'_1 \\ B'_1 \end{bmatrix} \tag{2.28}$$

$$\begin{bmatrix} A'_1 \\ B'_1 \end{bmatrix} = P_1 D_1^{-1} D_2 \begin{bmatrix} A'_2 \\ B'_2 \end{bmatrix} \tag{2.29}$$

$$\begin{bmatrix} A'_2 \\ B'_2 \end{bmatrix} = P_2 D_2^{-1} D_3 \begin{bmatrix} A'_3 \\ B'_3 \end{bmatrix} \tag{2.30}$$

$$\vdots$$

$$\begin{bmatrix} A'_N \\ B'_N \end{bmatrix} = P_N D_N^{-1} D_N \begin{bmatrix} A'_{N+1} \\ B'_{N+1} \end{bmatrix}. \tag{2.31}$$

As previously mentioned, the amplitude of the incident field A_0 is known and $B'_{N+1} = 0$, assuming that there is no an electrical wave coming from the substrate.

To know the amplitudes of the electric field, the assumption here is that: $A_0 = 1$, $B_{N+1} = 0$. Moreover, the components of the matrix $M = D_0^{-1}\left(\prod_{i=1}^{N} D_i P_i D_i^{-1}\right) D_{N+1}$ could be found only knowing the parameters of the materials and the incident angle of the wave, both for p and s-polarization. Using the equation (2.22), the value of B_0 can be found from:

$$r = \frac{B_0}{A_0} = \frac{M_{21}}{M_{11}} \rightarrow B_0 = A_0 \frac{M_{21}}{M_{11}}$$

Knowing the values of A_0 and B_0, the values of A'_1 and B'_1 are determined, using equation (2.28), likewise, A'_2 and B'_2 can be found from (2.29), and so on, the A'_i and B'_i quantities can be calculated recurrently through simulations, getting a function of the electric field module through the inner layers versus the thickness. For the i-th specific layer either p or s-polarization the expression (2.32) is helpful to calculate the module of electric field:

$$|\mathbf{E}(z)| = \left|A_i e^{ik_{iz}(z-d_i)} + B_i e^{-ik_{iz}(z-d_i)}\right| \quad if \quad d_i < z < d_{i+1} \tag{2.32}$$

A trilayer geometry was simulated for the geometry BK7||Au||SiO_2 ||Au||Air. For a wavelength $\lambda = 633nm$, the refraction index are: $n_1 = 1.51$, $n_2 = 0.1834 + i3.4332$, $n_3 = 1.4570$, $n_4 = 0.1834 + 3.4334i$, $n_5 = 1$, the inner layer thickness $d_1 = 40nm$, $d_2 = 50nm$, $d_3 = 5nm$. The functions for reflectance,

transmittance and absorptance as function of the angle of incidence are shown in the figure 2.8 for p polarization, there is a plasmon angle on $\theta_p = 50.3°$. The reflectance search its maximum value on $\theta = 44.1°$ (total internal reflection). The module of electric field for p and s modes are in the figure 2.9. The red vertical lines in the electric field module functions determine the change of materials of the inner layers.

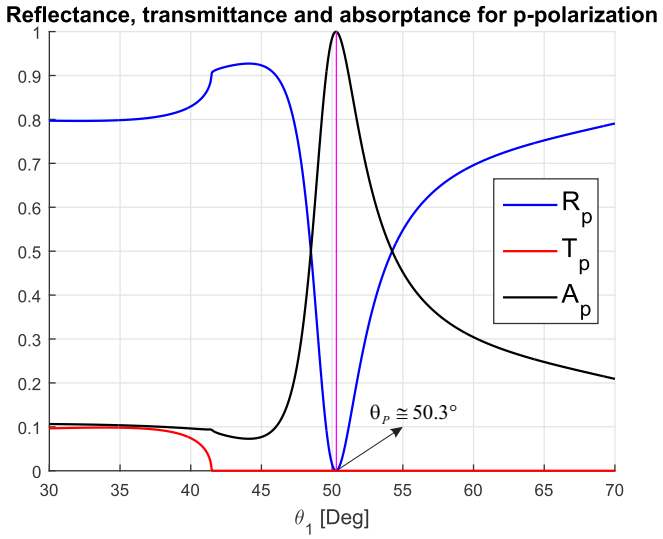

FIGURE 2.8: Optical functions for p-polarization for the geometry BK7||Au(40)||SiO_2(50) ||Au (5)||Air for $\lambda = 633nm$

The discontinuity of the module of electric field on p-polarization is related to the boundary condition (1.5). The module of electric field in s-polarization represented the continuity in the boundary condition (1.6). Both graphics are simulated in the plasmon angle ($\theta_P = 50.3°$), and for the inner layers (Au (40)|| SiO_2(50)||Au (5)) the values between brackets are the thickness in nanometers of each layer.

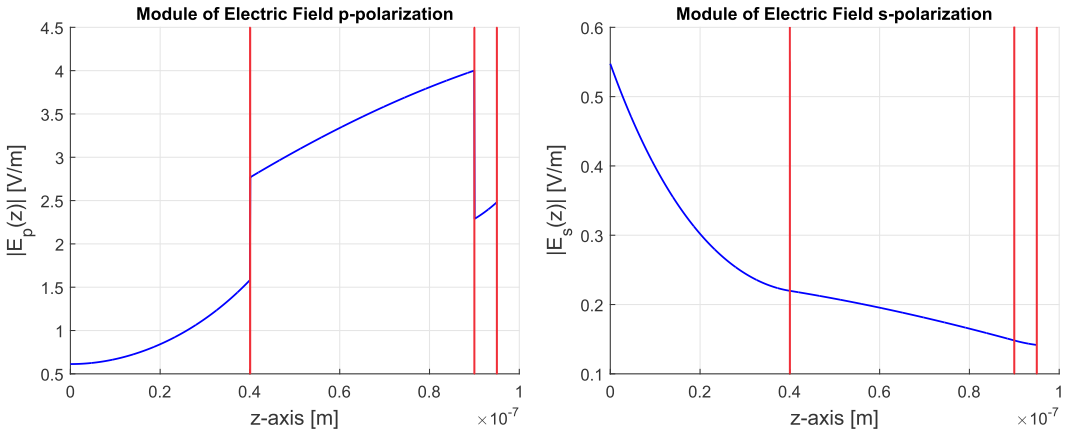

FIGURE 2.9: Electric field modulus for s and p-polarization in the inner layers of the geometry BK7||Au(40)||SiO_2(50) ||Au (5)||Air for plasmon angle $\theta_p = 50.3°$.

Two more electric fields were calculated for two angles of incidence $\theta_1 = 20°$ (Figure 2.10) and $\theta_2 = 0°$ (Figure 2.11). When there is an angle of incidence of $\theta_2 = 0°$ the electric field for polarizations s and p are the same due to both are parallel to the materials interface.

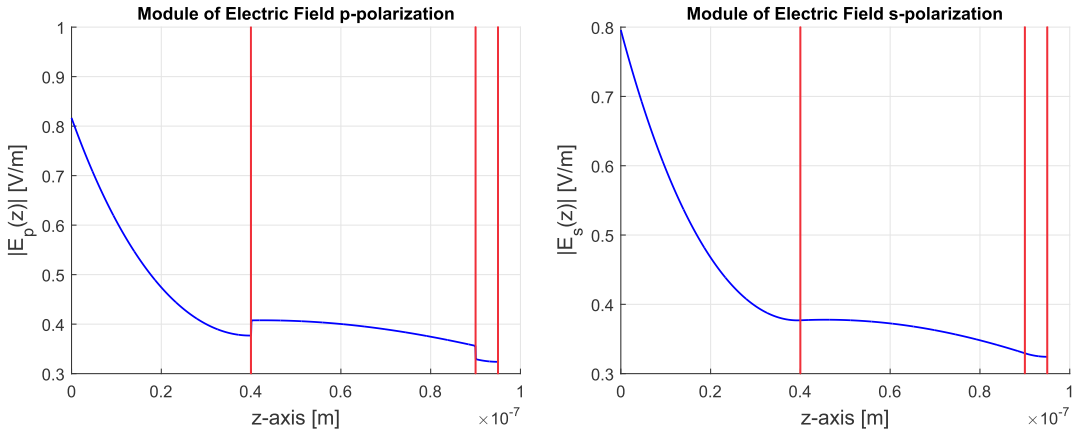

FIGURE 2.10: Electric field modulus for s and p-polarization in the inner layers of the geometry SiO||Au (40)|| BK7 (50)||Au (5)||Air for an angle of $\theta = 20°$.

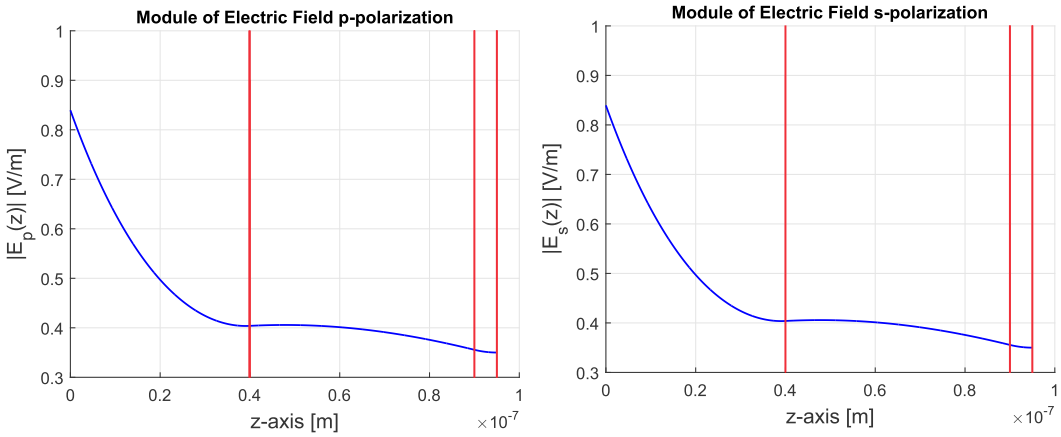

FIGURE 2.11: Electric field modulus for s and p-polarization in the inner layers of the geometry SiO||Au (40)|| BK7 (50)||Au (5)||Air for normal incidence $\theta = 0°$.

2.3 Flux diagram for optical functions isotropic media

In the figure 2.12 is shown the flux diagram followed to find the Fresnel coefficients and optical functions with angular dependence for any number isotropic media.

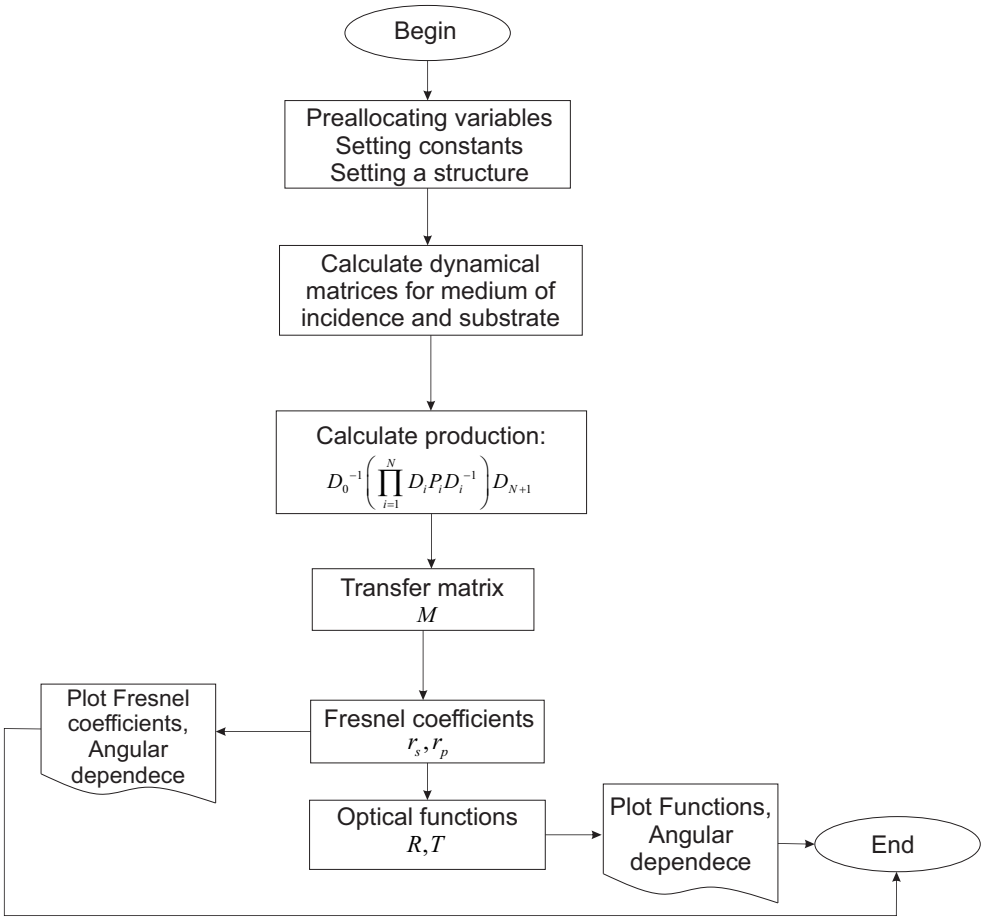

FIGURE 2.12: Flux diagram Fresnel coefficients and optical functions for a multilayer of isotropic media

2.4 Flux diagram for module of electric field - isotropic media

In the figure 2.13 is shown the flux diagram followed to find the module of electric field depending on the transversal coordinate of the structure.

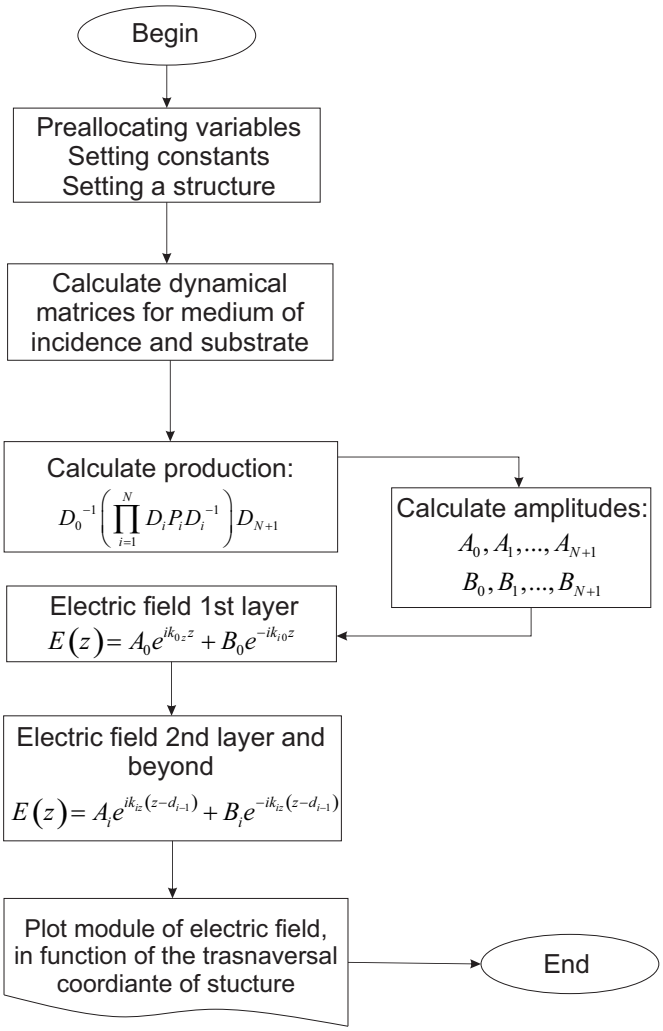

FIGURE 2.13: Flux diagram of module of electric field for a multilayer of isotropic materials

Chapter 3

Optics anisotropic multilayer thin films

3.1 Introduction

This chapter is about the optics of multilayer anisotropic thin films. The permittivity of the media now has the form of dielectric tensor of rank 2. Initially the Yeh's 4×4 matrix formulation is studied, and then the immersion model proposed by Cojocaru is used to simulate multilayer thin films for Fresnel coefficients and optical functions. Generalized Abelés relations emerge in the limit of isotropy. In addition, module of electric field is derived from immersion model. The results found are contrasted to those calculated in isotropic media and to those reported in the literature. Finally, scattering matrix approach is considered in the treatment of anisotropic multilayer thin film, improving numerical calculations finding the Transversal Magneto-Optic Kerr Effect (TMOKE).

3.2 Generalities of anisotropic media

In presence of anisotropic media there are several methods to find Fresnel coefficients and consequently optical functions. Yeh, for example (Yeh, 1980) uses the 4×4 transfer matrix method, Mansuripur (Mansuripur, 1990), on the other hand, uses 2×2 matrices as well as Cojocaru (Cojocaru, 2000) using the immersion model, in which each anisotropic layer is embedded between two isotropic layers of thickness zero. The scattering matrix method developed initially by Ko and Sambles (Ko and Sambles, 1988) is used to treat numerical overflow in electrical field calculations and thick layers above $1mm$. This method was taken by Caballero et. al. (Caballero, García-Martín, and Cuevas, 2012) presenting a generalization of the propagation of electromagnetic waves with nanostructured magneto-optical systems.

The propagation of monochromatic waves in anisotropic media has several changes in contrast to isotropic media. First, the modes p and s are coupled, which means that a p incident wave will reflect and refract a combination of waves p and s and reversely. Second, there are two refracted waves with different phase velocities, phenomena known as birefringence. Therefore, the dielectric constant of isotropic media turns on a tensor of rank 2, represented by a 3×3 matrix. Other physical characteristics of propagation will be mentioned latter along with the development of the theory.

Theoretical description of anisotropic multilayer systems initiates recalling the equation that relates the displacement and electric field vector:

$$\mathbf{D} = \varepsilon\mathbf{E} \tag{3.1}$$

In the isotropic media ε was a constant real or complex[1]. For anisotropic media, at a definied frequency, this variable turns into a the dielectric tensor, which in non-magnetic and transparent media is symmetric and real. It is always possible to chose three mutually orthogonal axis such that the off-diagonal elements are zero and can be written in the form according to (Yeh, 1980; Landry and Maldonado, 1995):

$$\varepsilon = A \begin{bmatrix} \varepsilon_1 & 0 & 0 \\ 0 & \varepsilon_2 & 0 \\ 0 & 0 & \varepsilon_3 \end{bmatrix} A^{-1} = \begin{bmatrix} \varepsilon_{xx} & \varepsilon_{xy} & \varepsilon_{xz} \\ \varepsilon_{yx} & \varepsilon_{yy} & \varepsilon_{yz} \\ \varepsilon_{zx} & \varepsilon_{zy} & \varepsilon_{zz} \end{bmatrix} \tag{3.2}$$

The components of the diagonal are called principal dielectric constants, A is the rotation matrix which is orthogonal ($A^{-1} = A^T$) and has the form gave by Diebel (Diebel, 2006):

$$A = \begin{bmatrix} \cos\psi\cos\phi - \cos\theta\sin\phi\sin\psi & -\sin\psi\cos\phi - \cos\theta\sin\phi\cos\psi & \sin\theta\sin\phi \\ \cos\psi\sin\phi + \cos\theta\sin\phi\sin\psi & -\sin\psi\sin\phi + \cos\theta\cos\phi\cos\psi & -\sin\theta\cos\phi \\ \sin\theta\sin\psi & \sin\theta\cos\psi & \cos\theta \end{bmatrix} \tag{3.3}$$

The angles ϕ, θ and ψ are called Euler angles and depend on the direction of the coordinates axis on the laboratory relatives to the axis of the optical axis of the anisotropic medium.

Recalling the electric and magnetic field for isotropic media can be written as:

$$\mathbf{E} = \mathbf{E}_0 e^{i(\mathbf{k}\cdot\mathbf{r}-\omega t)} \tag{3.4}$$

$$\mathbf{H} = \mathbf{H}_0 e^{i(\mathbf{k}\cdot\mathbf{r}-\omega t)} \tag{3.5}$$

The wave vector can be written in the form $\mathbf{k} = \frac{\omega}{c} n\mathbf{s}$, where $\mathbf{s}$ is an unitary vector in the direction of propagation. Replacing the electric and magnetic fields in the Maxwell equations (1.3, 1.4), turns into:

$$\mathbf{k}\times\mathbf{E} = \omega\mu\mathbf{H} \tag{3.6}$$

$$\mathbf{k}\times\mathbf{H} = -\omega\varepsilon\mathbf{E} \tag{3.7}$$

Replacing (3.6) in (3.7):

$$\mathbf{k}\times(\mathbf{k}\times\mathbf{E}) + \omega^2\mu\varepsilon\mathbf{E} = 0 \tag{3.8}$$

The previous equation is known as *momentum space equation*. The matrix form of the equation (3.8) can be written as:

$$\begin{bmatrix} \omega^2\mu\varepsilon_{xx} - k_y^2 - k_z^2 & \omega^2\mu\varepsilon_{xy} + k_x k_y & \omega^2\mu\varepsilon_{xz} + k_x k_z \\ \omega^2\mu\varepsilon_{yx} + k_x k_y & \omega^2\mu\varepsilon_{yy} - k_x^2 - k_z^2 & \omega^2\mu\varepsilon_{yz} + k_y k_z \\ \omega^2\mu\varepsilon_{zx} + k_x k_z & \omega^2\mu\varepsilon_{zy} + k_y k_z & \omega^2\mu\varepsilon_{zz} - k_x^2 - k_y^2 \end{bmatrix} \begin{bmatrix} E_x \\ E_y \\ E_z \end{bmatrix} = \begin{bmatrix} 0 \\ 0 \\ 0 \end{bmatrix} \tag{3.9}$$

The non trivial plane wave solutions are found where the determinant of the left side matrix (system matrix) goes to zero. The determinant of the system equals to zero with the off-diagonal components of the dielectric tensor being zero, leads an equation that can be drawn in three-dimensional space with the axis k_x, k_y and k_z, the generated surface in the momentum space $\mathbf{k}$, is called **normal surface**, consisting

[1] In a more general terms for isotropic media ε is called a dielectrical function that depends on the angular frequency ω of the incident radiation.

in general of two shells with four common points, see figure 3.1. The two lines passing through opposite points are called *optical axis*, those will be the directions of isotropy.

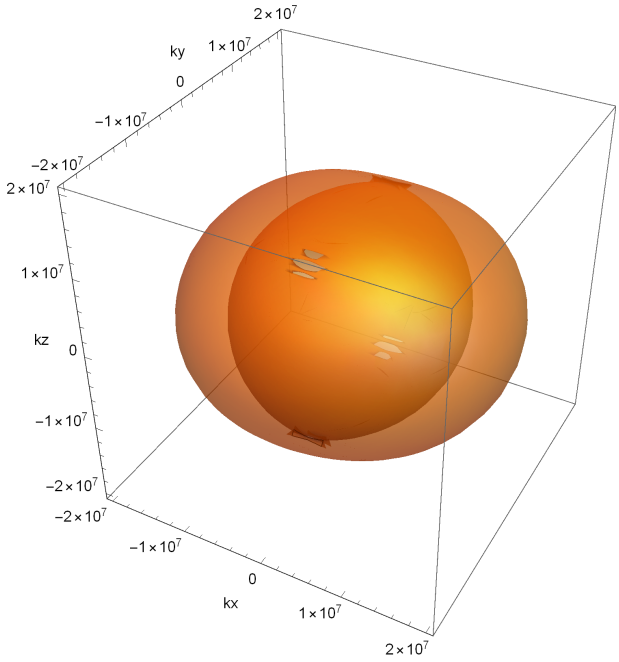

FIGURE 3.1: General form of the normal surface consisting of two spheroids with four common points. The line passing through of opposite points define optical axis.

The diagonal components of the dielectric tensor in equation (3.2) describe the optical anisotropy of the medium. Let $\varepsilon_{xx} = n_x^2$, $\varepsilon_{yy} = n_y^2$ and $\varepsilon_{zz} = n_z^2$. When n_x, n_y and n_z are different, there are two optical axis in the medium, the material is called *Biaxial*, the normal surface consists of one sphere intercepted by an ellipsoid having four common points, see figure 3.1, drawing a line between the two opposite intercepts gives the two optical axes. If two principal index are equal the medium is called *Uniaxial*, the sphere and the ellipsoid have now two common points, the optical axes will be z-axis, in this case $n_o^2 = \frac{\varepsilon_x}{\varepsilon_0} = \frac{\varepsilon_y}{\varepsilon_0}$ is called *ordinary index* and $n_e^2 = \frac{\varepsilon_z}{\varepsilon_0}$is the *extraordinary index*. The uniaxial anisotropic media could be positive (if $n_0 < n_e$) or negative (if $n_0 > n_e$), a bidimensional representation of the biaxial and uniaxial normal surface in the xz-plane is shown in the figure 3.2, the dotted red lines are the optical axis on biaxial media.

The displacement vector $\mathbf{D}$ in isotropic media is parallel to electric field vector $\mathbf{E}$, they are related by the electric constant ε; real or complex as seen in chapters 1 and 2. In presence of anisotropic media the relation between $\mathbf{D}$ and $\mathbf{E}$ is via dielectric tensor so, the mentioned vectors are not parallel anymore. Now $\mathbf{k}$ is orthogonal to $\mathbf{D}$ instead of $\mathbf{E}$, so $\mathbf{D}$, $\mathbf{E}$ and $\mathbf{k}$ are coplanar. The direction of the propagation is in the Poynting's direction vector $\mathbf{S} = c^2\epsilon_0\mathbf{E}\times\mathbf{B}$, that in general is different to $\mathbf{k}$. In the figure 3.3 there is an schematic representation of the considered vectors.

A monochromatic wave travelling through an isotropic medium that passes to an anisotropic one will be refracted in two waves. In total there will be four waves, two refracted and two reflected from the third medium. The schematic representation of a ray travelling from an incident isotropic medium to an anisotropic medium, is shown in the figure 3.4, the third medium (substrate) is isotropic too. The red horizontal dotted lines correspond to the tangential component of the wave that is the same for all media

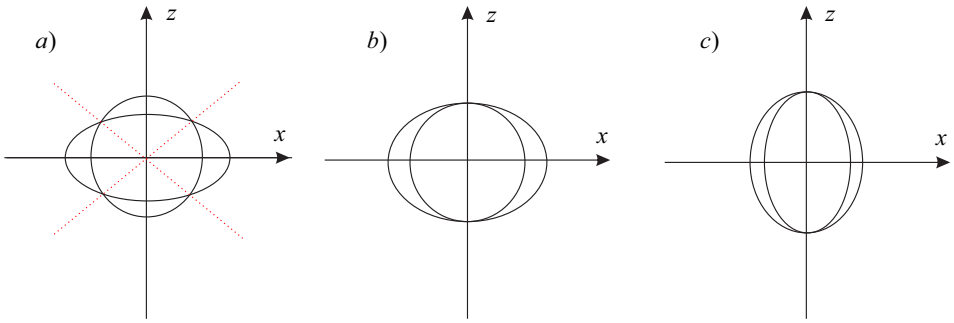

FIGURE 3.2: Schematic representation of the normal surface cuts. a) Biaxial material. Its refraction indexes are different $n_{xx} \neq n_{yy} \neq n_{zz}$, b) positive uniaxial materials $n_o < n_e$ and c) negative uniaxial materials. $n_o > n_e$. For uniaxial materials the optical axis is the z-axis.

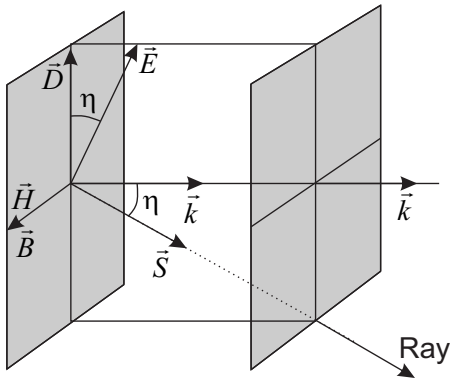

FIGURE 3.3: Schematic representation the vectors $\mathbf{E}, \mathbf{D}, \mathbf{H}, \mathbf{B}, \mathbf{k}$ and $\mathbf{S}$ in an anisotropic media.

due to boundary conditions (Snell's Law).

3.3 Yeh's 4×4 matrix formulation

In order to find the Fresnel coefficients and optical functions in anisotropic layers, initially the procedure used by Yeh (Yeh, 1980) is studied. Let $e^{i(\mathbf{k}\cdot\mathbf{r}-\omega t)} = e^{i(k_x x + k_y y + k_z z - \omega t)}$ the electric field, defining $k_x = \alpha$, $k_y = \beta$ and $k_z = \gamma$, then the electric field can be written in the form $e^{i(\alpha x + \beta y + \gamma z - \omega t)}$. Due to the media is considered homogeneous on xy-plane, α and β are constants and the γ component can be found from the determinant of the left side of the matrix equation (3.9). There are four (4) real or complex values of γ (or k_z) shown in the figure 3.4.

According to Yeh the electric field polarization of the partial waves has the form:

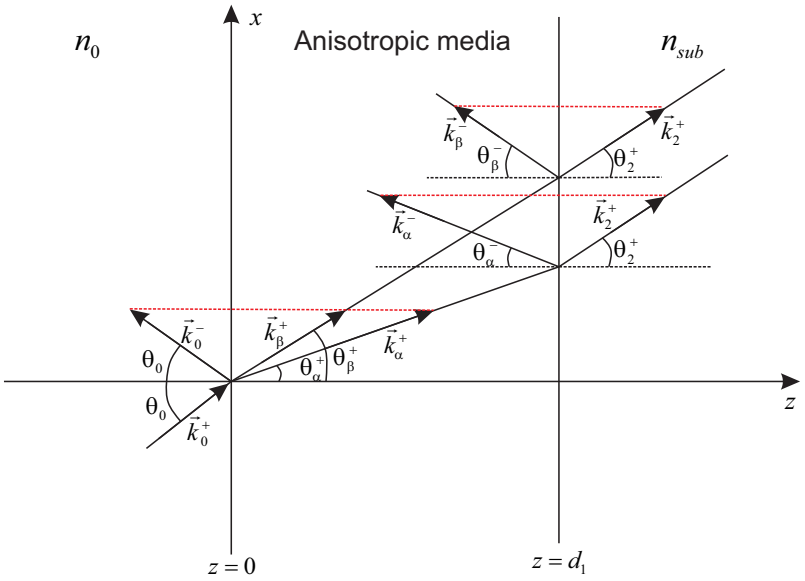

FIGURE 3.4: Propagation of monochromatic planar light wave into an anisotropic media. Two refracted waves travel back and forward in the anisotropic medium. n_0 and n_{sub} are the refraction index of the incident medium and refraction index of the substrate, respectively. The xz-plane is the plane of incidence of the wave.

$$\mathbf{p}_\sigma = N_\sigma \begin{bmatrix} (\omega^2\mu\varepsilon_{yy} - \alpha^2 - \gamma_\sigma^2)(\omega^2\mu\varepsilon_{zz} - \alpha^2 - \beta^2) - (\omega^2\mu\varepsilon_{yz} + \beta\gamma_\sigma)^2 \\ (\omega^2\mu\varepsilon_{yz} + \beta\gamma_\sigma)(\omega^2\mu\varepsilon_{zx} + \alpha\gamma_\sigma) - (\omega^2\mu\varepsilon_{xy} + \alpha\beta)(\omega^2\mu\varepsilon_{zz} - \alpha^2 - \beta^2) \\ (\omega^2\mu\varepsilon_{xy} + \alpha\beta)(\omega^2\mu\varepsilon_{yz} + \beta\gamma_\sigma) - (\omega^2\mu\varepsilon_{xz} + \alpha\gamma_\sigma)(\omega^2\mu\varepsilon_{yy} - \alpha^2 - \gamma_\sigma^2) \end{bmatrix} \tag{3.10}$$

The constant N_σ normalizes the vector $\mathbf{p}$ and $\sigma = 1, 2, 3, 4$.
Assuming non-magnetic media, the layered media have dielectric permitivitties given by the tensors:

$$\varepsilon = \begin{cases} \varepsilon(0) & if \quad z < 0 \\ \varepsilon(1) & if \quad z_0 < z < z_1 \\ \varepsilon(2) & if \quad z_1 < z < z_2 \\ \vdots & \\ \varepsilon(N) & if \quad z_{N-1} < z < z_N \\ \varepsilon(N+1) & if \quad z_N < z < z_{N+1} \end{cases}$$

The electric field in the n-th layer will be in the direction $\mathbf{p}_\sigma(n)$, and will have an amplitude for each layer given by $A_\sigma(n)$:

$$\mathbf{E} = \sum_{\sigma=1}^{4} A_\sigma(n)\mathbf{p}_\sigma(n)e^{i(\alpha x+\beta y+\gamma_\sigma(n)(z-z_n)-\omega t)} \tag{3.11}$$

As well as the electric field, the magnetic field is given by:

$$\mathbf{H} = \sum_{\sigma=1}^{4} A_\sigma(n)\mathbf{q}_\sigma(n)e^{i(\alpha x+\beta y+\gamma_\sigma(n)(z-z_n)-\omega t)},$$

where, due to the Maxwell equations (1.3) and (1.4):

$$\mathbf{q}_\sigma(n) = \frac{c}{\omega\mu}\mathbf{k}_\sigma(n) \times \mathbf{p}_\sigma(n)$$

and:

$$\mathbf{k}_\sigma(n) = \alpha\mathbf{x} + \beta\mathbf{y} + \gamma_\sigma(n)\mathbf{z},$$

Imposing the boundary conditions on of E_x, E_y, H_x and H_y at the interface $z = z_{n-1}$:

$$\begin{aligned}
\sum_{\sigma=1}^{4} A_\sigma(n-1)\mathbf{p}_\sigma(n-1)\cdot\mathbf{x} &= \sum_{\sigma=1}^{4} A_\sigma(n)\mathbf{p}_\sigma(n)\cdot\mathbf{x}e^{i\gamma_\sigma(n)t_n} \\
\sum_{\sigma=1}^{4} A_\sigma(n-1)\mathbf{p}_\sigma(n-1)\cdot\mathbf{y} &= \sum_{\sigma=1}^{4} A_\sigma(n)\mathbf{p}_\sigma(n)\cdot\mathbf{y}e^{i\gamma_\sigma(n)t_n} \\
\sum_{\sigma=1}^{4} A_\sigma(n-1)\mathbf{q}_\sigma(n-1)\cdot\mathbf{x} &= \sum_{\sigma=1}^{4} A_\sigma(n)\mathbf{q}_\sigma(n)\cdot\mathbf{x}e^{i\gamma_\sigma(n)t_n} \\
\sum_{\sigma=1}^{4} A_\sigma(n-1)\mathbf{q}_\sigma(n-1)\cdot\mathbf{y} &= \sum_{\sigma=1}^{4} A_\sigma(n)\mathbf{q}_\sigma(n)\cdot\mathbf{y}e^{i\gamma_\sigma(n)t_n},
\end{aligned}$$

where t_n is the thickness of the n-th layer. The four previous equations can be rewritten in matrix form:

$$\begin{bmatrix} A_1(n-1) \\ A_2(n-1) \\ A_3(n-1) \\ A_4(n-1) \end{bmatrix} = D^{-1}(n-1)D(n)P(n) \begin{bmatrix} A_1(n) \\ A_2(n) \\ A_3(n) \\ A_4(n) \end{bmatrix},$$

where

$$D(n) = \begin{bmatrix} \mathbf{x}\cdot\mathbf{p}_1(n) & \mathbf{x}\cdot\mathbf{p}_2(n) & \mathbf{x}\cdot\mathbf{p}_3(n) & \mathbf{x}\cdot\mathbf{p}_4(n) \\ \mathbf{y}\cdot\mathbf{q}_1(n) & \mathbf{y}\cdot\mathbf{q}_2(n) & \mathbf{y}\cdot\mathbf{q}_3(n) & \mathbf{y}\cdot\mathbf{q}_4(n) \\ \mathbf{y}\cdot\mathbf{p}_1(n) & \mathbf{y}\cdot\mathbf{p}_2(n) & \mathbf{y}\cdot\mathbf{p}_3(n) & \mathbf{y}\cdot\mathbf{p}_4(n) \\ \mathbf{x}\cdot\mathbf{q}_1(n) & \mathbf{x}\cdot\mathbf{q}_2(n) & \mathbf{x}\cdot\mathbf{q}_3(n) & \mathbf{x}\cdot\mathbf{q}_4(n) \end{bmatrix} \tag{3.12}$$

and

$$P(n) = \begin{bmatrix} e^{i\gamma_1(n)t_n} & 0 & 0 & 0 \\ 0 & e^{i\gamma_2(n)t_n} & 0 & 0 \\ 0 & 0 & e^{i\gamma_3(n)t_n} & 0 \\ 0 & 0 & 0 & e^{i\gamma_4(n)t_n} \end{bmatrix} \tag{3.13}$$

As well as isotropic media, the matrices $D(n)$ are called *Dynamical matrices* and $P(n)$ are the *Propagation matrices*. The transfer matrix is defined by: $T_{n-1} = D^{-1}(n-1)D(n)P(n)$. The amplitudes A_1 and A_3 (k_α^+, k_β^+) are travelling in the same direction from left to right while A_2 and A_4 (k_α^-, k_β^-) are the amplitudes of waves that travels from right to left. Assuming that there is no waves coming from the right side of the multilayer system, setting C_p for the amplitude of the transmitted wave p-polarized and C_s for the amplitude of the transmitted wave s-polarized, the matrix can be written as:

$$\begin{bmatrix} A_p \\ B_p \\ A_s \\ B_s \end{bmatrix} = \left(\prod_{n=1}^{N+1} T_{n-1,n} \right) \begin{bmatrix} C_p \\ 0 \\ C_s \\ 0 \end{bmatrix} \tag{3.14}$$

The thickness $t_{N+1} \equiv 0$. The subscripts s and p are the modes TE and TM respectively.

The matrix method presented is useful to describe the Fresnel coefficients for reflection and transmission for multilayer thin film anisotropic media. Due to mode coupling in the interfaces, there is eight complex amplitudes that can be expressed in terms of matrix elements. Having in mind that there is no waves incident from the right side of the multilayer ($D_p = D_s = 0$), then:

$$\begin{bmatrix} A_p \\ B_p \\ A_s \\ B_s \end{bmatrix} = \begin{bmatrix} M_{11} & M_{12} & M_{13} & M_{14} \\ M_{21} & M_{22} & M_{23} & M_{24} \\ M_{31} & M_{32} & M_{33} & M_{34} \\ M_{41} & M_{42} & M_{43} & M_{44} \end{bmatrix} \begin{bmatrix} C_p \\ 0 \\ C_s \\ 0 \end{bmatrix} \tag{3.15}$$

The Fresnel coefficients in terms of the transfer matrix are given by:

$$r_{ss} = \frac{M_{21}M_{33} - M_{23}M_{31}}{M_{11}M_{33} - M_{13}M_{31}} \tag{3.16}$$

$$r_{sp} = \frac{M_{41}M_{33} - M_{43}M_{31}}{M_{11}M_{33} - M_{13}M_{31}} \tag{3.17}$$

$$r_{ps} = \frac{M_{11}M_{23} - M_{21}M_{13}}{M_{11}M_{33} - M_{13}M_{31}} \tag{3.18}$$

$$r_{pp} = \frac{M_{11}M_{43} - M_{41}M_{13}}{M_{11}M_{33} - M_{13}M_{31}} \tag{3.19}$$

$$t_{ss} = \frac{M_{33}}{M_{11}M_{33} - M_{13}M_{31}} \tag{3.20}$$

$$t_{sp} = \frac{-M_{31}}{M_{11}M_{33} - M_{13}M_{31}} \tag{3.21}$$

$$t_{ps} = \frac{-M_{13}}{M_{11}M_{33} - M_{13}M_{31}} \tag{3.22}$$

$$t_{pp} = \frac{M_{11}}{M_{11}M_{33} - M_{13}M_{31}} \tag{3.23}$$

These eight complex amplitudes are spectrally correlated.

3.4 Considerations Yeh's method

Based on the described theory in the previous section, it is possible to find the functions for Fresnel coefficients depending on the angle of incidence. First of all, the Euler angles for each media must be known. Then, the refraction indexes of the dielectric tensor for each material. α (or k_x) and β (or k_y) components must be known as well as the constants c, ω and μ and finally the thickness of each inner layer. The angle of incidence is the independent variable. A program was designed in order to calculate the Fresnel coefficients following the next steps:

1. γ_σ's values from the moment equation are calculated.
2. Knowing the values of γ_σ's will find $\mathbf{p}_\sigma, N_\sigma, \mathbf{k}_\sigma, \mathbf{q}_\sigma$ ($\sigma = 1, 2, 3, 4$) for each θ_0.
3. The dynamic matrices are obtained for all layers, and propagation matrices are calculated for the inner layers.
4. The data collected allowed to find a product of the transfer matrices, and finally the components of the resultant matrix are found.
5. Fresnel coefficients are calculated through the equations (3.16-3.23).

Due to the structure of the matrix formulation 4×4, two special cases had to be considered:

- $\alpha \neq 0$ and $\beta \neq 0$
- The method does not work in the limits of isotropy.

Now we are going to demonstrate why this two cases could not be had in the Yeh's approach.

3.4.1 Must be satisfied: $\alpha \neq 0$ and $\beta \neq 0$

The **x** and **y** components of the incident wave (i.e. α and β) none can be zero. The two cases are analysed:

1. $\alpha = 0$. If α goes to zero, $\hat{\mathbf{y}}$ and $\hat{\mathbf{z}}$ components of the electric field vector are both zero, equation (3.10), consequently the second row in the dynamic matrix is zero ($\mathbf{p}_\sigma \cdot \hat{\mathbf{y}} = 0$). Hence the matrix is singular (has not inverse), so the transfer matrix could no be found.
2. $\beta = 0$. If the $\hat{\mathbf{y}}$ component of the incident wave vector ($\beta = k_y$) is null, $\hat{\mathbf{y}}$ component of the electric field vector becomes zero in the equation (3.10). Again the second row in the dynamic matrix has a row of zeros and the production could not be done.

3.4.2 4×4 Matrix fails in the limit of isotropy

A multilayer thin film structure not always has anisotropic media. Some layers could be isotropic or have induced magnetic anisotropy. Below there is a description of why the 4×4 matrix formulation could not work in isotropic layers. First, recall the moment equation:

$$\mathbf{k} \times (\mathbf{k} \times \mathbf{E}) - \omega^2 \mu \varepsilon \mathbf{E} = \mathbf{0}$$

Being ε the dielectric tensor given by equation (3.2). The equation (3.9) have non trivial solutions for the electric field vector (**E**) if the determinant of the system is zero, so:

$$\begin{vmatrix} \omega^2\mu\varepsilon_{xx} - \beta^2 - \gamma^2 & \omega^2\mu\varepsilon_{xy} + \alpha\beta & \omega^2\mu\varepsilon_{xz} + \alpha\gamma \\ \omega^2\mu\varepsilon_{yx} + \alpha\beta & \omega^2\mu\varepsilon_{yy} - \alpha^2 - \gamma^2 & \omega^2\mu\varepsilon_{yz} + \beta\gamma \\ \omega^2\mu\varepsilon_{xz} + \alpha\gamma & \omega^2\mu\varepsilon_{yz} + \beta\gamma & \omega^2\mu\varepsilon_{zz} - \alpha^2 - \beta^2 \end{vmatrix} = 0 \tag{3.24}$$

For isotropic materials, the off-diagonal elements $(\varepsilon_{xy}, \varepsilon_{yx}, \varepsilon_{xz}, \varepsilon_{zx}, \varepsilon_{yz}, \varepsilon_{zy})$ are 0 and the diagonal elements are equals $(\varepsilon_{xx} = \varepsilon_{yy} = \varepsilon_{zz} = \varepsilon)$. The determinant becomes:

$$\begin{vmatrix} \omega^2\mu\varepsilon - \beta^2 - \gamma^2 & \alpha\beta & \alpha\gamma \\ \alpha\beta & \omega^2\mu\varepsilon - \alpha^2 - \gamma^2 & \beta\gamma \\ \alpha\gamma & \beta\gamma & \omega^2\mu\varepsilon - \alpha^2 - \beta^2 \end{vmatrix} = 0 \tag{3.25}$$

Solving the determinant via cofactors:

$$\begin{aligned} &\left(\omega^2\mu\varepsilon - \beta^2 - \gamma^2\right)\left(\left(\omega^2\mu\varepsilon - \alpha^2 - \gamma^2\right)\left(\omega^2\mu\varepsilon - \alpha^2 - \beta^2\right) - \beta^2\gamma^2\right) \\ &\quad - \alpha\beta\left(\alpha\beta\left(\omega^2\mu\varepsilon - \alpha^2 - \beta^2\right) - \alpha\beta\gamma^2\right) + \alpha\gamma\left(\alpha\beta^2\gamma - \alpha\gamma\left(\omega^2\mu\varepsilon - \alpha^2 - \gamma^2\right)\right) = 0 \end{aligned}$$

Doing the algebra, lead us to a quartic equation in γ:

$$\gamma^4 + 2\left(\left(\alpha^2 + \beta^2\right) - \omega^2\mu\varepsilon\right)\gamma^2 + \left(\alpha^2 + \beta^2 - \omega^2\mu\varepsilon\right)^2 = 0$$

Factoring:

$$\left(\gamma^2 + \alpha^2 + \beta^2 - \omega^2\mu\varepsilon\right)\left(\gamma^2 + \alpha^2 + \beta^2 - \omega^2\mu\varepsilon\right) = 0$$

γ has two solutions with algebraic multiplicity 2:

$$\gamma^2 = \omega^2\mu\varepsilon - \alpha^2 - \beta^2$$

Hence:

$$\gamma = \pm\sqrt{\omega^2\mu\varepsilon - \alpha^2 - \beta^2} \tag{3.26}$$

On the other hand, the polarization vector is given by the equation (3.10), where $N_\sigma = \frac{1}{|\mathbf{p}|}$, normalizes the vector $\mathbf{p}$. The dynamic matrix (3.12) in its first and fourth rows has the projection of the x-axis of $\mathbf{p}$, and the y-axis projections are on the second and third rows.

The polarization vector in presence of isotropic media is:

$$\mathbf{p} = N_\sigma \begin{bmatrix} \left(\omega^2\mu\varepsilon - \alpha^2 - \gamma^2\right)\left(\omega^2\mu\varepsilon - \alpha^2 - \beta^2\right) - (\beta\gamma)^2 \\ \alpha\beta\gamma^2 - \alpha\beta\left(\omega^2\mu\varepsilon - \alpha^2 - \beta^2\right) \\ \alpha\beta^2\gamma - \alpha\gamma\left(\omega^2\mu\varepsilon - \alpha^2 - \gamma^2\right) \end{bmatrix}$$

To know which values of γ make the components of $\hat{\mathbf{x}}$ and $\hat{\mathbf{y}}$ equals to 0 in the polarization vector, they can be equalled to zeros, so, for the y component:

$$\begin{aligned}
\alpha\beta\gamma^2 - \alpha\beta\left(\omega^2\mu\varepsilon - \alpha^2 - \beta^2\right) &= 0 \\
\alpha\beta\left(\gamma^2 - \omega^2\mu\varepsilon - \alpha^2 - \beta^2\right) &= 0 \\
\gamma^2 - \left(\omega^2\mu\varepsilon + \alpha^2 + \beta^2\right) &= 0 \\
\gamma^2 &= \omega^2\mu\varepsilon - \alpha^2 - \beta^2
\end{aligned}$$

Then

$$\gamma = \pm\sqrt{\omega^2\mu\varepsilon - \alpha^2 - \beta^2} \tag{3.27}$$

The condition on γ states that the y component becomes 0 if the equation (3.27) is satisfied. The value of γ is the same for both procedures (equations (3.26) and (3.27)), so in multilayer structure with isotropic materials the dynamical matrix has always a row of zeros. Then it is impossible to calculate the transfer matrix. The previous argument proves that 4×4 formulation matrix is useless to calculate Fresnel coefficients and optical functions for isotropic media.

This issue was previously pointed out by Li and colaborators (Li, Sullivan, and Parsons, 1988). They solved it combining the Yeh (Yeh, 2005) and Berreman (Berreman, 1972) methods. There are several other ways to analyze the propagation of light on anisotropic media. One widely referenced is proposed by M. Mansuripur (Mansuripur, 1990) in which a 2×2 matrix method is derived. Another one is the simplified form for the 4×4 propagation matrix of a general homogeneous biaxial layer proposed by Abdulhalim (Abdulhalim, 1999). One approach for solving the propagation of light in anisotropic media was developed by Cojocaru in two moments. First, solving the particular case for one anisotropic layer embedded in two isotropic media (Cojocaru, 1997) as is shown in figure 3.4, and then developing a generalized matrix method using the fact that each anisotropic layer is between two isotropic media of thickness zero (Cojocaru, 2000). Within the limits of isotropy the relations found are reduced to the Abelès relations (Abelès, 1948). Scattering matrix approach is widely referenced and used by several authors; between them (Ko and Sambles, 1988; Cotter, Preist, and Sambles, 1995; Whittaker and Culshaw, 1999; Caballero, García-Martín, and Cuevas, 2012).

3.5 Cojocaru's method

Searching for a general method to simulate the propagation of coherent light in anisotropic multilayer thin films here we reviwed the Yeh's method. Nevertheless, Yeh's method does not work on the isotropic limits. Therefore, we here review the Cojocaru's method initially for one anisotropic medium in order to find the Fresnel coefficients. The medium of incidence (n_0) and the substrate (n_s) are considered isotropic. Boundary conditions are used to relate amplitudes of the incident and reflected fields inside the inner layer. Propagation of monochromatic waves inside anisotropic medium require to solve the moment space equation (3.8) or equivalently (3.9) for k_z. M. Mansuripur (Mansuripur, 1990) has found a way to write the fourth order polynomial in the way:

$$\zeta^4 + q_3\zeta^3 + q_2\zeta^2 + q_1\zeta + q_0 = 0, \tag{3.28}$$

where the coefficients of the equation (q_0, q_1, q_2, q_3) are given in the appendix B. This coefficients only dependent on the relative permitivitties of the dielectric tensor, the angle of incidence and $\xi = n_0 \sin\theta_0$. Based on the figure 3.4, the propagation vector on the incident medium can be written as:

$$\mathbf{k}_0^{\pm} = \frac{\omega}{c}\left(\xi\hat{\mathbf{x}} \pm \zeta\hat{\mathbf{z}}\right), \tag{3.29}$$

where, $\zeta = n_0 \cos\theta_0$. Four solutions are obtained from the equation (3.28) that determine the z-component of wave vector inside the anisotropic layer. The four solutions will be written as $\zeta = \zeta_\alpha^+, \zeta_\beta^+, \zeta_\alpha^-, \zeta_\beta^-$, the symbol + and − in the exponent of ζ is referred to an incident (+) or reflected (−) wave. The refractive indexes are given by:

$$n = \left[\xi^2 + \zeta^2\right]^{\frac{1}{2}} \tag{3.30}$$

In addition, the refracted angle is:

$$\theta = \arccos\left(\frac{\zeta}{n}\right) \tag{3.31}$$

The four values of ζ give four values of n, n_α^+, n_α^-, n_β^+ and n_β^- and consequently four values of θ that will be θ_α^+, θ_α^-, θ_β^+ and θ_β^-. The four values of θ are represented by the figure 3.4. When the inner layer is isotropic $\zeta_\alpha^+ = \zeta_\beta^+$, $\theta_\alpha^+ = \theta_\beta^+$ and $n_\alpha^+ = n_\beta^+$, that is the same for $\zeta_\alpha^- = \zeta_\beta^-$, $\theta_\alpha^- = \theta_\beta^-$ and $n_\alpha^- = n_\beta^-$, also if the medium is uniaxial $\zeta_\alpha = \zeta_o$, $\theta_\alpha = \theta_o$ and $n_\alpha = n_o$, where the subscript o is for the ordinary index, also, $\zeta_\beta = \zeta_e$, $\theta_\beta = \theta_e$ and $n_\beta = n_e$, are the variables for the extraordinary index. This approach was simulated and the results were contrasted with those obtained for isotropic media given the desire values for three isotropic media. Setting the thickness of the anisotropic layer equals to zero, the results are the same as two isotropic media (simple interface).

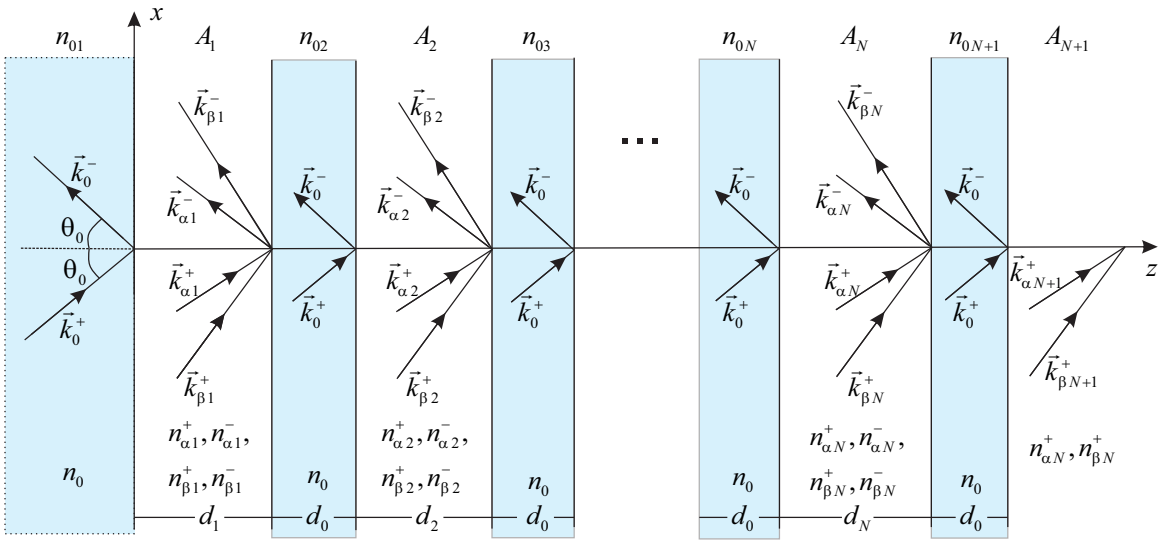

FIGURE 3.5: Anisotropic multilayer thin films structure with the immersion model, the blue pale colors are the isotropic media. The rays represent the four waves (two incident $k_{\alpha j}^+$, $k_{\beta j}^+$ and two reflected $k_{\alpha j}^-$, $k_{\beta j}^-$) in each anisotropic layer. The distances $d_0 = 0$ for all isotropic media immerse between two anisotropic layers and $n_{0j} = n_{01}$, for $0 \leq j \leq N+1$.

The general form proposed by E. Cojocaru (Cojocaru, 2000) uses the immersion model, where each layer is suppose to be immerse between two isotropic layers with refractive index equal to the medium of incidence n_0, see figure 3.5. The immersion model makes possible to set a boundary conditions for each layer easily, defining transmission (3.32), reflection (3.33) and propagation (3.34) by 2×2 matrices given by:

$$\tau_j^{\pm} = \frac{2\zeta_0}{\delta_j^{\pm}} \begin{bmatrix} a_{\beta j}^{\pm} & \pm b_{\beta j}^{\pm} \\ -a_{\alpha j}^{\pm} & \mp b_{\alpha j}^{\pm} \end{bmatrix} \tag{3.32}$$

$$\rho_j^{\pm} = \frac{1}{\delta_j^{\pm}} \begin{bmatrix} \rho_{j11}^{\pm} & \rho_{j12}^{\pm} \\ \rho_{j21}^{\pm} & \rho_{j21}^{\pm} \end{bmatrix} \tag{3.33}$$

$$X_j^{\pm}\Big|_{z_j} = \begin{bmatrix} e^{\pm i\frac{\omega}{c}\zeta_{\alpha}^{\pm} z_l} & 0 \\ 0 & e^{\pm i\frac{\omega}{c}\zeta_{\beta}^{\pm} z_l} \end{bmatrix} \tag{3.34}$$

Where, $i = \sqrt{-1}$, $z_l = \sum_{j=1}^{l} d_m$, the constants $a_{\pm}^{\sigma}$, $b_{\pm}^{\sigma}$ and $\delta_j^{\pm}$ are given by:

$$a_{\pm}^{\sigma} = n_0 e_x \pm n\cos(\eta) h_y \cos\theta_0 \tag{3.35}$$

$$b_{\pm}^{\sigma} = \zeta_0 e_y \pm n\cos(\eta) h_x \tag{3.36}$$

$$\delta_j^{+} = a_{\beta j+}^{+} b_{\alpha j-}^{+} - a_{\alpha j+}^{+} b_{\beta j-}^{+} \tag{3.37}$$

$$\delta_j^{-} = a_{\beta j-}^{-} b_{\alpha j+}^{-} - a_{\alpha j-}^{-} b_{\beta j+}^{-} \tag{3.38}$$

Where, $\sigma = \pm$ refers to the incident (+) and reflected (−) waves, η is the walk-off angle, between the electric field vector and the displacement vector (see figure 3.3) and θ_0 is the angle of incidence of the wave. The values of e_x, e_y, h_x, h_y are the components of the unit vectors in the direction of the electric and magnetic field in the anisotropic media ($\hat{\mathbf{e}} = (e_x, e_y, e_z)$, $\hat{\mathbf{h}} = (h_x, h_y, h_z)$), finally the subscript j refers to the j-th layer.

The components for dynamic reflection matrices, $\rho_j^{\pm}$, are:

$$\begin{aligned} \rho_{11j}^{\pm} &= a_{\beta j\pm}^{\pm} b_{\alpha j\pm}^{\mp} - a_{\beta j\pm}^{\mp} b_{\beta j\mp}^{\pm} \\ \rho_{12j}^{\pm} &= a_{\beta j\pm}^{\pm} b_{\beta j\pm}^{\mp} - a_{\beta j\pm}^{\mp} b_{\beta j\mp}^{\pm} \\ \rho_{21j}^{\pm} &= a_{\alpha j\pm}^{\mp} b_{\alpha j\pm}^{\pm} - a_{\alpha j\pm}^{\pm} b_{\beta j\mp}^{\mp} \\ \rho_{22j}^{\pm} &= a_{\alpha j\pm}^{\mp} b_{\alpha j\pm}^{\pm} - a_{\beta j\pm}^{\pm} b_{\beta j\mp}^{\mp} \end{aligned}$$

In each anisotropic layer a 4×4 transfer matrix M_j is found via:

$$M_j = \left(\tilde{\tau}_j\right)^{-1} \tilde{\rho}_j \left(\tilde{\chi}_j\right)^{-1} \left(\tilde{\rho}_j\right)^{-1} \tilde{\tau}_j \tag{3.39}$$

The expressions for $\tilde{\tau}_j$, $\tilde{\rho}_j$ and $\tilde{\chi}_j$, are given by:

$$\tilde{\tau}_j = \begin{bmatrix} \tau_j^+ & O_2 \\ O_2 & \tau_j^- \end{bmatrix} \tag{3.40}$$

$$\tilde{\rho}_j = \begin{bmatrix} \rho_j^+ & I_2 \\ I_2 & \rho_j^- \end{bmatrix} \tag{3.41}$$

$$\tilde{\chi}_j = \begin{bmatrix} \chi_j^- & I_2 \\ I_2 & \chi_j^+ \end{bmatrix} \tag{3.42}$$

The matrices (3.40, 3.41, 3.42) are block matrices where each component is a 2×2 matrix. The matrices $\tau_j^{\pm}$ are defined by the equation (3.32), as well as the matrices $\rho_j^{\pm}$ are given by (3.33), $\chi_j^{\pm} = X_j^{\pm}\Big|_{d_j}$. I_2 is the 2×2 identity matrix and O_2 is the 2×2 zero matrix.

The product of all transfer matrices corresponding to anisotropic layers $M = \prod_{j=1}^{N} M_j$, gives a unique 4×4 matrix which can be written in block matrix as follows:

$$M = \begin{bmatrix} A & B \\ C & D \end{bmatrix}$$

For the substrate we define:

$$\begin{aligned} r_s &= \left(\tau_{N+1}^-\right)^{-1} \rho_{N+1}^- \tau_{N+1}^+ \\ t_s &= \tau_{N+1}^+ \end{aligned}$$

The 2×2 matrices that define the Fresnel coefficients are given by:

$$r = (C + Dr_s)(A + Br_s)^{-1} \tag{3.43}$$

$$t = t_s (A + Br_s)^{-1} \tag{3.44}$$

The Fresnel coefficients for reflection in the r matrix are given by: $r_{11} = r_{ss}, r_{12} = r_{sp}, r_{21} = r_{ps}, r_{22} = r_{pp}$, in a similar way for the transmission coefficients $t_{11} = t_{ss}, t_{12} = t_{sp}, t_{21} = t_{ps}, t_{22} = t_{pp}$. If the j-th layer is isotropic with refraction index n_i, the matrices (3.32, 3.33, 3.34) are replaced by:

$$\chi_j^{\pm} = \begin{bmatrix} e^{\mp i \frac{\omega}{c} d_j \zeta_j} & 0 \\ 0 & e^{\mp i \frac{\omega}{c} d_j \zeta_j} \end{bmatrix} \tag{3.45}$$

$$\tau_j^{\pm} = \begin{bmatrix} t_{sj} & 0 \\ 0 & t_{pj} \end{bmatrix} \tag{3.46}$$

$$\rho_j^{\pm} = \begin{bmatrix} r_{sj} & 0 \\ 0 & r_{pj} \end{bmatrix}, \tag{3.47}$$

where $\zeta_j = n_j \cos\theta_j$, θ_j is the refraction angle, t_{sj}, t_{pj}, r_{sj} and r_{pj} are the Fresnel coefficients for s and p modes at the interface j, that can be calculated by the equations (1.16, 1.17, 1.26, 1.27).

3.6 Module of electric field based on Cojocaru's method

The goal in this section is to find the amplitudes of incident and reflected electric field in each layer through the immersion Cojocaru's model (Cojocaru, 2000). First of all, set the electrical field vector in the j and $0j$-th layer as:

$$\mathbf{E}_j^{\sigma} = \begin{bmatrix} E_{\alpha j}^{\sigma} \\ E_{\beta j}^{\sigma} \end{bmatrix} \tag{3.48}$$

$$\mathbf{E}_{0j}^{\sigma} = \begin{bmatrix} E_{sj}^{\sigma} \\ E_{pj}^{\sigma} \end{bmatrix}, \tag{3.49}$$

where, $\sigma = \pm$ for incident and reflected fields, the subscript j denotes the material layer, the subscripts α and β are the waves in the j-th anisotropic media and the subscripts s and p refers to the polarization of the wave in the media $0j$

If there are three materials the boundary conditions in the immersion model states that:

$$\tau_1^{+}\mathbf{E}_{01}^{+} = \mathbf{E}_1^{+} + \rho_1^{+}\mathbf{E}_1^{-}, \tag{3.50}$$

$$\tau_1^{-}\mathbf{E}_{01}^{-} = \rho_1^{-}\mathbf{E}_1^{+} + \mathbf{E}_1^{-}, \tag{3.51}$$

$$X_1^{+}\Big|_{z_1}\mathbf{E}_1^{+} + \rho_1^{+}X_1^{-}\Big|_{z_1}\mathbf{E}_1^{-} = \tau_1^{+}X_0^{+}\Big|_{z_1}\mathbf{E}_{02}^{+}, \tag{3.52}$$

$$X_1^{-}\Big|_{z_1}\mathbf{E}_1^{-} + \rho_1^{-}X_1^{+}\Big|_{z_1}\mathbf{E}_1^{+} = \tau_1^{-}X_0^{-}\Big|_{z_1}\mathbf{E}_{02}^{-}, \tag{3.53}$$

$$\tau_2^{+}X_0^{+}\Big|_{z_1}\mathbf{E}_{02}^{+} = X_2^{+}\Big|_{z_1}\mathbf{E}_2^{+}, \tag{3.54}$$

$$\tau_2^{-}X_0^{-}\Big|_{z_1}\mathbf{E}_{02}^{-} = \rho_2^{-}X_2^{+}\Big|_{z_1}\mathbf{E}_2^{+}, \tag{3.55}$$

where, $X_0^{\pm}\Big|_{z_j} = e^{\pm i\frac{\omega}{c}z_j\zeta_0}$ and $X_j^{\pm}\Big|_{z_j}$ is given by the equation (3.34).

The transmission ($\tau_j^{\pm}$), reflection ($\rho_j^{\pm}$), propagation ($X_j^{\pm}$) matrices as well as Fresnel coefficients r and t are known through the equations (3.32), (3.33), (3.34), (3.43) and (3.44), respectively. Therefore, $\mathbf{E}_{01}^{-} = r\mathbf{E}_{01}^{+}$ and $X_2^{+}\Big|_{z_N}\mathbf{E}_2^{+} = t\mathbf{E}_{01}^{+}$ can be solved for $\mathbf{E}_{01}^{-}$ and $\mathbf{E}_2^{+}$, having in mind that $\mathbf{E}_{01}^{+}$ is the amplitude of the incident wave.

For both polarizations the vector $\mathbf{E}_{01}^{+}$ can be define as (equation (3.49)):

$$\vec{\mathbf{E}}_{01s}^{+} = \begin{bmatrix} 1 \\ 0 \end{bmatrix}$$

$$\vec{\mathbf{E}}_{01p}^{+} = \begin{bmatrix} 0 \\ 1 \end{bmatrix}$$

The first component of the vector corresponds to the s-polarization while the second correspond to the p-polarization. Then, the vectors $\mathbf{E}_{01}^{-}$ and $\mathbf{E}_2^{+}$ can be found immediately (equations (3.50) and (3.55)).

Using the equations (3.50) and (3.51) is possible to find the vectors of electric field incident $\mathbf{E}_1^+$ and reflected $\mathbf{E}_1^-$ in the intermediate layer for three materials.

The module of electric field for p-polarization has the shape (a similar expression is obtained for s-polarization):

$$|\mathbf{E}_p| = |E_{p1}^+ e^{i\frac{\omega}{c}\zeta_\alpha^+ z} + E_{p2}^+ e^{i\frac{\omega}{c}\zeta_\beta^+ z} + E_{p3}^- e^{i\frac{\omega}{c}\zeta_\alpha^- z} + E_{p4}^- e^{i\frac{\omega}{c}\zeta_\beta^- z}| \tag{3.56}$$

Where, $E_{p1,2}^+$ are components of the incident field and $E_{p3,4}^-$ are the components of the reflected field in the inner layer.

In general, if there are more than two inner layers, the way to find the amplitudes of the electric fields either s or p-polarized will be (see figure 3.19):

1. Choose the polarization state in order to know $\mathbf{E}_{01}^+$. In appendix C there is a table with the Jones vectors of some typical polarization states (Yeh, 2005).
2. Use the Fresnel coefficients (r,t) and the propagation matrix $X_{N+1}^+\Big|_{z_N}$ to find $\mathbf{E}_{01}^-$ and $\mathbf{E}_{N+1}^+$ (the layer $N+1$ is the substrate).
3. Calculate $\mathbf{E}_1^\pm$ with the known values and the first two equations from boundary conditions as presented above.
4. Use the latest two equations from the boundary conditions to find the amplitudes $\mathbf{E}_{0N+1}^\pm$.
5. Determine the vectors $\mathbf{E}_N^\pm$ with the equations (3.54) and (3.55) in the boundary conditions.
6. With the result found in the previous item, find the vectors $\mathbf{E}_{0N}^\pm$.
7. Evaluate the number of layers left and go back to the item 5 to repeat the algorithm until the layer number 2.

The previous steps were followed to obtain the module of electric field. The algorithm is exemplified through the flux diagram shown in the figure 3.19 and programmed in matlab 2015.

Explicit relations for $\mathbf{E}_N^+$, $\mathbf{E}_N^-$, $\mathbf{E}_{0N}^+$ and $\mathbf{E}_{0N}^-$ are presented in equations (3.57), (3.58), (3.59) and (3.60).

$$\mathbf{E}_N^- = \left[\left(\rho_N^+ - \left(\rho_N^-\right)^{-1}\right) X_N^-\Big|_{z_N}\right]^{-1} \left(\tau_N^+ X_0^+\Big|_{z_N} \mathbf{E}_{0N+1}^+ - \left(\rho_N^-\right)^{-1} X_0^-\Big|_{z_N} \mathbf{E}_{0N+1}^-\right) \tag{3.57}$$

$$\mathbf{E}_N^+ = \left(X_N^+\Big|_{z_N}\right)^{-1} \left[\tau_N^+ X_0^+\Big|_{z_N} \mathbf{E}_{0N+1}^+ - \rho_N^+ X_N^-\Big|_{z_N} \mathbf{E}_N^-\right] \tag{3.58}$$

$$\mathbf{E}_{0N}^+ = \frac{1}{X_0^+\Big|_{z_{N-1}}} \left(\tau_N^+\right)^{-1} \left[X_N^+\Big|_{z_{N-1}} \mathbf{E}_N^+ + \rho_N^+ X_N^-\Big|_{z_{N-1}} \mathbf{E}_N^-\right] \tag{3.59}$$

$$\mathbf{E}_{0N}^- = \frac{1}{X_0^-\Big|_{z_{N-1}}} \left(\tau_N^-\right)^{-1} \left[\rho_N^- X_N^-\Big|_{z_{N-1}} \mathbf{E}_N^+ + \tau_N^+ X_0^+\Big|_{z_{N-1}} \mathbf{E}_N^-\right] \tag{3.60}$$

3.7 Scattering Matrix Approach

3.7.1 Introduction

D. Y. K. Ko and J. R. Sambles (Ko and Sambles, 1988) developed a method called *Scattering matrix*. They present a formalism for modeling electromagnetic wave propagation in stratified media. There are two advantages of this method: in one hand its numerical estability. On the other hand, the possibility of implement thick layers ($> 1\mu m$). This approach was taken up by Cotter, Priest & Sambles (Cotter, Preist, and Sambles, 1995) who use this method in the presence of multilayer diffraction gratings allowing to obtain reflectance for thick layers as function of the angle of incidence. Later Whittaker and Culshaw (Whittaker and Culshaw, 1999) use the approach to calculate reflectivity and emission spectra for multilayer dielectric waveguides in a structured patterned holes. Following the patterned multilayer systems, recently Caballero, García-Martín and Cuevas (Caballero, García-Martín, and Cuevas, 2012) use the generalized form of this method to find the reflectivity and TMOKE as functions of wavelength for perforated Fe films with circular holes in a periodically array. The present development uses the fundamentals of the previous documents and follow principally the scattering matrix approach described by (Caballero, García-Martín, and Cuevas, 2012) and Moncada, E. (Moncada, 2015).

The scattering matrix method couples the incoming to the outgoing waves in a structured system of materials. The electromagnetic waves can be divided in two sets, the forward and backward modes represented as ($\mathbf{a}_i$) and ($\mathbf{b}_i$), respectively. The waves are chosen such that the plane of incidence is in the xz-axis. A relation between forward and backward waves in the incident medium and arbitrary medium n can be related by the expression:

$$\begin{bmatrix} \mathbf{a}_n \\ \mathbf{b}_0 \end{bmatrix} = S(0,n) \begin{bmatrix} \mathbf{a}_0 \\ \mathbf{b}_n \end{bmatrix} \tag{3.61}$$

In the equation (3.61) the coefficients of forward modes are contained in the variable $\mathbf{a}$ while coefficients of backward modes are contained in the variable $\mathbf{b}$. The matrix $\mathbf{S}(0,n)$ are called *scattering matrix* and is calculated later as an iterative process, finding first the *interface matrices* coupling the amplitudes of two adjacent layers as is shown in the equation (3.62).

$$\begin{bmatrix} \mathbf{a}_n \\ \mathbf{b}_n \end{bmatrix} = I(n,n+1) \begin{bmatrix} \mathbf{a}_{n+1} \\ \mathbf{b}_{n+1} \end{bmatrix} \tag{3.62}$$

Figure 3.6 shows an schematic representation of the forward (incoming - $\mathbf{a}_l$) and backward (outgoing - $\mathbf{b}_l$) waves.

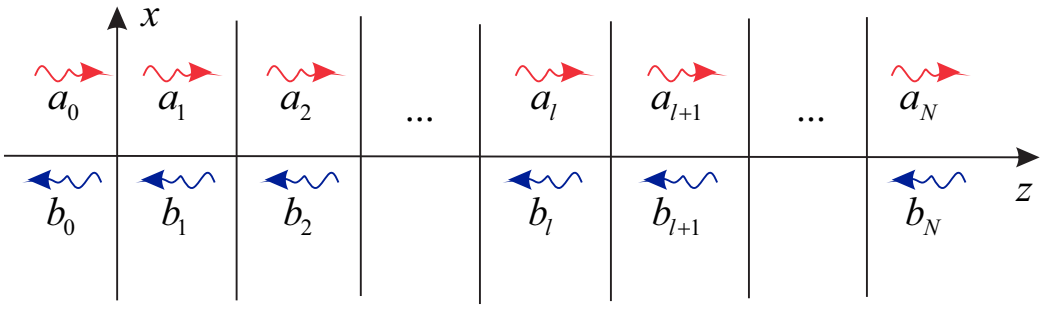

FIGURE 3.6: Forward and backward amplitudes in a multilayer structure.

Mathematical formulation of scattering matrices are presented above with purpose of finding interface and scattering matrices. The reflection and transmission matrices are found for s and p-polarizations.

3.7.2 Mathematical formulation of scattering matrix method

The starting point as presented for Yeh's and Cojocaru's method are the Maxwell equations. Particularly the Ampere and Faraday laws. Also the constitutive relations for the displacement $\mathbf{D}$ and magnetic induction $\mathbf{B}$, for an anisotropic material given as follows:

$$\mathbf{D} = \varepsilon_0 \hat{\varepsilon} \mathbf{E} \tag{3.63}$$

$$\mathbf{B} = \mu_0 \hat{\mu} \mathbf{H} \tag{3.64}$$

Where the relative permittivity and permeability are now dielectric and magnetic tensors of rank 2, that can be represented as 3×3 matrices as follows:

$$\varepsilon = \begin{bmatrix} \varepsilon_{xx} & \varepsilon_{xy} & \varepsilon_{xz} \\ \varepsilon_{yx} & \varepsilon_{yy} & \varepsilon_{yz} \\ \varepsilon_{zx} & \varepsilon_{zy} & \varepsilon_{zz} \end{bmatrix} \quad \mu = \begin{bmatrix} \mu_{xx} & \mu_{xy} & \mu_{xz} \\ \mu_{yx} & \mu_{yy} & \mu_{yz} \\ \mu_{zx} & \mu_{zy} & \mu_{zz} \end{bmatrix} \tag{3.65}$$

Assuming harmonic time dependence $e^{-i\omega t}$ the electric field can be rescaled as $\omega \varepsilon_0 \mathbf{E} \rightarrow \mathbf{E}$, where $\frac{\omega}{c} \rightarrow \omega$, leading the equations (1.3) and (1.4) in non-conducting media to:

$$\nabla \times \mathbf{E} = i\omega^2 \hat{\mu} \mathbf{H} \tag{3.66}$$

$$\nabla \times \mathbf{H} = -i\hat{\varepsilon} \mathbf{E} \tag{3.67}$$

Also, the electric and magnetic fields are written in the moment representation as

$$\mathbf{E}(\mathbf{r}, z) = e^{i\mathbf{k}\cdot\mathbf{r}} e^{iqz} \left[e_x \hat{\mathbf{x}} + e_y \hat{\mathbf{y}} + e_z \hat{\mathbf{z}} \right] \tag{3.68}$$

$$\mathbf{H}(\mathbf{r}, z) = e^{i\mathbf{k}\cdot\mathbf{r}} e^{iqz} \left[h_x \hat{\mathbf{x}} + h_y \hat{\mathbf{y}} + h_z \hat{\mathbf{z}} \right] \tag{3.69}$$

Where $\mathbf{k} = (k_x, k_y)$ is the wave vector parallel to the interfaces. Replacing the equations (3.68) and (3.69) into the equations (3.66) and (3.67) the curl $\nabla \times \mathbf{E}$ can be written as:

$$\nabla \times \mathbf{E} = \begin{vmatrix} \mathbf{i} & \mathbf{j} & \mathbf{k} \\ \frac{\partial}{\partial x} & \frac{\partial}{\partial y} & \frac{\partial}{\partial z} \\ e^{i\mathbf{k}\cdot\mathbf{r}} e^{iqz} e_x & e^{i\mathbf{k}\cdot\mathbf{r}} e^{iqz} e_y & e^{i\mathbf{k}\cdot\mathbf{r}} e^{iqz} e_z \end{vmatrix} \tag{3.70}$$

$$\nabla \times \mathbf{E} = e^{i\mathbf{k}\cdot\mathbf{r}} e^{iqz} \left[(k_y e_z - q e_y)\mathbf{i} - (k_x e_z - q e_x)\mathbf{j} + (k_x e_y - k_y e_x)\mathbf{k} \right] \tag{3.71}$$

By the equation (3.66) is found the system of equations:

$$\begin{aligned} k_y e_z - q e_y &= h_x \omega^2 \\ q e_x - k_x e_z &= h_y \omega^2 \\ k_x e_y - k_y e_x &= h_z \omega^2 \end{aligned}$$

System that can be written in a matrix form as:

$$\begin{bmatrix} 0 & -q & k_y \\ q & 0 & -k_x \\ -k_y & k_x & 0 \end{bmatrix} \begin{bmatrix} e_x \\ e_y \\ e_z \end{bmatrix} = \omega^2 \begin{bmatrix} h_x \\ h_y \\ h_z \end{bmatrix}$$

In a compact form:

$$C^T \mathbf{e} = \omega^2 \hat{\mu} \mathbf{h} \tag{3.72}$$

In a similar way, solving the curl of the magnetic field vector $\nabla \times \mathbf{H}$:

$$\nabla \times \mathbf{H} = \begin{vmatrix} \mathbf{i} & \mathbf{j} & \mathbf{k} \\ \frac{\partial}{\partial x} & \frac{\partial}{\partial y} & \frac{\partial}{\partial z} \\ e^{i\mathbf{k}\cdot\mathbf{r}} e^{iqz} h_x & e^{i\mathbf{k}\cdot\mathbf{r}} e^{iqz} h_y & e^{i\mathbf{k}\cdot\mathbf{r}} e^{iqz} h_z \end{vmatrix} \tag{3.73}$$

$$\nabla \times \mathbf{H} = e^{i\mathbf{k}\cdot\mathbf{r}} e^{iqz} \left[(k_y h_z - q h_y)\mathbf{i} - (k_x h_z - q h_x)\mathbf{j} + (k_x h_y - k_y h_x)\mathbf{k} \right] \tag{3.74}$$

By the equation (3.67) the system of equations emerge:

$$\begin{matrix} k_y h_z - q h_y \\ q h_x - k_x h_z \\ k_x h_y - k_y h_x \end{matrix} = -\hat{\varepsilon} \begin{bmatrix} e_x \\ e_y \\ e_z \end{bmatrix}$$

System that can be written in a matrix form as:

$$\begin{bmatrix} 0 & q & -k_y \\ -q & 0 & k_x \\ k_y & -k_x & 0 \end{bmatrix} \begin{bmatrix} h_x \\ h_y \\ h_z \end{bmatrix} = \hat{\varepsilon} \begin{bmatrix} e_x \\ e_y \\ e_z \end{bmatrix}$$

In a compact form:

$$C\mathbf{h} = \hat{\varepsilon} \mathbf{e} \tag{3.75}$$

The matrix C is antisymmetric ($A^T = -A$). The electric or magnetic field can be eliminated from the equations (3.72) and (3.75) in order to obtain the components of the electric or magnetic field[2] setting $\mathbf{h} = h_x\hat{\mathbf{x}} + h_y\hat{\mathbf{y}} + h_z\hat{\mathbf{z}}$ and $\mathbf{e} = e_x\hat{\mathbf{x}} + e_y\hat{\mathbf{y}} + e_z\hat{\mathbf{z}}$ and eliminating the $\mathbf{e}$ variable the system becomes in a unique equation given by:

$$\left(C^T \hat{\eta} C - \omega^2 \hat{\mu} \right) \mathbf{h} = \begin{bmatrix} 0 \\ 0 \\ 0 \end{bmatrix} \tag{3.77}$$

Defining the antisymmetric matrix C and $\hat{\eta}$ as:

[2] If the variable to be eliminated is $\mathbf{h}$, emerge the equation:

$$\left(\frac{1}{\omega^2} C C^T - \hat{\varepsilon} \right) \mathbf{e} = \begin{bmatrix} 0 \\ 0 \\ 0 \end{bmatrix} \tag{3.76}$$

which is an alternative form of the moment space equation and written in terms of its components lead us to equation 3.9. An alternative deduction for the electric field is found on the Appendix D

$$C \equiv \begin{bmatrix} 0 & q & -k_y \\ -q & 0 & k_x \\ k_y & -k_x & 0 \end{bmatrix} \tag{3.78}$$

$$\hat{\eta} \equiv \hat{\varepsilon}^{-1} \tag{3.79}$$

Which defines an eigenvalue problem for ω^2. This problem can be set as a problem of non-linear eigenvalues problem in q. First, using the constitutive relation for magnetic induction ($\nabla \cdot \mathbf{B} = 0$), being $\mathbf{B} = \mu\mathbf{H}$, in order to simplify the process for all subsequence analysis $\mu = \hat{1}$, (3×3 identity matrix). The divergence $\nabla \cdot \mathbf{H} = 0$ gives the z-component of the magnetic vector in terms of the x- and y-components:

$$h_z = -\frac{1}{q}\left(k_x h_x + k_y h_y\right) \tag{3.80}$$

Replacing the latest equation in the first two identities in equation (3.77), the matrix system in h_x and h_y becomes:

$$\left(A_2 q^2 + A_1 q + A_0 + A_{-1}\frac{1}{q}\right)\begin{bmatrix} h_x \\ h_y \end{bmatrix} = \begin{bmatrix} 0 \\ 0 \end{bmatrix} \tag{3.81}$$

The matrices 2×2 A_i are given by:

$$A_2 = \begin{bmatrix} \eta_{yy} & -\eta_{yx} \\ -\eta_{xy} & \eta_{xx} \end{bmatrix} \tag{3.82}$$

$$A_1 = A_1^{(a)} + A_1^{(b)} \tag{3.83}$$

$$A_0 = A_0^{(a)} + A_0^{(b)} - \omega^2 I_2 \tag{3.84}$$

$$A_{-1} = \begin{bmatrix} k_x k_y^2 \eta_{zx} - k_x^2 k_y \eta_{zy} & k_y^3 \eta_{zx} - k_x k_y^2 \eta_{zy} \\ k_x^3 \eta_{zy} - k_x^2 k_y \eta_{zx} & k_x^2 k_y \eta_{zy} - k_x k_y^2 \eta_{zx} \end{bmatrix} \tag{3.85}$$

where:

$$A_1^{(a)} = \begin{bmatrix} -k_y \eta_{zy} & k_y \eta_{zx} \\ k_x \eta_{zy} & -k_x \eta_{zx} \end{bmatrix} \qquad A_1^{(b)} = \begin{bmatrix} -k_y \eta_{yz} & k_x \eta_{yz} \\ k_y \eta_{xz} & -k_x \eta_{xz} \end{bmatrix} \tag{3.86}$$

$$A_0^{(a)} = \begin{bmatrix} k_y^2 \eta_{zz} & -k_x k_y \eta_{zz} \\ -k_x k_y \eta_{zz} & k_x^2 \eta_{zz} \end{bmatrix} \qquad A_0^{(b)} = \begin{bmatrix} k_x^2 \eta_{yy} - k_x k_y \eta_{yx} & k_x k_y \eta_{yy} - k_y^2 \eta_{yx} \\ k_x k_y \eta_{xx} - k_x^2 \eta_{xy} & k_y^2 \eta_{xx} - k_x k_y \eta_{xy} \end{bmatrix} \tag{3.87}$$

$$I_2 = \begin{bmatrix} 1 & 0 \\ 0 & 1 \end{bmatrix} \tag{3.88}$$

The equation (3.81) can be solved via Matlab with the command `polyeig` or can be linearized as is shown by Caballero, García-Martín & Cuevas (Caballero, García-Martín, and Cuevas, 2012) and is exemplified above in section 3.7.5. The equation (3.81) returns six eigenvalues and six eigenvectors of the system. Two of the eigenvalues are always zero, that is the trivial solution, when there is no wave propagating in the layers, the other four can be categorized as q_1, q_2 for positive imaginary part and p_1, p_2 for values with negative imaginary part. The corresponding eigenvectors $\phi_1 = \begin{bmatrix} \phi_{x_1} \\ \phi_{y_1} \end{bmatrix}$, $\phi_2 = \begin{bmatrix} \phi_{x_2} \\ \phi_{y_2} \end{bmatrix}$, for $q_{1,2}$

values and $\psi_1 = \begin{bmatrix}\psi_{x_1}\\ \psi_{y_1}\end{bmatrix}$, $\psi_2 = \begin{bmatrix}\psi_{x_2}\\ \psi_{y_2}\end{bmatrix}$, for $p_{1,2}$ values. The total magnetic and electric fields ($\mathbf{e}(z)$, $\mathbf{h}(z)$) propagating towards z-direction inside the inner layer of a multilayer structure are given by:

$$\mathbf{h}(z) = \sum_{i=1}^{2}\left(\begin{bmatrix}\phi_{x_n}\\ \phi_{y_n}\\ \phi_{z_n}\end{bmatrix} e^{iq_n z} a_n + \begin{bmatrix}\psi_{x_n}\\ \psi_{y_n}\\ \psi_{z_n}\end{bmatrix} e^{-ip_n(d-z)} b_n\right) \tag{3.89}$$

The coefficients a_n and b_n correspond to the forward and backward waves and d is the thickness of the layer. The equation (3.75) can be used to write the electric field as:

$$\mathbf{e}(z) = \sum_{i=1}^{2}\left(\hat{\eta}C_{q_n}\begin{bmatrix}\phi_{x_n}\\ \phi_{y_n}\\ \phi_{z_n}\end{bmatrix} e^{iq_n z} a_n + \hat{\eta}C_{p_n}\begin{bmatrix}\psi_{x_n}\\ \psi_{y_n}\\ \psi_{z_n}\end{bmatrix} e^{-ip_n(d-z)} b_n\right) \tag{3.90}$$

The matrix C_{q_n} and C_{p_n} are found from the expression (3.78) replacing q by the eigenvalues $q_{1,2}$ and $p_{1,2}$. The tangential components of the electric and magnetic fields are continuous along the all slabs so $\mathbf{e}_{||} = \begin{bmatrix}-e_y\\ e_x\end{bmatrix}$ and $\mathbf{h}_{||} = \begin{bmatrix}h_x\\ h_y\end{bmatrix}$ are describe using the equations (3.89) and (3.90) through the expressions:

$$\mathbf{h}_{||}(z) = \Phi_+ f_+(z)\,\mathbf{a} + \Phi_- f_-(d-z)\,\mathbf{b} \tag{3.91}$$

Using the equation (3.75) and doing the algebra, the parallel electric field is given by:

$$\begin{aligned}\mathbf{e}_{||}(z) = &\left(A_0^{(b)}\Phi_+ q^{-1} + A_1^{(b)}\Phi_+ + A_2\Phi_+ q\right) f_+(z)\,\mathbf{a}\\ &+ \left(A_0^{(b)}\Phi_- p^{-1} + A_1^{(b)}\Phi_- + A_2\Phi_- p\right) f_-(d-z)\,\mathbf{b}\end{aligned} \tag{3.92}$$

Where, $A_0^{(b)}$, $A_1^{(b)}$ and A_2, are defined by the equations (3.86), (3.87) and (3.82), respectively. Also:

$$\mathbf{a} = \begin{bmatrix}a_1\\ a_2\end{bmatrix} \qquad \mathbf{b} = \begin{bmatrix}b_1\\ b_2\end{bmatrix}$$

$$q = \begin{bmatrix}q_1 & 0\\ 0 & q_2\end{bmatrix} \qquad p = \begin{bmatrix}p_1 & 0\\ 0 & p_2\end{bmatrix}$$

$$q^{-1} = \begin{bmatrix}\frac{1}{q_1} & 0\\ 0 & \frac{1}{q_2}\end{bmatrix} \qquad p^{-1} = \begin{bmatrix}\frac{1}{p_1} & 0\\ 0 & \frac{1}{p_2}\end{bmatrix}$$

$$f_+(z) = \begin{bmatrix}e^{iq_1 z} & 0\\ 0 & e^{iq_2 z}\end{bmatrix} \qquad f_-(d-z) = \begin{bmatrix}e^{-ip_1(d-z)} & 0\\ 0 & e^{-ip_2(d-z)}\end{bmatrix}$$

$$\Phi_+ = \begin{bmatrix}\phi_{x_1} & \phi_{x_2}\\ \phi_{y_1} & \phi_{y_2}\end{bmatrix} \qquad \Phi_- = \begin{bmatrix}\psi_{x_1} & \psi_{x_2}\\ \psi_{y_1} & \psi_{y_2}\end{bmatrix}$$

The equations (3.91) and (3.92) can be written in a compactness way as:

$$\begin{bmatrix}\mathbf{e}_{||}(z)\\ \mathbf{h}_{||}(z)\end{bmatrix} = M\begin{bmatrix}f_l^{+}(z)\,\mathbf{a}\\ f_l^{-}(d_l - z)\,\mathbf{b}\end{bmatrix} \tag{3.93}$$

The matrix M is define by the 2×2 block matrices by:

$$M_{11} = A_0^{(b)}\Phi_+ q^{-1} + A_1^{(b)}\Phi_+ + A_2\Phi_+ q, \tag{3.94}$$
$$M_{12} = A_0^{(b)}\Phi_- p^{-1} + A_1^{(b)}\Phi_- + A_2\Phi_- p, \tag{3.95}$$
$$M_{21} = \Phi_+ \tag{3.96}$$
$$M_{22} = \Phi_- \tag{3.97}$$

In order to find explicit expressions for $\mathbf{a}$ and $\mathbf{b}$ at the l-layer, the matrix scattering approach is shown above. This method relates the amplitudes of forward and backward waves in different layers. Let $\mathbf{a}_0$ and $\mathbf{b}_0$ the amplitudes for the forward and backward waves in the medium of incidence, $\mathbf{a}_l$ and $\mathbf{b}_l$ the waves in the l-th layer, $\mathbf{a}_N$ and $\mathbf{b}_N$ in the substrate (see figure 3.6).

The scattering between the layers 0 and l can be written in matrix form as:

$$\begin{bmatrix}\mathbf{a}_l \\ \mathbf{b}_0\end{bmatrix} = \begin{bmatrix}S_{11}(0,l) & S_{12}(0,l) \\ S_{21}(0,l) & S_{22}(0,l)\end{bmatrix}\begin{bmatrix}\mathbf{a}_0 \\ \mathbf{b}_l\end{bmatrix} \tag{3.98}$$

In a similar way the relation between the amplitudes at the layers l and N are related via:

$$\begin{bmatrix}\mathbf{a}_N \\ \mathbf{b}_l\end{bmatrix} = \begin{bmatrix}S_{11}(l,N) & S_{12}(l,N) \\ S_{21}(l,N) & S_{22}(l,N)\end{bmatrix}\begin{bmatrix}\mathbf{a}_l \\ \mathbf{b}_N\end{bmatrix} \tag{3.99}$$

Solving for $\mathbf{a}_l$ and $\mathbf{b}_l$ we have:

$$\mathbf{a}_l = [I_2 - S_{12}(0,l)\,S_{21}(l,N)]^{-1}\,[S_{11}(0,l)\,\mathbf{a}_0 + S_{12}(0,l)\,S_{22}(l,N)\,\mathbf{b}_N] \tag{3.100}$$
$$\mathbf{b}_l = [I_2 - S_{21}(l,N)\,S_{12}(0,l)]^{-1}\,[S_{21}(l,N)\,S_{11}(0,l)\,\mathbf{a}_0 + S_{22}(l,N)\,\mathbf{b}_N] \tag{3.101}$$

The matrix I_2 is the 2×2 identity matrix $I_2 = \begin{bmatrix}1 & 0 \\ 0 & 1\end{bmatrix}$. Analytical closed expressions for $S_{ij}(0,l)$ and $S_{ij}(l,N)$ are deduced above.

3.7.3 Scattering Matrices

The continuity of the parallel fields at the interface of the l-th and $l+1$-th layers in terms of the electric and magnetic fields are described by:

$$\begin{bmatrix}\mathbf{e}_{||}(d_l) \\ \mathbf{h}_{||}(d_l)\end{bmatrix}_l = \begin{bmatrix}\mathbf{e}_{||}(0) \\ \mathbf{h}_{||}(0)\end{bmatrix}_{l+1}$$

Where, d_l is the thickness of the l-th layer. Using the equation 3.93 in both sides of the previous equation, then:

$$\begin{bmatrix}f_l^+(d_l)\,\mathbf{a}_l \\ \mathbf{b}_l\end{bmatrix} = I(l,l+1)\begin{bmatrix}\mathbf{a}_{l+1} \\ f_l^-(d_{l+1})\,\mathbf{b}_{l+1}\end{bmatrix} \tag{3.102}$$

The matrix $I(l,l+1)$ is called *interface matrix* and is given by $I(l,l+1) = M_l^{-1}M_{l+1}$. The scattering process that can occur from one layer (l') to another (l) could be described by:

$$\begin{bmatrix}\mathbf{a}_l \\ \mathbf{b}_{l'}\end{bmatrix} = S(l',l)\begin{bmatrix}\mathbf{a}_{l'} \\ \mathbf{b}_l\end{bmatrix} \tag{3.103}$$

With the equations (3.102) and (3.103) and doing the appropriate algebra the components (2×2 matrices) of the scattering matrix $S(0,l)$ are given by:

$$\begin{aligned}
S_{11}(l',l+1) &= \left[I_{11}(l,l+1) - f_l^+(d_l)\,S_{12}(l',l)\,I_{21}(l,l+1)\right]^{-1} f_l^+(d_l)\,S_{11}(l',l)\\
S_{12}(l',l+1) &= \left[I_{11}(l,l+1) - f_l^+(d_l)\,S_{12}(l',l)\,I_{21}(l,l+1)\right]^{-1}\\
&\quad\times\left[-I_{12}(l,l+1) + f_l^+(d_l)\,S_{12}(l',l)\,I_{22}(l,l+1)\right] f_{l+1}^-(d_{l+1})\\
S_{21}(l',l+1) &= S_{22}(l',l)\,I_{21}(l,l+1)\,S_{11}(l',l+1) + S_{21}(l',l)\\
S_{22}(l',l+1) &= S_{22}(l',l)\,I_{21}(l,l+1)\,S_{12}(l',l+1) + S_{22}(l',l)\,I_{22}(l,l+1)\,f_{l+1}^-(d_{l+1})
\end{aligned} \tag{3.104}$$

The 2×2 block matrices are defined recurrently starting with $S(0,l) = I_4$, where I_4 is the 4×4 identity matrix.

Following a similar reasoning based on Moncada's work (Moncada, 2015), the scattering matrices $S(l,N)$ can be found from the boundary condition (3.103) rewritten as:

$$\mathbf{a}_{l+1} = I_{11}(l+1,l)\,f_l^+(d_l)\,\mathbf{a}_l + I_{12}(l+1,l)\,\mathbf{b}_l \tag{3.105}$$

$$f_{l+1}^-(d_{l+1})\,\mathbf{b}_{l+1} = I_{21}(l+1,l)\,f_l^+(d_l)\,\mathbf{a}_l + I_{22}(l+1,l)\,\mathbf{b}_l \tag{3.106}$$

Now the interface matrices are defined by $I(l+1,l) = M_{l+1}^{-1}M_l$, also:

$$\mathbf{a}_N = S_{11}(l+1,N)\,\mathbf{a}_{l+1} + S_{12}(l+1,N)\,\mathbf{b}_N \tag{3.107}$$

$$\mathbf{b}_{l+1} = S_{21}(l+1,N)\,\mathbf{a}_{l+1} + S_{22}(l+1,N)\,\mathbf{b}_N \tag{3.108}$$

Eliminating $\mathbf{a}_{l+1}$ and $\mathbf{b}_{l+1}$ from the equations (3.105) - (3.108)

$$\begin{aligned}
S_{22}(l,N) &= \left[I_{22}(l+1,l) - f_{l+1}^-(d_{l+1})\,S_{21}(l+1,N)\,I_{12}(l+1,l)\right]^{-1}\\
&\quad\times f_{l+1}^-(d_{l+1})\,S_{22}(l+1,N)\\
S_{21}(l,N) &= \left[I_{22}(l+1,l) - f_{l+1}^-(d_{l+1})\,S_{21}(l+1,N)\,I_{12}(l+1,l)\right]^{-1}\\
&\quad\times\left[f_{l+1}^-(d_{l+1})\,S_{21}(l+1,N)\,I_{11}(l+1,l)\,f_l^+(d_l) - I_{21}(l+1,l)\,f_l^+(d_l)\right]\\
S_{11}(l,N) &= S_{11}(l+1,N)\,I_{11}(l+1,l)\,f_l^+(d_l) + S_{11}(l+1,N)\,I_{12}(l+1,l)\,S_{21}(l,N)\\
S_{12}(l,N) &= S_{12}(l+1,N) + S_{11}(l+1,N)\,I_{12}(l+1,l)\,S_{22}(l,N)
\end{aligned} \tag{3.109}$$

The matrices $S(l,N)$ are calculated iteratively from the end to the structure, but in this case the initial set up is the matrix $S(N,N) = I_4$.

3.7.4 Reflection and Transmission Amplitudes

The transmission and reflection matrices relate the incident with the transmitted and reflected fields, respectively. In terms of the electric field they can be written as:

$$\begin{bmatrix} E_{x,0}^{(r)} \\ E_{y,0}^{(r)} \end{bmatrix} = R_0 \begin{bmatrix} E_{x,0}^{(i)} \\ E_{y,0}^{(i)} \end{bmatrix} \tag{3.110}$$

$$\begin{bmatrix} E_{x,N}^{(t)} \\ E_{y,N}^{(t)} \end{bmatrix} = T_0 \begin{bmatrix} E_{x,0}^{(i)} \\ E_{y,0}^{(i)} \end{bmatrix} \tag{3.111}$$

The super index denote the reflected (r), transmitted (t) and incident (i) field components of the wave at the layer 0 and N. Assuming both, the medium of incidence and the substrate isotropic, the resulting eigenvalues are degenerate ($q_1 = q_2 = -p_1 = -p_2$), from the equations (3.93) and (3.66) is possible obtain:

$$E_{x,0} = \left[\left(M_{0,21}a_{0,1} + M_{0,22}a_{0,2}\right)e^{iq_0 z} + \left(M_{0,23}b_{0,1} + M_{0,24}b_{0,2}\right)e^{-iq_0 z}\right]e^{i\mathbf{k}\cdot\mathbf{r}} \tag{3.112}$$

$$-E_{y,0} = \left[\left(M_{0,11}a_{0,1} + M_{0,12}a_{0,2}\right)e^{iq_0 z} + \left(M_{0,13}b_{0,1} + M_{0,14}b_{0,2}\right)e^{-iq_0 z}\right]e^{i\mathbf{k}\cdot\mathbf{r}} \tag{3.113}$$

The matrix $M_{0,ij}$ denote the element in the row i and column j of the 4×4 M-matrix in the medium of incidence. The M-matrix is defined by the equations (3.94)-(3.97). The propagation mode of the wave is **x** ($E_{y,0} = 0$) or **y** ($E_{x,0} = 0$). In the first case the forward propagating term in equation (3.112) must be zero and:

$$a_{0,1} = -\frac{M_{0,12}}{M_{0,11}}a_{0,2} \tag{3.114}$$

The amplitude $a_{0,2}$ is set as 1. The components of the reflection matrix $R_{0,11}$ and $R_{0,21}$ are found setting $E_{y,0} = 0$ (x-polarization) in a similar way $R_{0,12}$ and $R_{0,22}$ are found setting $E_{x,0} = 0$ (y-polarization), then for x-polarization:

$$R_{0,11} = \frac{E^{(r)}_{x,0}}{E^{(i)}_{x,0}} = \frac{M_{0,23}b_{0,1} + M_{0,24}b_{0,2}}{M_{0,21}a_{0,1} + M_{0,22}a_{0,2}} \tag{3.115}$$

$$R_{0,21} = \frac{E^{(r)}_{y,0}}{E^{(i)}_{x,0}} = -\frac{M_{0,13}b_{0,1} + M_{0,14}b_{0,2}}{M_{0,21}a_{0,1} + M_{0,22}a_{0,2}} \tag{3.116}$$

For y-polarization $a_{0,2} = -\frac{M_{0,21}}{M_{0,22}}a_{0,1}$ the reflection matrix components $R_{0,12}$, $R_{0,22}$ are:

$$R_{0,12} = \frac{E^{(r)}_{x,0}}{E^{(i)}_{y,0}} = -\frac{M_{0,23}b_{0,1} + M_{0,24}b_{0,2}}{M_{0,11}a_{0,1} + M_{0,12}a_{0,2}} \tag{3.117}$$

$$R_{0,22} = \frac{E^{(r)}_{y,0}}{E^{(i)}_{y,0)}} = \frac{M_{0,13}b_{0,1} + M_{0,14}b_{0,2}}{M_{0,11}a_{0,1} + M_{0,12}a_{0,2}} \tag{3.118}$$

Since there is no incident wave from the substrate, $\mathbf{b}_N = 0$, and from equations (3.93) and (3.66) we obtain:

$$E_{x,N} = \left(M_{N,21}a_{N,1} + M_{N,22}a_{N,2}\right)e^{iq_N z}e^{i\mathbf{k}\cdot\mathbf{r}} \tag{3.119}$$

$$-E_{y,N} = \left(M_{N,11}a_{N,1} + M_{N,12}a_{N,2}\right)e^{iq_N z}e^{i\mathbf{k}\cdot\mathbf{r}} \tag{3.120}$$

The previous expressions with the equations (3.111) - (3.113) give $T_{N,11}$ and $T_{N,21}$ components for x-polarization:

$$T_{N,11} = \frac{E^{(t)}_{x,N}}{E^{(i)}_{x,0}} = \frac{M_{N,21}a_{N,1} + M_{N,22}a_{N,2}}{M_{0,21}a_{0,1} + M_{0,22}a_{0,2}} \tag{3.121}$$

$$T_{N,21} = \frac{E^{(t)}_{y,N}}{E^{(i)}_{x,0}} = -\frac{M_{N,11}a_{N,1} + M_{N,12}a_{N,2}}{M_{0,21}a_{0,1} + M_{0,22}a_{0,2}} \tag{3.122}$$

For y-polarization $T_{N,12}$ and $T_{N,22}$ components are given by:

$$T_{N,12} = \frac{E^{(t)}_{x,N}}{E^{(i)}_{y,0}} = -\frac{M_{M,21}a_{N,1} + M_{N,22}a_{N,2}}{M_{0,11}a_{0,1} + M_{0,12}a_{0,2}} \tag{3.123}$$

$$T_{N,22} = \frac{E^{(t)}_{y,N}}{E^{(i)}_{y,0}} = \frac{M_{N,11}a_{N,1} + M_{N,12}a_{N,2}}{M_{0,11}a_{0,1} + M_{0,12}a_{0,2}} \tag{3.124}$$

The amplitudes: $\mathbf{b}_0$ and $\mathbf{a}_N$ are given by: $\mathbf{b}_0 = S_{21}(0,N)\,\mathbf{a}_0$ and $\mathbf{a}_N = S_{11}(0,N)\,\mathbf{a}_0$ according with (Whittaker and Culshaw, 1999).

Due to the coordinate axis in which the waves are treated is the xyz coordinate system, a convenient transformation is set the wave in a sp-basis, so the figure 3.7 shows an schematic representation of the sp bases in a xyz coordinate system.

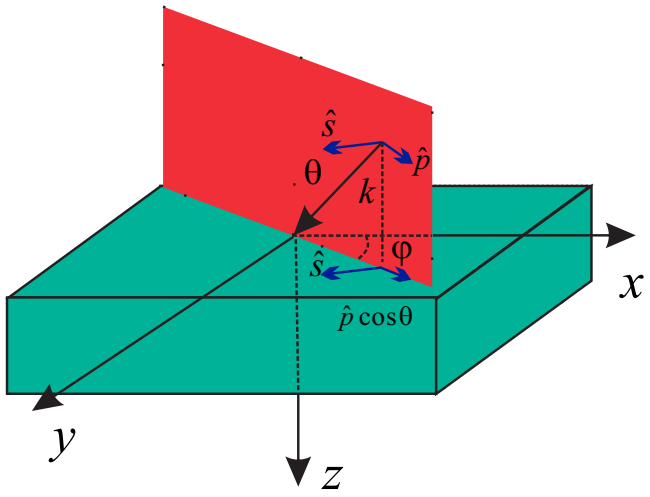

FIGURE 3.7: Polarization states s and p in a xyz coordinate system, θ is the angles of incidence and ψ is the azimuthal angle that will be zero for all purposes of the numerical simulations

The transformation is given by the relations:

$$R_0^{(sp)} = U^{-1} R_0 U \tag{3.125}$$
$$T_N^{(sp)} = U^{-1} T_N U \tag{3.126}$$

The transformation matrix U is:

$$U = \begin{bmatrix} -\sin\psi & \cos\psi \\ \cos\theta\cos\psi & \cos\theta\sin\psi \end{bmatrix} \tag{3.127}$$

3.7.5 Linearised equation of eigenvectors

In order to find the explicit expression of eigenvalues and the eigenvecotrs of the equation (3.81) there is a linearising process introduced by Caballero and colaborators (Caballero, García-Martín, and Cuevas, 2012). Multiplying both sides of equation (3.81) by q and setting $\begin{bmatrix} h_x \\ h_y \end{bmatrix} = \begin{bmatrix} \phi_x \\ \phi_y \end{bmatrix} = \phi$, is possible write:

$$q^3 A_2\phi + q^2 A_1\phi + qA_0\phi + A_{-1}\phi = 0$$

An equivalent matrix form is:

$$\begin{bmatrix} q\phi \\ q^2\phi \\ A_{-1}\phi + qA_0\phi + q^2A_1\phi \end{bmatrix} = \begin{bmatrix} q\phi \\ q^2\phi \\ -q^3A_2\phi \end{bmatrix}$$

Doing the substitutions $\lambda_n = q^{n-1}\phi$ for $n = 1, 2, 3$ and $A_{n-1} = B_n$, the previous matrix identity can be written as:

$$\begin{bmatrix} \lambda_2 \\ \lambda_3 \\ B_0\lambda_1 + B_1\lambda_2 + B_2\lambda_3 \end{bmatrix} = q \begin{bmatrix} \lambda_1 \\ \lambda_2 \\ -B_3\lambda_3 \end{bmatrix}$$

Or,

$$\begin{bmatrix} 0 & 1 & 0 \\ 0 & 0 & 1 \\ B_0 & B_1 & B_2 \end{bmatrix} \begin{bmatrix} \lambda_1 \\ \lambda_2 \\ \lambda_3 \end{bmatrix} = q \begin{bmatrix} 1 & 0 & 0 \\ 0 & 1 & 0 \\ 0 & 0 & -B_3 \end{bmatrix} \begin{bmatrix} \lambda_1 \\ \lambda_2 \\ \lambda_3 \end{bmatrix} \tag{3.128}$$

Where $\mathbf{0}_2$ is the 2×2 matrix of zeros, and 1 is the 2×2 identity matrix.
Setting,

$$AL = \begin{bmatrix} 0 & 1 & 0 \\ 0 & 0 & 1 \\ B_0 & B_1 & B_2 \end{bmatrix} \qquad AR = \begin{bmatrix} 1 & 0 & 0 \\ 0 & 1 & 0 \\ 0 & 0 & -B_3 \end{bmatrix} \qquad \nu = \begin{bmatrix} \lambda_1 \\ \lambda_2 \\ \lambda_3 \end{bmatrix}$$

The equation (3.128) can be transformed into:

$$(AL)\,v = q\,(AR)\,v \tag{3.129}$$
$$(AR)^{-1}\,(AL)\,v = qv \tag{3.130}$$
$$Av = qv \tag{3.131}$$

Here, $A = (AR)^{-1}\,(AL)$. The equation 3.131 is a linear eigenvalues problem that is easily solved via linear algebra techniques.

3.8 Optical and Magneto-Optical Activity

In materials as quartz, or sugar solution, there is a natural optical rotation of the electric field through the optical axes as mentioned by Yariv and Yeh (Yariv and Yeh, 1984). If light is viewed from the source has a right gyration, the material is dextro-rotatory. Else, if light rotates toward the left is called levo-rotatory. This rotation is present mathematically on the dielectric tensor that is now Hermitian so $\varepsilon_{ij} = \varepsilon_{ij}^{*}$. The electric field density can be written as:

$$\mathbf{D} = \varepsilon_a \mathbf{E} + i\varepsilon_o \mathbf{G} \times \mathbf{E}$$

Where ε_a is the dielectric tensor in absence of optical activity, $\mathbf{G}$ is the gyration vector and is parallel to propagation direction. The cross product of $\mathbf{G}$ with $\mathbf{E}$ is defined as: $\mathbf{G} \times \mathbf{E} = [\mathbf{G}]\mathbf{E}$ so $\mathbf{D} = (\varepsilon_a + i\varepsilon_o[\mathbf{G}])\,\mathbf{E}$, then, the Hamiltonian dielectric tensor is $\varepsilon = \varepsilon_a + i\varepsilon_o[\mathbf{G}]$.

In isotropic or uniaxial anisotropic media, the effect of the term $i\varepsilon_o \mathbf{G} \times \mathbf{E}$ is to cause rotation of the light linearly polarized.

The change rate of $\mathbf{E}$ respect to media length z is:

$$\frac{d\mathbf{E}}{dz} = \frac{\pi}{\lambda n}\mathbf{G} \times \mathbf{E}$$

Where n is the refraction index. The rotation angle per length unit (specific rotatory power) is given by:

$$\varrho = \frac{\pi}{\lambda n} G \tag{3.132}$$

Where, $G = |\mathbf{G}|$.

In presence of a external magnetic field some materials can exhibit this rotatory power. This effect is known as *Faraday Effect*, in this case the rotation is proportional to the magnetic field along the light propagation:

$$\mathbf{G} = \gamma \mathbf{B}$$

Where γ is the medium magneto-gyration coefficient. In an optically active medium, the rotation sense has a fixed relation with the propagation direction. In the Faraday Effect the rotation has a fixed relation with the magnetic field $\mathbf{B}$, and the equation (3.132) will be:

$$\varrho = \frac{\pi\gamma}{\lambda n} B \tag{3.133}$$
$$\varrho = VB \tag{3.134}$$

Where V is called Bernet constant.

Brewster found that transparent substances normally isotropic, can be turn on anisotropy optically via mechanic effort, this phenomena is called: mechanic birefringence, photoelasticity or effort birrefringence as commented by Hecht (Hecht, 2017).

3.8.1 The Magneto-optic Kerr Effect

The magneto optic Kerr effect (MOKE) is a description of the behaviour of linear polarized light when is reflected by a medium affected by a external magnetic field. The way that polarization changes depends on the orientation of the external magnetic field (or its magnetization), related to the plane of the surface and the plane of incidence. There are three known geometries related with the orientation of the external magnetic field described by Armelles et. al. and Zvezdin and Kotov (Armelles et al., 2013; Zvezdin and Kotov, 1997). The Polar geometry (PMOKE) in which the magnetic field is perpendicular to the material surface, Longitudinal (LMOKE) where the magnetic field is in incident plane and inplane to the surface and Transversal (TMOKE) where the magnetic field is perpendicular to the surface, and parallel to the incidence plane. See figure 3.8 for the three configurations previously described. The later has several applications on optical data storage as describe by Zvezdin and Kotov (Zvezdin and Kotov, 1997).

$$\varepsilon = \begin{bmatrix} \varepsilon & a\Pi_z & a\Pi_y \\ -a\Pi_z & \varepsilon & -a\Pi_x \\ -a\Pi_y & a\Pi_x & \varepsilon \end{bmatrix} \tag{3.135}$$

A tensor for isotropic material has the principal components equals ($\varepsilon_{xx} = \varepsilon_{yy} = \varepsilon_{zz} = \varepsilon$) and the off-diagonal elements zero which change its values with magnetization or with an external magnetic field. The new shape of the tensor is described by the equation (3.2), all the elements off the diagonal are antisymmetrical and represents the magneto-optic constants of the material found experimentally. The polar, longitudinal and transversal magneto-optic Kerr effect lead to a particular forms of the equation (3.2), they are described in the relations given by (3.136):

$$\hat{\varepsilon}_P = \begin{bmatrix} \varepsilon & a\Pi & 0 \\ -a\Pi & \varepsilon & 0 \\ 0 & 0 & \varepsilon \end{bmatrix} \quad \hat{\varepsilon}_L = \begin{bmatrix} \varepsilon & 0 & 0 \\ 0 & \varepsilon & -a\Pi \\ 0 & a\Pi & \varepsilon \end{bmatrix} \quad \hat{\varepsilon}_T = \begin{bmatrix} \varepsilon & 0 & a\Pi \\ 0 & \varepsilon & 0 \\ -a\Pi & 0 & \varepsilon \end{bmatrix} \tag{3.136}$$

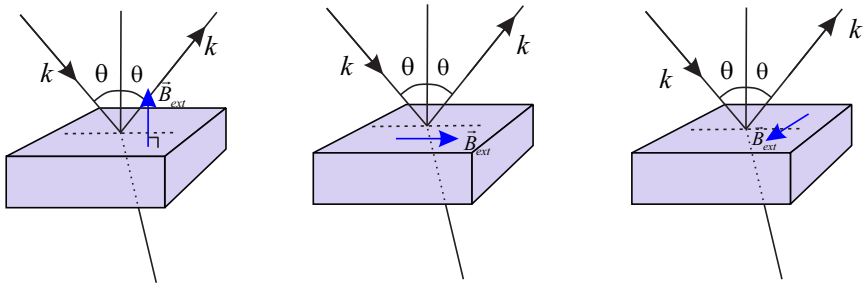

FIGURE 3.8: Three geometries for the Kerr effect . (Left) Polar, (Center) Longitudinal, (Right) Transversal. The vector $\vec{\mathbf{B}}_{ext}$ indicates the external magnetic field.

3.9 Numerical Results

3.9.1 Cojocaru's method - Optical Functions for isotropic media

In the isotropic regime the method proposed by Cojocaru lead us to generalized Abelés relations (Abelès, 1948 & Heavens, 1991). The flux diagram in the figure 3.18 shows a path to calculate Fresnel coefficients and optical functions of reflectance, transmittance and absorptance. Several geometries were tested, beginning with two dielectric media (simple interface), passing through Kretschmann-Raether geometries to a trilayer BK7 ||Au||Si O_2 ||Au||Air, analysed in chapter 2.

Total Internal Reflection

The first geometry tested was the dielectric interface BK7||Air, with $\lambda = 633nm$. The refraction indexes are $n_0 = 1.51$ and $n_1 = 1$ previously analysed in chapter 1, the Fresnel coefficients for reflection and transmission, as well as the optical functions for reflectance and transmittance, they were calculated for p-polarization and s-polarization giving the same results of the chapter 2, see figure 3.9.

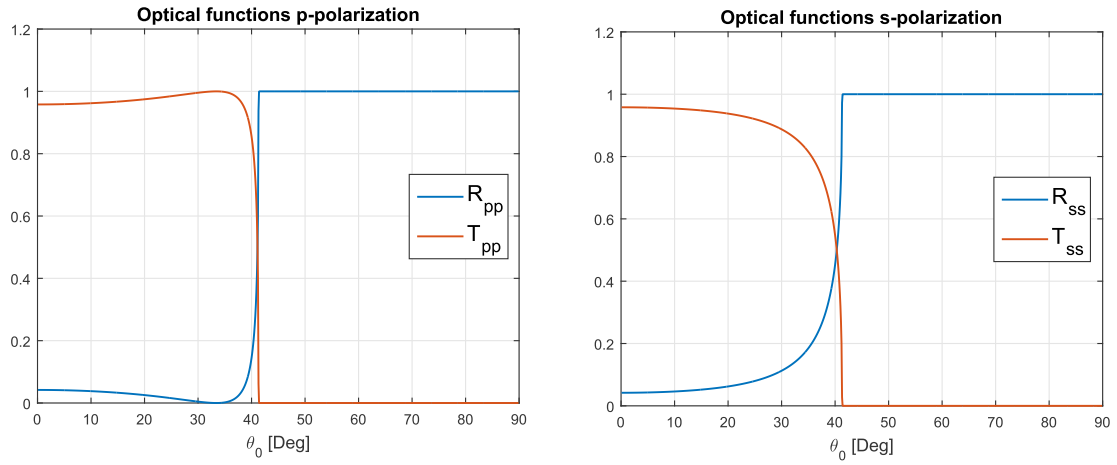

FIGURE 3.9: Optical functions for s and p-polarizations in simple interface BK7||Air for $\lambda = 633nm$ using the Cojocaru's method

Kretschmann-Raether geometry

The second multilayer system tested was the Kretschmann-Raether geometry of a gold isotropic layer embedded in optical glass as medium of incidence and air as substrate. Unusual absorptions are present at a particular angle called plasmon angle, then a representative function is one in which the reflectance, transmittance and absorptance are drawn. A simulation was made for the same range of incident angles as in chapter 2 (from $\theta = 40°$ to $\theta = 50°$). The figure 3.10 shows this representation for all range of incident angles and a subinterval from $\theta_0 = 40°$ to $\theta_0 = 50°$ where the absorption takes place. The constants for this geometry are: $n_{BK7} = 1.51$, $n_{Au} = 0.1834 + 3.4332i$ and $n_{Air} = 1$, the wavelength is $\lambda = 633nm$ and a thickness of gold $d_1 = 47nm$. The results are the same found in the chapter 2 and reported by (Raether, 1988), (Sambles, Bradbery, and Yang, 1991) and (Herreño-Fierro, 2016).

The trilayer BK7 ||Au||Si O_2 ||Au||Air was simulated, the obtained functions are the same that the figure 2.8.

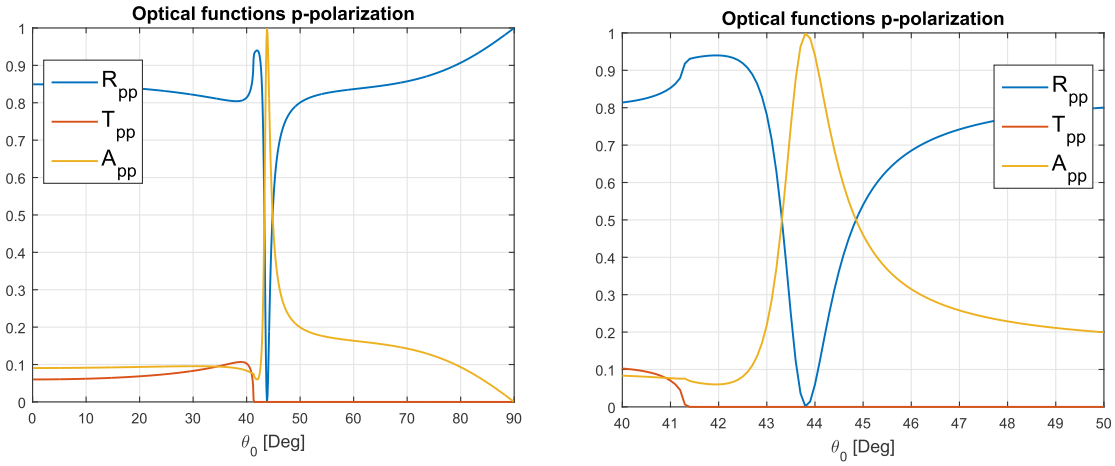

FIGURE 3.10: Optical functions for the Kretschmann & Raether geometry. (Left) For all angles of incidence, (right) For a range of angles of incidence $40° \leq \theta_0 \leq 50°$

3.9.2 Cojocaru's method - Optical Functions for anisotropic media

Cojocaru's method require know the constants $a_\alpha^\pm$, $a_\beta^\pm$, $b_\alpha^\pm$ and $b_\beta^\pm$ with the purpose of finding the transmission and reflection matrices, then the electric and magnetic field unitary vectors must be known. To do that, the study of Laundry and Maldonado (Landry and Maldonado, 1995) is useful on the treatment of anisotropic media. The solutions of the quartic equation are ordered in a way such that we know which one is ζ_α^+, ζ_α^-, ζ_β^+ and ζ_β^-, this is possible because the values of n are known, with the increment of the real part of each value of n the normal wave vector z-component will increase so θ will decrease. Then, we calculate the propagation unit vector $\hat{\mathbf{k}}$ for each ζ for any anisotropic medium. An auxiliary matrix J is calculated as follows:

$$J = \epsilon - n^2 I_3 \tag{3.137}$$

Where I_3 is the 3×3 identity matrix, n have four values n_α^+, n_α^-, n_β^+, n_β^- determined by the equation (3.30), ε is the dielectric tensor given by the equation (3.2). All Euler angles must be known by the user to calculate rotation matrix (3.3). After having the J-matrix the adjugate matrix of J is found $adj(J)$, so there are three possibilities, each one of the will give a possible electric unit vector for electrical field:

1. If J is nonsingular $\det(J) \neq 0$, then the unit electric field vector is $\hat{\mathbf{e}} = adj(J) \cdot \hat{\mathbf{k}}$.
2. If J is singular $\det(J) = 0$ and planar $adj(J) \neq \mathbf{0}_3$, then $\hat{\mathbf{e}}$ is any non zero column of $adj(A)$
3. If J is singular $\det(J) = 0$ and linear $adj(J) = \mathbf{0}_3$, then $\hat{\mathbf{e}}$ is any non zero column of J.

Where, the $\mathbf{0}_3$ is the 3×3 zero matrix. The displacement unit vector can be found from $\mathbf{d} = \varepsilon\hat{\mathbf{e}}$ and $\hat{\mathbf{d}} = \frac{\mathbf{d}}{|\mathbf{d}|}$. The walk-off angle between the electric field vector and displacement vector can be found from the relation (for each ζ and each angle of incidence):

$$\eta = -sign\left(\hat{\mathbf{k}} \cdot \hat{\mathbf{e}}\right) \cos^{-1}\left(\hat{\mathbf{d}} \cdot \hat{\mathbf{e}}\right) \tag{3.138}$$

The magnetic field unit vector is determined via:

$$\hat{\mathbf{h}} = \hat{\mathbf{k}} \times \hat{\mathbf{d}} \tag{3.139}$$

Having the values of $\hat{\mathbf{e}} = (e_x, e_y, e_z)$, $\hat{\mathbf{h}} = (h_x, h_y, h_z)$, η and n for each wave in each anisotropic medium, the constants given by the equations (3.36 - 3.38) can be calculated. Therefore, the matrices for reflection, transmission and propagation can be computed. Hence the propagation matrix will be well defined. A bilayer structure compound of Air ||Biaxial||Biaxial||BK7 was tested the refraction index are, for the air $n_0 = 1$, for both biaxial layers $n_x = 1.60$, $n_y = 1.65$, $n_z = 2.25$ and the substrate $n_{sub} = 1.5$. The thickness of each layer is the same $d = 207.5nm$. The Euler angles are $\psi = 15°$, $\phi = 45°$, $\theta = 45°$, for the first biaxial layer, for second biaxial layer the Euler angles are given by: $\psi = 165°$, $\phi = 135°$, $\theta = 135°$, results of reflectance and transmittance for both polarizations were above the unit so we do not include them. We are still working on this issue.

3.9.3 Cojocaru's method - Optical Functions for Induced anisotropy for magnetooptic media

There are two geometries with magneto-optic activity that are simulated in order to contrast with. The first one is the trilayer Au||Co||Au embedded in glass as incidence media and air as substrate, studied by Herreño and Patño (Herreño-Fierro and Patiño, 2015) with a wavelength $\lambda = 532nm$. The polarization of the wave (vectors $\hat{\mathbf{e}}$ and $\hat{\mathbf{h}}$) given by the appendix C via Jones vectors can be introduced in the program but for all polarization states the results are the same. The figure 3.11 shows optical functions in p-polarization with angular dependence.

Another geometry sufficiently reported (Balasubramanian, Marathay, and Macleod, 1988, Mansuripur, 1990, Abdulhalim, 1999) is compound by Air || SiO_2 || SbTe || SiO_2 || Al || BK7, layer SbTe is magneto-optic, the refractive index for air $n_0 = 1$, silicon dioxide refractive index is $n_1 = 1.4528$ with a thickness $d_{SiO_2} = 143.2nm$, the magneto-optic layer SbTe has a relative epsilon $\varepsilon_{xx} = \varepsilon_{yy} = \varepsilon_{zz} = \varepsilon_r = -4.8984 + 19.415i$ with off-diagonal elements $\varepsilon_{xy} = -\varepsilon_{yx} = 0.4322 + 0.0058i$, $\varepsilon_{xz} = \varepsilon_{zx} = \varepsilon_{yz} = \varepsilon_{zy} = 0$, $d_{SbTe} = 20nm$, the third layer as the same of the first SiO_2 with $n_3 = 1.4528$ and $d_{SiO_2} = 143.2nm$. The metal layer Aluminium has a refractive index $n_{Al} = 2.72 + 8.21i$, with a thickness $d_{Al} = 500nm$ and finally the substrate BK7 has a refractive index $n_{BK7} = 1.51$, the wavelength is $\lambda = 830nm$. The reflectance (R_{ss}, R_{sp}, R_{ps}, R_{pp}) is shown in the figure 3.11 (left). Note that reflectance R_{sp} and R_{ps} are the same and have been scaled by a factor of 1000. Obtained results are not the same as the reported in the literature, the shape is similar but numerically the values does not reproduce the results. We are still working on this issue.

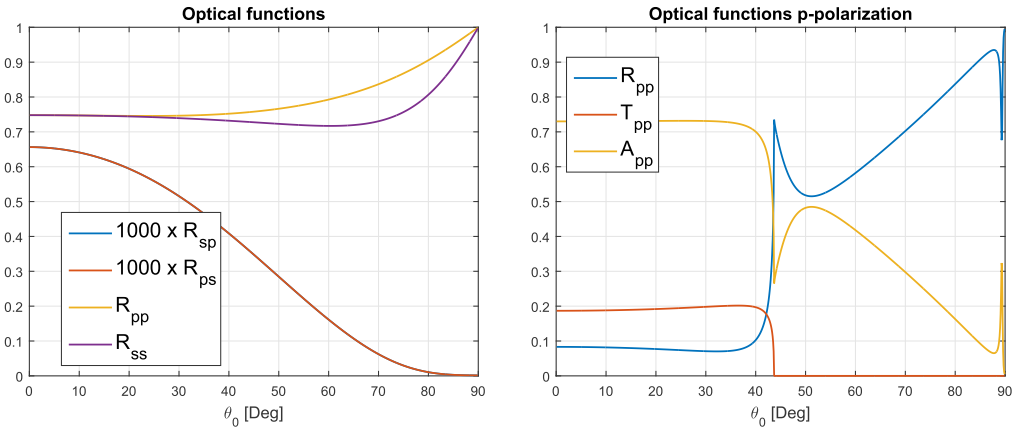

FIGURE 3.11: (left) Reflectance with angular dependence for a magneto-optic geometry Air || SiO_2 || SbTe || SiO_2 || Al || BK7 for a wavelength $\lambda = 830nm$. (Right) Optical functions with angular dependence for a magneto-optic geometry BK7||Au||Co||Au||Air for a wavelength $\lambda = 532nm$ and p-polarization. The thickness of the inner layers $d_{Au} = 14.1nm$, $d_{Co} = 10.2nm$, $d_{Au} = 0.5nm$.

3.9.4 Scattering matrix method - Optical Functions for isotropic media

The scattering matrix method is the second followed method for calculate optical functions for isotropic and magneto-optic induced anisotropic media. The obtained results are summarized here for the same previous geometries tested via Cojocaru's method, the simple interface BK7||Air for $\lambda = 633nm$, the Krestchamnn & Raether geometry BK7||Au||Air for $\lambda = 633nm$ with $d_{Au} = 47nm$. Figures 3.12 and 3.13.

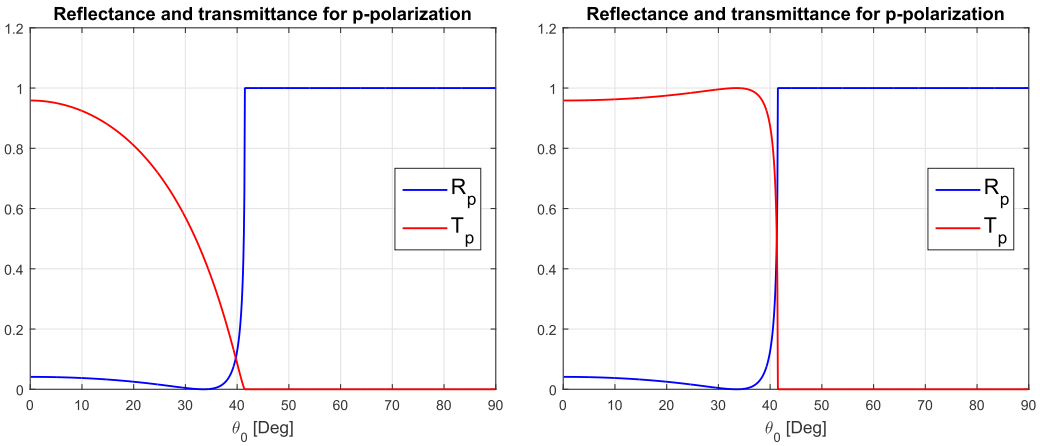

FIGURE 3.12: Optical functions with angular dependence for simple interface BK7||Air for $\lambda = 633nm$ calculated with the scattering matrix method. (Left) original results from the method. (Right) correcting the transmittance.

The method has an issue evidenced by the transmittance for p-polarization in both figures (the $R+T=1$ is not satisfied). An analytic algorithm can be developed in scattering matrix approach for isotropic simple

interface showing that the transmittance has an extra factor of $\frac{\sqrt{1-\left(\frac{n_1 \sin\theta_0}{n_2}\right)^2}}{\cos\theta_0}$, that is precisely the expression of (1.14). So, multiplying by $\frac{1}{\alpha}$ the value of the equation (3.121) the Fresnel coefficient and consequently the transmittance has the shape obtained in chapter 1.

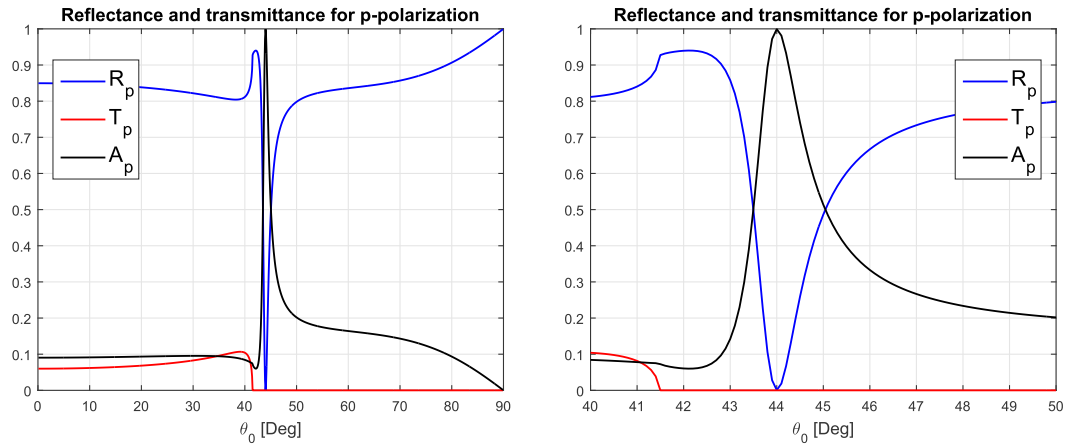

FIGURE 3.13: Optical functions with angular dependence for the Kretschmann & Raether geometry BK7|| Au ||Air for a wavelength $\lambda = 633nm$. For all angles of incidence, (right) For a range of angles of incidence $40° \leq \theta_0 \leq 50°$.

3.9.5 Scattering matrix method - Optical Functions for induced anisotropy for magneto-optic media

As well as the isotropic and anisotropic media calculated via Cojocaru's method and contrasted by the scattering matrix method, the induced anisotropy for magneto-optic media geometries were also calculated by means of scattering matrix method for the geometries tested before with the Cojocaru's method.

The first one is the geometry BK7||Au||Co||Au||Air (left) figure 3.14. The second one is the geometry Air || SiO_2 || SbTe || SiO_2 || Al || BK7, (right) figure 3.14. The optical functions have similar behaviour but, they do not have equal numerical results. Also, the cross polarization R_{sp} and R_{ps} the values are totally differents. Results which differs from those given in (Balasubramanian, Marathay, and Macleod, 1988), (Mansuripur, 1990) and (Abdulhalim, 1999). Nevertheless, experimental results for trilayer Au||Co|| Au, shows data for the reflectance closest to the scattering matrices (Herreño-Fierro and Patiño, 2015).

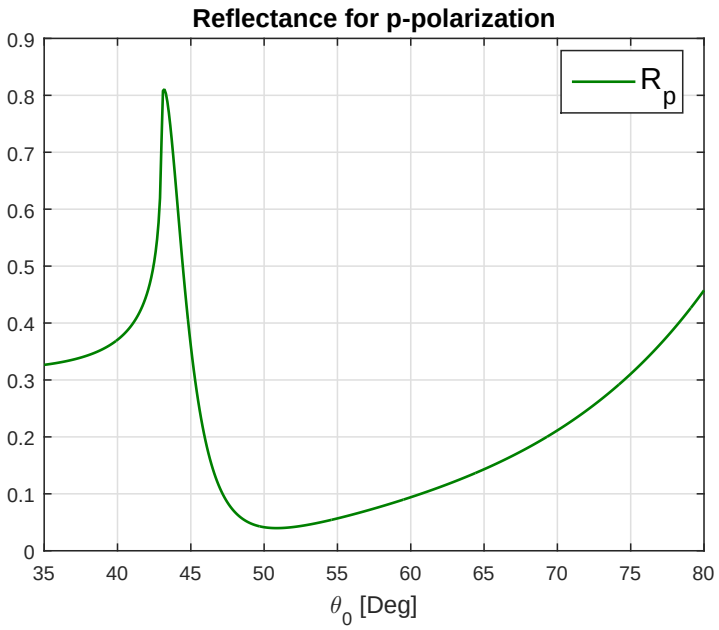

FIGURE 3.14: Reflectance with angular dependence for a magneto-optic geometry BK7||Au(14.1)||Co(10.2)||Au(0.5)||Air for a wavelength $\lambda = 533nm$ and p-polarization.

3.10 Numerical Results - Module of electric field

3.10.1 Cojocaru's electric field

Once the steps of the algorithm were conceived, some known geometries were studied. The first geometry tested was Kretschamnn-Raether, the functions obtained were compared with previous results found from the Airy's formulas and 2×2 matrix method in chapter 2. Setting the same structure parameters the results are in the figure 3.15 for an angle of incidence 40° and 43.84°.

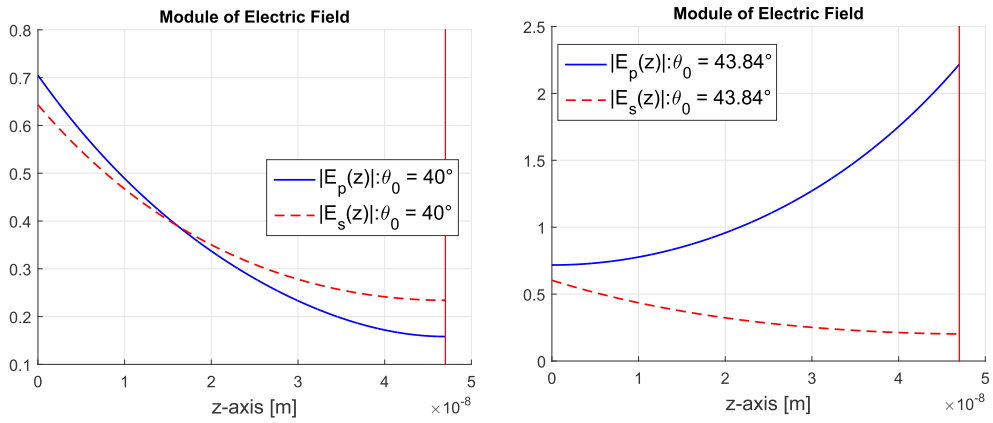

FIGURE 3.15: Electric field module for Kretschmann geometry in the inner layer (Gold) with a wavelength of $\lambda = 633nm$ for p-polarization, gold has a thickness of $d_1 = 47nm$.

One geometry tested in chapter 2 was the SiO||Au||BK7||Au||Air. The electric field module was

plotted for three different angles for p and s-polarization respectively, thought electric fields becomes larger that results obtained for isotropic multilayer at the end of chapter 2.
In the geometry BK7||Au||Co||Au||Air the non-diagonal elements of the dielectric tensor can be modified, by means of an external magnetic field, due to the cobalt layer. The electric field was calculated in $\theta = 44°$ for two polarizations as is shown in the figure 3.16.

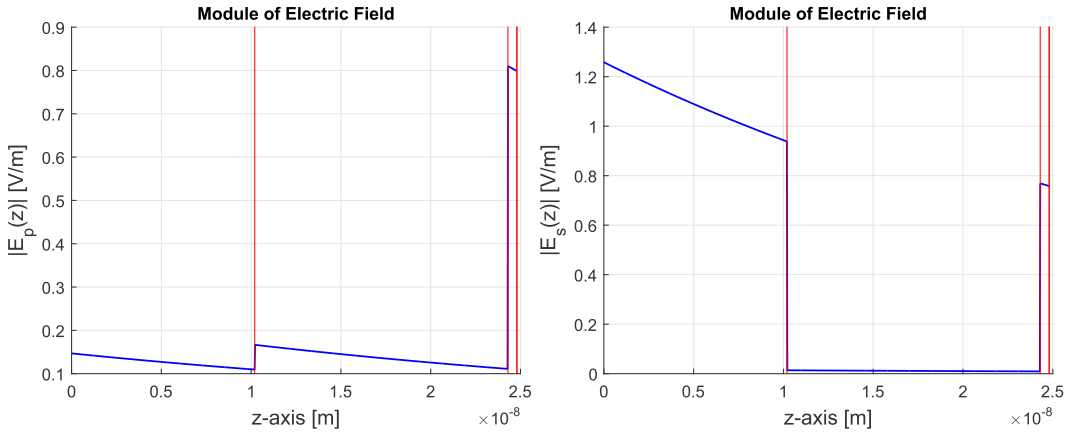

FIGURE 3.16: Electric field module for trilayer Au||Co||Au, angle of incidence $\theta_0 = 44°$ with a wavelength of $\lambda = 532nm$ for (left) p-polarization and (right) s-polarization.

3.11 Numerical Results - Magneto-optic signal

The magneto-optic signal is a measurable quantity calculated for magneto-optic Kerr effect polar, longitudinal and transversal (Armelles et al., 2013). The expression for polar and longitudinal have the same formula, given by:

$$\theta + i\psi = \frac{r_{ps}(\Pi)}{r_{pp}} \tag{3.140}$$

While the transversal has the shape:

$$\frac{\Delta R_{pp}(\Pi)}{R_{pp}} = \frac{R(+M) - R(-M)}{R(0)} \tag{3.141}$$

The figure 3.17 shows a function of the TMOKE (Transversal Magneto-optic Kerr Effect) for the trilayer Au||Co||Au whose optical functions were previously simulated via scattering matrix in the figure 3.14. The function obtained has a behaviour described by Herreño (Herreño-Fierro and Patiño, 2015) for thicknesses Au bottom 14.1nm, Co 10.2nm and Au top 0.5nm for each mentioned layer.

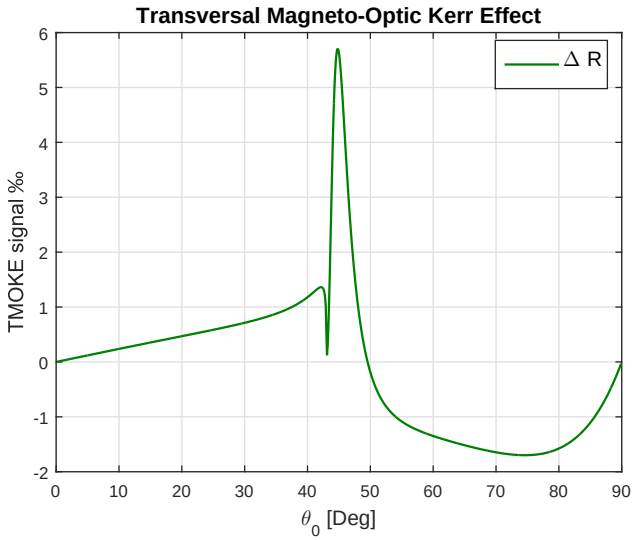

FIGURE 3.17: TMOKE signal for the trilayer geometry BK7||Au(14.1)||Co(10.2)||Au(0.5)||Air for $\lambda = 532nm$ with angular dependence. Note the vertical axis is in per thousand (‰).

3.12 Flux diagram - Optical functions Cojocaru's method

In the figure 3.18 is shown the flux diagram followed to find the Fresnel coefficients and optical functions with angular dependence:

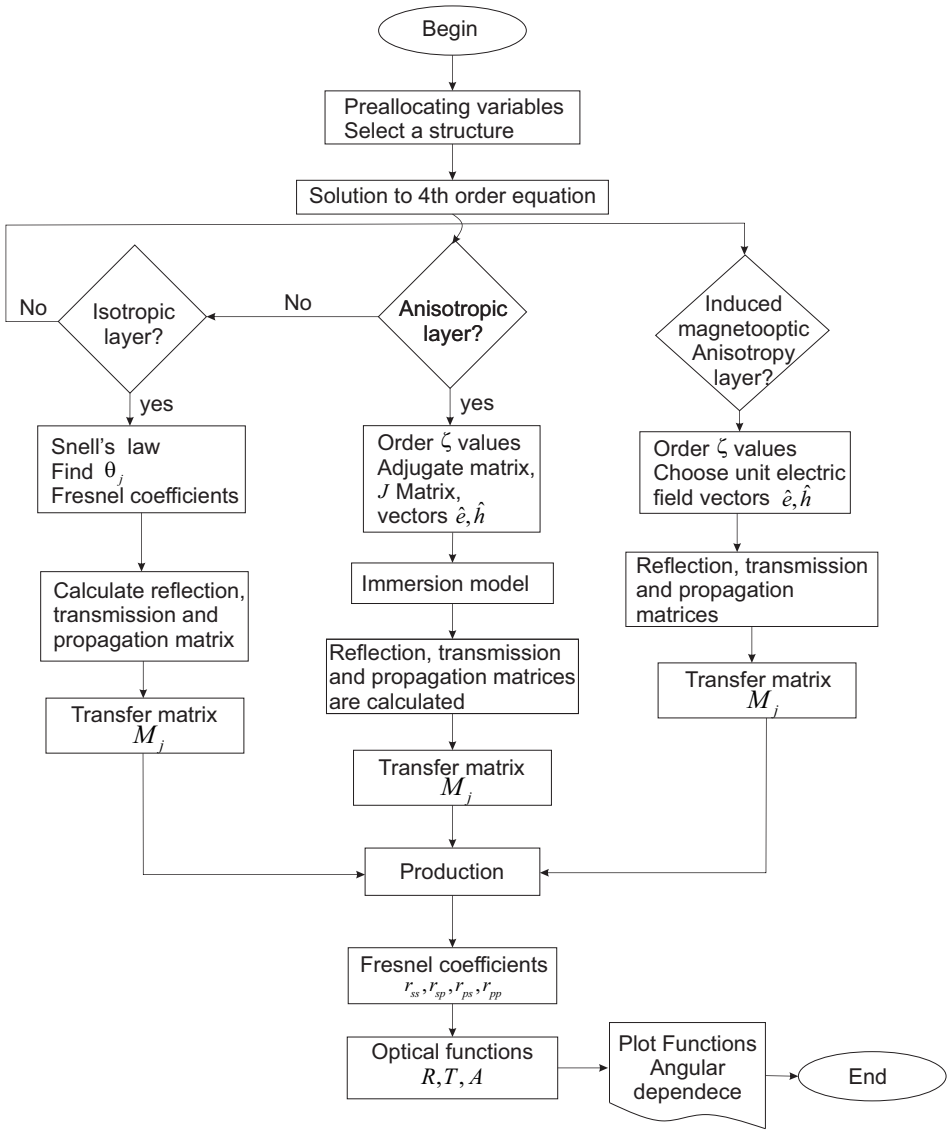

FIGURE 3.18: Flux diagram using the immersion model to find Fresnel coefficients and optical functions

3.13 Flux diagram electric field - Cojocaru's method

In the figure 3.19 is shown the flux diagram followed to find the amplitudes of the electric field in each anisotropic layer using the immersion model proposed by Cojocaru:

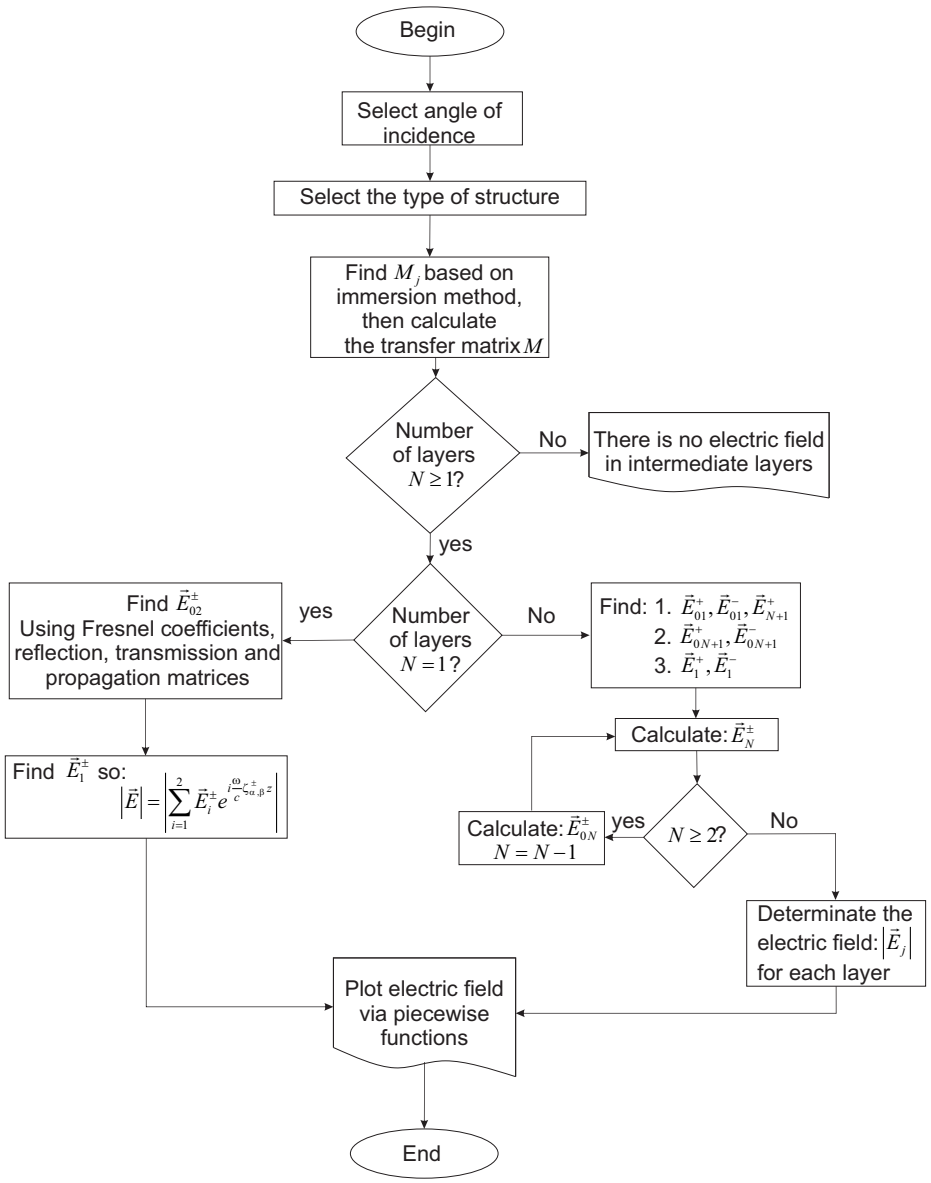

FIGURE 3.19: Flux diagram using the immersion model to find amplitude of electric fields in each layer for a multilayer anisotropic media

Chapter 4

Discussion & Conclusions

Propagation of light in multilayer thin film structures were studied for isotropic and anisotropic layers. All the treatment began with the study of the theory reported in textbooks, articles and doctorate thesis, leading the equations to an algorithm that allowed to compute and plot the Fresnel coefficients, the measurable response optical functions (reflectance and transmittance), and the distribution of the electric field along the structure, as function of the angle of incidence of the radiation to the illuminated surface. Some of the obtained curves were contrasted with those from the textbooks, articles and doctoral thesis. From the methods treated, there are autonomous deductions and corrections of the methods. Here, we discuss the results obtained for different systems, starting from a single interface addressed in chapter one, passing through a multilayer thin film isotropic layers and ending with the study of anisotropic multilayers. In each deduction the starting point was the Maxwell equations, when necessary these equations were recalled and modified for a particular approach.

The first system was the simple interface. For that, we deduced analytical expressions for Fresnel coefficients and optical functions with angular dependence. Figures 1.4 and right side of 1.6 show the same behaviour of those reported by Eugene Hecht (Hecht, 2017). The simulations found in a simple interface with a conducting surface (see figure 1.11) can be contrasted with results by P. Yeh (Yeh, 2005). The same shape of the reflectance (for both polarizations states, s and p) was obtained for any interface dielectric-metal, although the amplitudes of the reflectance can be different depending on the wavelength and the metal involved.

For interaction of waves with matter in one thin film layer (monolayer), we initially studied the Airy's formulas. Fresnel coefficients were represented only analytically and optical functions were directly computed for the Kretschmann & Raether geometry, finding the result in Fig. 2.3 which have the desire shape compared with those obtained by C. Herreño-Fierro and colaborators (Herreño-Fierro, 2016). Distribution of electric field along the transversal coordinate of the structure was derived in an autonomous way and then it was simulated for the so called plasmon angle obtained for the Kretschmann & Raether configuration. The calculations in figure 2.5 shows an enhancement for the distribution of electric field in p-polarization where unusual absorptions take effect.

Optics of multilayer thin film was studied through the 2×2 transfer matrix method. This approach leads to M-matrix for isotropic layers, it was useful to find Fresnel coefficients and consequently optical functions. An algorithm was created with purpose to know the optical functions of multilayer structures. Based on the program designed an optimization of the multilayer Au || SiO_2 || Au was found in the work of Palencia-Barrera, and collaborators (Palencia-Barrera, 2018). The figure 2.8 contains the results for the simulated optical functions of a trilayer showing an unusual abosorption at an angle of incidence of 50.3°. Also the program was used to control the effectiveness of optical response work of L. P. Quiroga-Sánchez

and collaborators (Quiroga-Sáchez, 2018).

The procedure of 2×2 transfer matrices was used to derive in an autonomous way the total amplitudes of the electric field backward and forward in each layer. The method was able to simulate the total distribution of electric field. Functions left and right in figure 2.9 were obtained from the simulation based in the analytical method found as a function of the z-axis trasnversal to the structure. The results helped to develop the work of A. X. Rodríguez-Rodríguez and collaborators (Rodríguez-Rodríguez, 2018).

The implementation of 4×4 transfer matrix method developed by Yeh shows inefficient behaviour in the limit of isotropy. A demonstration was carried out to show this fact, as well as the mandatory fact that neither of the wave components could be zero. Searching for a method that simulate isotropic and anisotropic multilayer thin film structures the Cojocaru's approach was studied, its method gives quite good results for isotropic media, but for magneto-optic anisotropy the calculations (see Fig. 3.11) differ from the graphics reported by Mansuripur (Mansuripur, 1990) and by C. Herreño-Fierro and colaborators (Herreño-Fierro and Patiño, 2015). In addition, the electric field was derived, based on the immersion model and its simulations gave the same results for monolayer isotropic systems, but for two or more inner layers there was an unjustified increment for the distribution of electric field for the same structure Au || SiO_2 || Au.

Finally, scattering matrix method was studied and programmed. The obtained optical functions in isotropic media are consistent with previous results except for the transmittance. It was necessary to add a factor in order to obtain the correct shape. In presence of magneto-optic layers the algorithm for p-polarization in reflectance gave precise functions in the trilayer (Au || Co || Au) for reflectance as is shown in the figure 3.14. Polar, longitudinal and transversal magneto-optic Kerr effect can be calculated in the algorithm created. TMOKE signal in trilayer Au(14.1) || Co(10.2) || Au(0.5) was simulated using the scattering matrix approach. The result of the simulation have the same shape with those found by Herreño-Fierro and Patiño (Herreño-Fierro and Patiño, 2015), but its amplitude is twice that one reported.

The algorithm created has an advantage over previous works, that is the implementation of models for isotropic and anisotropic media via software having a tool that allow users to do simulations for any number of layers knowing the response previously to the lab work, saving money, time and material, using the experimental setup only to test the simulations created.

In future works for isotropic media an algorithm for multilayer thin film can be created for optical functions depending on the wavelength (or equivalently eV) of the electromagnetic incident wave. This treatment need the data base of materials to be simulated which can be downloaded from available data bases like that popular from Mikhail Polyanskiy: *Refractive Index Data Base* (Polyanskiy, 2016).

Another future work could be a Graphic User Interface (GUI), convenient to readily obtain results as a previous process of the experimental set-up. This can include the results for isotropic media including optical functions as a function of the angle of incidence or the wavelength of the incident source and module of electric field. This GUI could have the option to manage anisotropic media for optical functions and electric field using scattering matrix approach giving as outputs the optical functions, module of electric field and the magneto-optic Kerr effect signal.

Following the same line for the future works, an online version of the propagating of light in stratified media can be build for open access to users all around the world in order to amplify the social reach and

to obtain a feedback and possible issues or bugs of the implemented code.

Finally, but not less important, from this master thesis, emerged two articles to be published that will be mentioned above:

- **Title:** *Optical functions using the scattering matrix approach for isotropic and magneto-optic media*
  Authors: B, Garibello-Suan, N. Avilán-Vargas, C. Herreño-Fierro and J. A. Galvis.
  Overview: The scattering matrix method is used to calculate optical functions introducing the correction factor α. Numerical results are shown for isotropic and magneto-optic multilayers.

- **Title:** *Formalism of transfer matrix* 4×4 *for anisotropic multilayered media in the limits of isotropy*
  Authors: B, Garibello-Suan, N. Avilán-Vargas, C. Herreño-Fierro and J. A. Galvis
  Overview: This article shows how the matrix transfer method 4×4 does not work in the limits of isotropy, the analytical deduction presented in the chapter 3 it is taken to write the article.

Some research developed in cooperation with Universidad Distrital and Universidad de los Andes are implementing experimental measures of multilayer thin films making use of the algorithms created in this thesis. Specific applications, simulations and experimental results will be shown in the papers:

- **Title:** *Effective Media Model and Sensitivity to Dielectric Environment of Plasmonic Properties of Gold Thin Films* To be published.
  Authors: A. X. Rodríguez-Rodríguez, B. Garibello-Suan, L. P. Quiroga-Sánchez, E. Patiño, and C. A. Herreño-Fierro.

- **Title:** *Plasmonic Enhancement of the Refractive and Magneto-optical Kerr Effect in Multilayer Continuos Systems* To be published.
  Authors: L. P. Quiroga-Sánchez, B. Garibello-Suan, E. Patiño, and C. A. Herreño-Fierro.

Appendix A

Appendix A

A.1 Electric Field p-polarization, normal component deduction

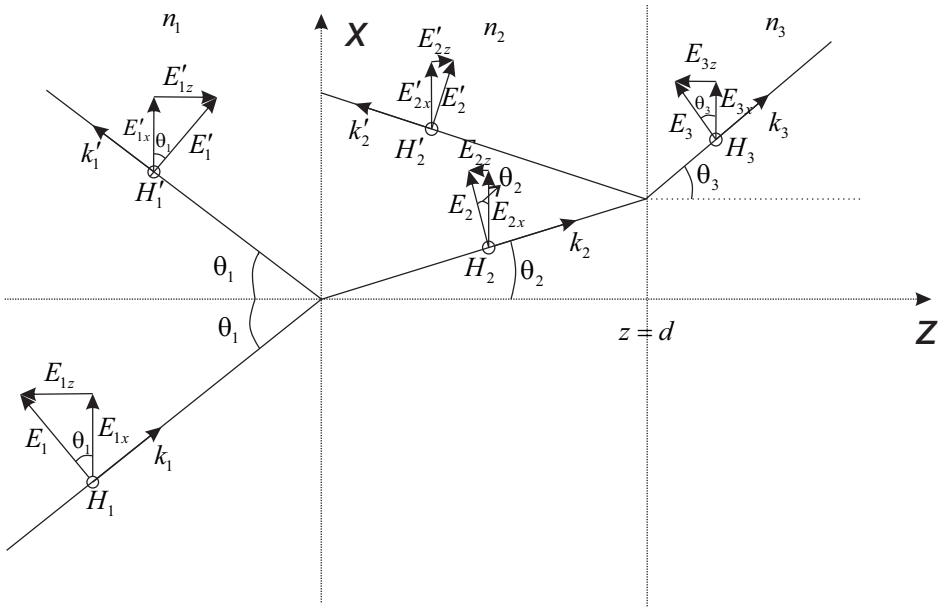

FIGURE A.1: p-Polarization for a oblique inicident wave through two nonconducting media

For p-polarization the figure 1.2 is a reference in which the electric fields can be decomposed as is shown below on the figure A.1. The components in the x-axes were studied on the chapter 2. In the case of normal components along z-direction, we must use the boundary condition 1.5 with $\rho_z = 0$, and define the electric field along z in the form:

$$E_z(z) = \begin{cases} \left(-A_p e^{ik_{1z}z} + B_p e^{-ik_{1z}z}\right) \sin\theta_1 & if \quad z < 0 \\ \left(-C_p e^{ik_{2z}z} + D_p e^{-ik_{2z}z}\right) \sin\theta_2 & if \quad 0 < z < d \\ \left(-F_p e^{ik_{3z}(z-d)}\right) \sin\theta_3 & if \quad z > d \end{cases} \tag{A.1}$$

Applying the boundary condition 1.5 for $z = 0$ and $z = d$, the Snell's Law for the interfaces 1||2 and 2||3 ($n_1 \sin\theta_1 = n_2 \sin\theta_2 = n_3 \sin\theta_3$) and assuming $A_p = 1$, $B_p = r_p$ and $F_p = t_p$ will give:

$$\begin{aligned} n_1(-1 + r_p) &= n_2(-C_p + D_p) \\ n_2(-C_p e^{ik_{2z}d} + D_p e^{-ik_{2z}d}) &= -n_3 t_p \end{aligned}$$

Solving for C_p and D_p:

$$\begin{aligned} C_p &= \frac{1 - r_p - \beta_{12}\beta_{23}t_p e^{ik_{2z}d}}{\beta_{12}(1 - e^{2ik_{2z}d})} \\ D_p &= \frac{1 - r_p}{\beta_{12}} - \frac{1 - r_p - \beta_{12}\beta_{23}t_p e^{ik_{2z}d}}{\beta_{12}(1 - e^{2ik_{2z}d})}. \end{aligned}$$

Where $\beta_{12} = \frac{n_2}{n_1}$, $\beta_{23} = \frac{n_3}{n_2}$. The electric field was simulated for the Kretschmann configuration BK7||Au||Air, the module of the electric field has the shape of the figure A.2.

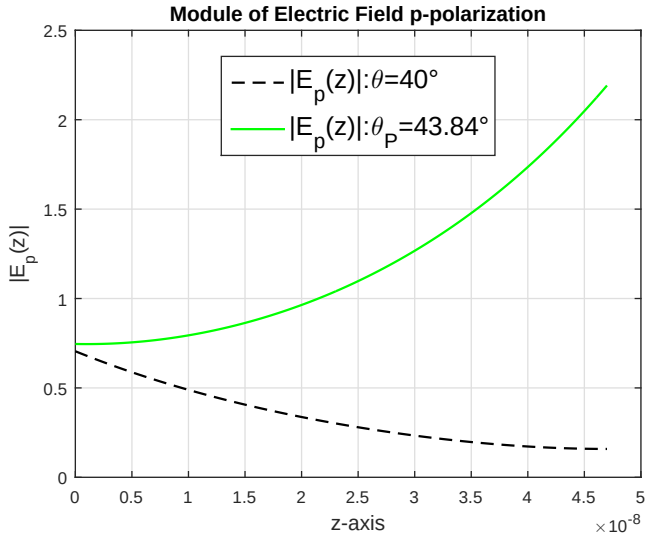

FIGURE A.2: Module of the electric field for p-polarization in the gold layer ($d = 47nm$) for Kretscmann configuration (deduction with normal components)

The shape of the figure A.2 is quite similar to the one presented in 2.5. Tabular data were obtained from the simulations and analyse, giving a zero error, which means that the two models are equivalent.

Appendix B

Appendix B

B.1 Coefficients of quartic equation

The coefficients of the moment space equation:

$$\zeta^4 + q_3\zeta^3 + q_2\zeta^2 + q_1\zeta + q_0 = 0 \tag{B.1}$$

$$\begin{aligned} q_0 = &\left(1 - \xi^2/\varepsilon_{zz}\right)\left[\varepsilon_{yy}\left(\varepsilon_{xx} - \xi^2\right) - \varepsilon_{xy}\varepsilon_{yx}\right] \\ &+ \left[\varepsilon_{xz}\left(\varepsilon_{yx}\varepsilon_{zy} - \varepsilon_{yy}\varepsilon_{zx}\right) + \varepsilon_{yz}\left[\varepsilon_{xy}\varepsilon_{zx} + \varepsilon_{zy}\left(\xi^2 - \varepsilon_{xx}\right)\right]\right]/\varepsilon_{zz} \end{aligned} \tag{B.2}$$

$$q_1 = \xi\left[\varepsilon_{xy}\varepsilon_{zx} + \varepsilon_{xz}\varepsilon_{yx} + \left(\xi^2 - \varepsilon_{xx}\right)\left(\varepsilon_{yz} + \varepsilon_{zy}\right)\right]/\varepsilon_{zz} \tag{B.3}$$

$$q_2 = \xi^2 - \varepsilon_{xx} - \varepsilon_{yy}\left(1 - \xi^2/\varepsilon_{zz}\right) + \left(\varepsilon_{xz}\varepsilon_{zx} + \varepsilon_{yz}\varepsilon_{zy}\right)/\varepsilon_{zz} \tag{B.4}$$

$$q_3 = \xi\left(\varepsilon_{yz} + \varepsilon_{zy}\right)/\varepsilon_{zz} \tag{B.5}$$

Appendix C

Appendix C

C.1 Jones Vectors for polarization states

Polarizations States	Jones Vectors
	$\begin{bmatrix}1\\0\end{bmatrix}$
	$\begin{bmatrix}0\\1\end{bmatrix}$
	$\frac{1}{\sqrt{2}}\begin{bmatrix}1\\1\end{bmatrix}$
	$\frac{1}{\sqrt{2}}\begin{bmatrix}1\\-1\end{bmatrix}$
	$\frac{1}{\sqrt{2}}\begin{bmatrix}1\\-i\end{bmatrix}$
	$\frac{1}{\sqrt{2}}\begin{bmatrix}1\\i\end{bmatrix}$
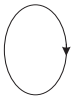	$\frac{1}{\sqrt{5}}\begin{bmatrix}1\\2i\end{bmatrix}$
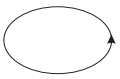	$\frac{1}{\sqrt{5}}\begin{bmatrix}2\\-i\end{bmatrix}$

TABLE C.1: Jones vector for polarization states

Appendix D

Appendix D

D.1 Scattering matrix alternative deduction based on the electric field

First of all the Maxwell equation:

$$\nabla \times \mathbf{E} = i\omega^2 \mu \mathbf{H} \tag{D.1}$$

Knowing that the electric and magnetic fields has the form (eliminating the temporal dependence):

$$\mathbf{E} = e^{i\mathbf{k}\cdot\mathbf{r}} e^{iqz} \left(e_x \hat{\mathbf{x}} + e_y \hat{\mathbf{y}} + e_z \hat{\mathbf{z}}\right) \tag{D.2}$$

$$\mathbf{H} = e^{i\mathbf{k}\cdot\mathbf{r}} e^{iqz} = \left(h_x \hat{\mathbf{x}} + h_y \hat{\mathbf{y}} + h_z \hat{\mathbf{z}}\right) \tag{D.3}$$

The rotational of the electric field will be:

$$\begin{aligned}
\nabla \times \mathbf{E} &= \begin{vmatrix} \hat{\mathbf{x}} & \hat{\mathbf{y}} & \hat{\mathbf{z}} \\ \frac{\partial}{\partial x} & \frac{\partial}{\partial y} & \frac{\partial}{\partial z} \\ e_x & e_y & e_z \end{vmatrix} \\
&= \left(\frac{\partial e_z}{\partial y} - \frac{\partial e_y}{\partial z}\right) \hat{\mathbf{x}} - \left(\frac{\partial e_z}{\partial x} - \frac{\partial e_x}{\partial z}\right) \hat{\mathbf{y}} + \left(\frac{\partial e_y}{\partial x} - \frac{\partial e_x}{\partial y}\right) \hat{\mathbf{z}} \\
&= ie^{i\mathbf{k}\cdot\mathbf{r}} e^{iqz} \left(\left(k_y e_z - q e_y\right) \hat{\mathbf{x}} - \left(k_x e_z - q e_x\right) \hat{\mathbf{y}} + \left(k_x e_y - k_y e_x\right) \hat{\mathbf{z}}\right)
\end{aligned}$$

Knowing that the magnetic field is given by equation (D.2), the Maxwell equation (D.1) becomes:

$$\left(k_y e_z - q e_y\right) \hat{\mathbf{x}} - \left(k_x e_z - q e_x\right) \hat{\mathbf{y}} + \left(k_x e_y - k_y e_x\right) \hat{\mathbf{z}} = h_x \omega^2 \hat{\mathbf{x}} + h_y \omega^2 \hat{\mathbf{y}} + h_z \omega^2 \hat{\mathbf{z}} \tag{D.4}$$

That is the same that:

$$\begin{aligned}
k_y e_z - q e_y &= h_x \omega^2 \\
q e_x - k_x e_z &= h_y \omega^2 \\
k_x e_y - k_y e_x &= h_z \omega^2
\end{aligned}$$

In matrix form the previous equations can be written in the form:

$$\begin{bmatrix} 0 & -q & k_y \\ q & 0 & -k_x \\ -k_y & k_x & 0 \end{bmatrix} \begin{bmatrix} e_x \\ e_y \\ e_z \end{bmatrix} = \omega^2 \begin{bmatrix} h_x \\ h_y \\ h_z \end{bmatrix} \tag{D.5}$$

In a compact form:

$$C^T \mathbf{e} = \omega^2 \mathbf{h} \tag{D.6}$$

Where T is the transpose of the antisymmetric matrix C. The electric field vector $\hat{e} = \begin{bmatrix} e_x \\ e_y \\ e_z \end{bmatrix}$, and the electric field vector $\hat{h} = \begin{bmatrix} h_x \\ h_y \\ h_z \end{bmatrix}$ and ω^2 is the angular frequency.

The Maxwell equation for curl of magnetic field stands:

$$\nabla \times \mathbf{H} = -i\hat{\varepsilon}\mathbf{E} \tag{D.7}$$

Where $\hat{\varepsilon}$ is the dielectric tensor. Replacing $\mathbf{E}$ and $\mathbf{H}$ by the equations (D.3) and (D.2):

$$\begin{aligned} \nabla \times \mathbf{H} &= \begin{vmatrix} \hat{\mathbf{x}} & \hat{\mathbf{y}} & \hat{\mathbf{z}} \\ \frac{\partial}{\partial x} & \frac{\partial}{\partial y} & \frac{\partial}{\partial z} \\ h_x & h_y & h_z \end{vmatrix} \\ &= \left(\frac{\partial h_z}{\partial y} - \frac{\partial h_y}{\partial z}\right)\hat{\mathbf{x}} - \left(\frac{\partial h_z}{\partial x} - \frac{\partial h_x}{\partial z}\right)\hat{\mathbf{y}} + \left(\frac{\partial h_y}{\partial x} - \frac{\partial h_x}{\partial y}\right)\hat{\mathbf{z}} \\ &= ie^{i\mathbf{k}\cdot\mathbf{r}}e^{iqz}\left(\left(k_y h_z - q h_y\right)\hat{\mathbf{x}} - \left(k_x h_z - q h_x\right)\hat{\mathbf{y}} + \left(k_x h_y - k_y h_x\right)\hat{\mathbf{z}}\right) \end{aligned}$$

Knowing that the electric field is given by equation (D.3), the Maxwell equation (D.7) becomes:

$$\left(k_y h_z - q h_y\right)\hat{\mathbf{x}} - \left(k_x h_z - q h_x\right)\hat{\mathbf{y}} + \left(k_x h_y - k_y h_x\right)\hat{\mathbf{z}} = \hat{\varepsilon}\left(e_x\hat{\mathbf{x}} + e_y\hat{\mathbf{y}} + e_z\hat{\mathbf{z}}\right) \tag{D.8}$$

In matrix form the previous equation can be written in the form:

$$\begin{bmatrix} 0 & q & -k_y \\ -q & 0 & k_x \\ k_y & -k_x & 0 \end{bmatrix}\begin{bmatrix} h_x \\ h_y \\ h_z \end{bmatrix} = \hat{\varepsilon}\begin{bmatrix} e_x \\ e_y \\ e_z \end{bmatrix} \tag{D.9}$$

In a compact form:

$$C\mathbf{h} = \hat{\varepsilon}\mathbf{e} \tag{D.10}$$

From equations (D.6) and (D.10) is possible obtain the electric or the magnetic field, so, finding the electric field:

$$\left(\frac{1}{\omega^2}CC^T - \hat{\varepsilon}\right)\mathbf{e} = \begin{bmatrix} 0 \\ 0 \\ 0 \end{bmatrix} \tag{D.11}$$

The equation (D.11) related the electric field components with the angular frequency (ω^2), the propagation vector components ($k_x, k_y, k_z = q$) in the matrix C and the dielectric tensor $\hat{\varepsilon}$.

In a long format, the equation (D.11) can be written as:

$$\left(\frac{1}{\omega^2}\begin{bmatrix}0 & q & -k_y\\ -q & 0 & k_x\\ k_y & -k_x & 0\end{bmatrix}\begin{bmatrix}0 & -q & k_y\\ q & 0 & -k_x\\ -k_y & k_x & 0\end{bmatrix}-\begin{bmatrix}\varepsilon_{xx} & \varepsilon_{xy} & \varepsilon_{xz}\\ \varepsilon_{yx} & \varepsilon_{yy} & \varepsilon_{yz}\\ \varepsilon_{zx} & \varepsilon_{zy} & \varepsilon_{zz}\end{bmatrix}\right)\begin{bmatrix}e_x\\ e_y\\ e_z\end{bmatrix}=\begin{bmatrix}0\\0\\0\end{bmatrix} \tag{D.12}$$

Doing the algebraic operations and multiplying by $-\omega^2$:

$$\begin{bmatrix}\omega^2\varepsilon_{xx}-k_y^2-q^2 & \omega^2\varepsilon_{xy}+k_xk_y & \omega^2\varepsilon_{xz}+k_xq\\ \omega^2\varepsilon_{yx}+k_xk_y & \omega^2\varepsilon_{yy}-k_x^2-q^2 & \omega^2\varepsilon_{yz}+k_yq\\ \omega^2\varepsilon_{zx}+k_xq & \omega^2\varepsilon_{zy}+k_yq & \omega^2\varepsilon_{zz}-k_x^2-k_y^2\end{bmatrix}\begin{bmatrix}e_x\\ e_y\\ e_z\end{bmatrix}=\begin{bmatrix}0\\0\\0\end{bmatrix} \tag{D.13}$$

Note that the equation (D.13) is exactly the same that (3.9). Furthermore, the matrix can be turn into a system:

$$\left(\omega^2\varepsilon_{xx}-k_y^2-q^2\right)e_x+\left(\omega^2\varepsilon_{xy}+k_xk_y\right)e_y+\left(\omega^2\varepsilon_{xz}+k_xq\right)e_z = 0 \tag{D.14}$$

$$\left(\omega^2\varepsilon_{yx}+k_xk_y\right)e_x+\left(\omega^2\varepsilon_{yy}-k_x^2-q^2\right)e_y+\left(\omega^2\varepsilon_{yz}+k_yq\right)e_z = 0 \tag{D.15}$$

$$\left(\omega^2\varepsilon_{zx}+k_xq\right)e_x+\left(\omega^2\varepsilon_{zy}+k_yq\right)e_y+\left(\omega^2\varepsilon_{zz}-k_x^2-k_y^2\right)e_z = 0 \tag{D.16}$$

Also, the Maxwell equation for the divergence of the displacement in free space becomes:

$$\nabla\cdot\mathbf{D}=0 \tag{D.17}$$

Replacing $\mathbf{D}=\varepsilon_0\hat{\varepsilon}\mathbf{E}$ and setting the electrical field as the equation (D.3), the divergence gives the equation:

$$k_x\left(\varepsilon_{xx}e_x+\varepsilon_{xy}e_y+\varepsilon_{xz}e_z\right)+k_y\left(\varepsilon_{yx}e_x+\varepsilon_{yy}e_y+\varepsilon_{yz}e_z\right)+q\left(\varepsilon_{zx}e_x+\varepsilon_{zy}e_y+\varepsilon_{zz}e_z\right)=0 \tag{D.18}$$

Solving for E_z:

$$e_z=-\frac{k_x\varepsilon_{xx}+k_y\varepsilon_{yx}+q\varepsilon_{zx}}{k_x\varepsilon_{xz}+k_y\varepsilon_{yz}+q\varepsilon_{zz}}e_x-\frac{k_x\varepsilon_{xy}+k_y\varepsilon_{yy}+q\varepsilon_{zy}}{k_x\varepsilon_{xz}+k_y\varepsilon_{yz}+q\varepsilon_{zz}}e_y \tag{D.19}$$

Replacing the equation D.19 into the equation D.13, lead us to a 2×2 equation system:

$$\begin{bmatrix}a_{11}d_{11}-a_{13}d_1 & a_{12}d_{11}-a_{13}d_2\\ a_{21}d_{11}-a_{23}d_1 & a_{22}d_{11}-a_{23}d_2\end{bmatrix}\begin{bmatrix}e_x\\ e_y\end{bmatrix}=\begin{bmatrix}0\\0\end{bmatrix} \tag{D.20}$$

Where:

$$
\begin{aligned}
a_{11} &= \omega^2\varepsilon_{xx} - k_y^2 - q^2 \\
a_{12} &= \omega^2\varepsilon_{xy} + k_x k_y \\
a_{13} &= \omega^2\varepsilon_{xz} + k_x q \\
a_{21} &= \omega^2\varepsilon_{yx} + k_x k_y \\
a_{22} &= \omega^2\varepsilon_{yy} + k_x^2 - q^2 \\
a_{23} &= \omega^2\varepsilon_{yz} + k_y q \\
d_1 &= k_x\varepsilon_{xx} + k_y\varepsilon_{yx} + q\varepsilon_{zx} \\
d_2 &= k_x\varepsilon_{xy} + k_y\varepsilon_{yy} + q\varepsilon_{zy} \\
d_{11} &= k_x\varepsilon_{xz} + k_y\varepsilon_{yz} + q\varepsilon_{zz}
\end{aligned}
$$

The equation D.20 can be written in terms of powers of q, multiplying first by $\frac{1}{q}$:

$$\left(A_2 q^2 + A_1 q + A_0 + A_{-1}\frac{1}{q}\right)\begin{bmatrix} e_x \\ e_y \end{bmatrix} = \begin{bmatrix} 0 \\ 0 \end{bmatrix} \tag{D.21}$$

The matrices A_2, A_1, A_0 and A_{-1} are given by:

$$A_2 = \begin{bmatrix} -\varepsilon_{zz} & 0 \\ 0 & -\varepsilon_{zz} \end{bmatrix} \tag{D.22}$$

$$A_1 = -k_x\begin{bmatrix} \varepsilon_{xz}+\varepsilon_{zx} & \varepsilon_{zy} \\ 0 & \varepsilon_{xz} \end{bmatrix} - k_y\begin{bmatrix} \varepsilon_{yz} & 0 \\ \varepsilon_{zx} & \varepsilon_{yz}+\varepsilon_{zy} \end{bmatrix} \tag{D.23}$$

$$
\begin{aligned}
A_0 = \omega^2\left(\varepsilon_{zz}\begin{bmatrix} \varepsilon_{xx} & \varepsilon_{xy} \\ \varepsilon_{yx} & \varepsilon_{yy} \end{bmatrix} - \varepsilon_{zx}\begin{bmatrix} \varepsilon_{xz} & 0 \\ \varepsilon_{yz} & 0 \end{bmatrix} - \varepsilon_{zy}\begin{bmatrix} 0 & \varepsilon_{xz} \\ 0 & \varepsilon_{yz} \end{bmatrix}\right) \\
- k_x^2\begin{bmatrix} \varepsilon_{xx} & \varepsilon_{xy} \\ 0 & \varepsilon_{zz} \end{bmatrix} - k_y^2\begin{bmatrix} \varepsilon_{zz} & 0 \\ \varepsilon_{yx} & \varepsilon_{yy} \end{bmatrix} - k_x k_y\begin{bmatrix} \varepsilon_{yx} & \varepsilon_{yy}-\varepsilon_{zz} \\ \varepsilon_{xx}-\varepsilon_{zz} & \varepsilon_{xy} \end{bmatrix}
\end{aligned} \tag{D.24}
$$

$$
\begin{aligned}
A_{-1} = \omega^2\left(k_x\begin{bmatrix} 0 & 0 \\ \varepsilon_{yx}-\varepsilon_{xx}\varepsilon_{yz} & \varepsilon_{xz}\varepsilon_{yy}-\varepsilon_{xy}\varepsilon_{yz} \end{bmatrix} + k_y\begin{bmatrix} \varepsilon_{xx}\varepsilon_{yz}-\varepsilon_{xz} & \varepsilon_{xy}\varepsilon_{yz}-\varepsilon_{xz} \\ 0 & 0 \end{bmatrix}\right) \\
+ k_x k_y\left(k_x\begin{bmatrix} 0 & 0 \\ \varepsilon_{xz} & -\varepsilon_{yz} \end{bmatrix} + k_y\begin{bmatrix} \varepsilon_{xz} & \varepsilon_{yz} \\ 0 & 0 \end{bmatrix}\right) + k_x^2\varepsilon_{xz}\begin{bmatrix} 0 & k_y \\ 0 & k_x \end{bmatrix} + k_y^2\varepsilon_{yz}\begin{bmatrix} -k_y & 0 \\ k_x & 0 \end{bmatrix}
\end{aligned} \tag{D.25}
$$

The process is realized assuming the permeability is $\mu = 1$

Bibliography

Abdulhalim, I (1999). "Analytic propagation matrix method for linear optics of arbitrary biaxial layered media". In: *Journal of Optics A: Pure and Applied Optics* 1.5, p. 646.

Abelès, Florin (1948). "Sur la propagation des ondes électromagnétiques dans les milieux sratifiés". In: *Annales de physique*. Vol. 12. 3. EDP Sciences, pp. 504–520.

Armelles, Gaspar et al. (2013). "Magnetoplasmonics: combining magnetic and plasmonic functionalities". In: *Advanced Optical Materials* 1.1, pp. 10–35.

Balasubramanian, K, AS Marathay, and HA Macleod (1988). "Modeling magneto-optical thin film media for optical data storage". In: *Thin Solid Films* 164, pp. 391–403.

Berreman, Dwight W (1972). "Optics in stratified and anisotropic media: 4× 4-matrix formulation". In: *Josa* 62.4, pp. 502–510.

Caballero, B, Antonio García-Martín, and JC Cuevas (2012). "Generalized scattering-matrix approach for magneto-optics in periodically patterned multilayer systems". In: *Physical Review B* 85.24, p. 245103.

Cojocaru, E (1997). "Generalized Abeles relations for an anisotropic thin film of an arbitrary dielectric tensor". In: *Applied optics* 36.13, pp. 2825–2829.

— (2000). "Simple recurrence matrix relations for multilayer anisotropic thin films". In: *Applied optics* 39.1, pp. 141–148.

Cotter, NPK, TW Preist, and JR Sambles (1995). "Scattering-matrix approach to multilayer diffraction". In: *JOSA A* 12.5, pp. 1097–1103.

Diebel, James (2006). "Representing attitude: Euler angles, unit quaternions, and rotation vectors". In: *Matrix* 58.15-16, pp. 1–35.

Griffiths, David J (2013). *Introduction to electrodynamics*. 4ed. Pearson, Addison-Wesley, p. 420.

Heavens, Oliver S (1991). *Optical properties of thin solid films*. Courier Corporation.

Hecht, E. (2017). *Optics*. Always learning. Pearson. ISBN: 9781292096933.

Herreño-Fierro, César Aurelio (2016). "Magnetoplasmónica de estructuras multicapa Au||Co||Au". In: *Ph.D, Thesis*, pp. 1–182.

Herreño-Fierro, César Aurelio and Edgar J Patiño (2015). "Maximization of surface-enhanced transversal magneto-optic Kerr effect in Au/Co/Au thin films". In: *physica status solidi (b)* 252.2, pp. 316–322.

Ko, D Yuk Kei and JR Sambles (1988). "Scattering matrix method for propagation of radiation in stratified media: attenuated total reflection studies of liquid crystals". In: *JOSA A* 5.11, pp. 1863–1866.

Landry, Gary D and Theresa A Maldonado (1995). "Complete method to determine transmission and reflection characteristics at a planar interface between arbitrarily oriented biaxial media". In: *JOSA A* 12.9, pp. 2048–2063.

Li, Zhan-Ming, Brian T Sullivan, and Robert R Parsons (1988). "Use of the 4× 4 matrix method in the optics of multilayer magnetooptic recording media". In: *Applied optics* 27.7, pp. 1334–1338.

Mansuripur, M (1990). "Analysis of multilayer thin-film structures containing magneto-optic and anisotropic media at oblique incidence using 2× 2 matrices". In: *Journal of Applied Physics* 67.10, pp. 6466–6475.

Moncada, E. (2015). "Light propagation and near-field radiative heat transfer in photonic structures containing anisotropic and dispersive materials". In: *Ph.D Thesis*, pp. 1–88.

Palencia-Barrera, Liseth Daniela (2018). “Caracterización y Optimización de Resonancias Plasmónicas en Estructuras Multicapas”. In: *Thesis*, pp. 1–59.

Polyanskiy, Mikhail N (2016). “Refractive index database”. In: URL: https://refractiveindex.info/.

Quiroga-Sáchez, Leidy Paola (2018). “Plasmones Superficiales en Sistemas Multicapas Au|SiO2”. In: *Thesis*, pp. 1–53.

Raether, Heinz (1988). “Surface plasmons on smooth surfaces”. In: *Surface plasmons on smooth and rough surfaces and on gratings*. Springer, pp. 4–39.

Reitz, John R, Frederick J Milford, and Robert W Christy (2008). *Foundations of electromagnetic theory*. Addison-Wesley Publishing Company.

Rodríguez-Rodríguez, Anyi Ximena (2018). “Sensibilidad al Entorno Dieléctrico de las Propiedades Plasmónicas de Películas Delgadas de Oro”. In: *Thesis*, pp. 1–43.

Sambles, JR, GW Bradbery, and Fuzi Yang (1991). “Optical excitation of surface plasmons: an introduction”. In: *Contemporary physics* 32.3, pp. 173–183.

Whittaker, DM and IS Culshaw (1999). “Scattering-matrix treatment of patterned multilayer photonic structures”. In: *Physical Review B* 60.4, p. 2610.

Windt, David L (1998). “IMD—Software for modeling the optical properties of multilayer films”. In: *Computers in physics* 12.4, pp. 360–370.

Yariv, Amnon and Pochi Yeh (1984). *Optical waves in crystals*. Vol. 5. Wiley New York.

Yeh, P. (2005). *Optical Waves in Layered Media*. Wiley Series in Pure and Applied Optics. Wiley. ISBN: 9780471731924.

Yeh, Pochi (1980). “Optics of anisotropic layered media: a new 4× 4 matrix algebra”. In: *Surface Science* 96.1-3, pp. 41–53.

Zvezdin Anatoliĭ, Konstantinovich and Viacheslav Alekseevich Kotov (1997). *Modern magnetooptics and magnetooptical materials*. CRC Press.